Photochemistry of Transition Metal Hydrides

Journal:	*Chemical Reviews*
Manuscript ID	Draft
Manuscript Type:	Thematic Review
Date Submitted by the Author:	n/a
Complete List of Authors:	Perutz, Robin; University of York, Chemistry Procacci, Barbara; University of York, Department of Chemistry

Photochemistry of Transition Metal Hydrides

Robin N Perutz* and Barbara Procacci*

Department of Chemistry, University of York, YO10 5DD, UK

Abstract

Photochemical reactivity associated with metal-hydrogen bonds is very widespread among metal hydride complexes and has played a critical part in opening up C-H bond activation and related fields. In recent research, it has allowed photocatalytic generation of hydrogen from aqueous media with well-defined reaction intermediates, and has been exploited to obtain NMR spectra of dilute solutions with a single pulse of an NMR spectrometer with the aid of para-hydrogen enhancement. Since photolysis can be performed on fast timescales and at extremely low temperature, metal-hydride photochemistry has enabled determination of the molecular structure and rates of reaction of highly reactive intermediates. We review the photoprocesses available to complexes with one, two or more M–H bonds, to metal dihydrogen complexes and to complexes with bridging hydride ligands. The majority of photochemical reactions are likely to be dissociative, occurring on femto- or pico-second timescales, but hydride complexes may be designed with equilibrated excited states that undergo different photochemical reactions, including excited state proton transfer or excited state hydride transfer. A few photochemical reactions have been analyzed by quantum dynamics calculations. We identify five characteristic photoprocesses of metal mono-hydride complexes associated with the M-H bond of which the most widespread are M-H homolysis and R-H reductive elimination. For metal dihydride complexes, by far the dominant photoprocess is reductive elimination of H_2. This reaction is usually reversed thermally, allowing a degenerate cycle to be established of H_2 reductive elimination and oxidative addition. This cycle may be used in to measure rates of reaction with H_2 up to the diffusion limit. Dihydrogen complexes typically lose H_2 photochemically and this photo-reaction may be employed in a similar way to that of dihydride complexes. Photocatalysis and photoelectrocatalysis with metal hydride complexes have been exploited for such reactions as formation of H_2 from protons and formic acid decomposition. Photocatalysis has also been applied to C-H functionalization reactions such as dehydrogenation of alkenes or borylation of arenes. The review is completed with a survey of transition metal hydride photochemistry organized by transition metal group.

CONTENTS

1. INTRODUCTION

Transition metal hydride complexes play roles in innumerable chemical reactions and catalytic processes. They illustrate formation of simple covalent bonds with transition metals and vary in character from acidic to hydridic. Furthermore, a large proportion of metal hydride complexes exhibit photochemical reactivity associated with the M-H bond(s). Although many examples of photochemical reactivity have long been known and have opened up new fields of research, we are not aware of any wide-ranging reviews of this subject. It was first reported by two groups independently in 1972 that metal dihydride complexes may undergo photochemical reductive elimination of H_2. Camus, Cocevar and Mestroni reported that cationic cobalt dihydrides $[Co(H)_2(NN)(PR_3)_2]^+$ (NN = 2,2'-bipyridine *or* 1,10-phenanthroline, R_3 = Bu_3, Pr_3, Et_3, Et_2Ph) exhibit photoinduced reductive elimination of H_2 under vacuum; the reaction is reversed thermally by restoring a hydrogen atmosphere.[1] In the same year, Giannotti and Green independently communicated that a tungsten dihydride, $Cp_2W(H)_2$ loses H_2 photochemically and undergoes insertion of the metal into the C-H bonds of benzene.[2] Since then, a variety of

photoprocesses have been observed that involve the metal-hydrogen bond(s) directly: dissociation of hydrogen atoms, reductive elimination of H_2 or RH (R = alkyl, silyl, etc.), hydrogen transfer, isomerization, and electron transfer. In addition, there may be photoprocesses involving other ligands. It is now clear that the majority of transition metal *cis*-dihydride complexes undergo photodissociation of H_2, provided that the relevant absorption bands are not obscured by other transitions with much higher absorption coefficients. The photoprocesses for monohydride complexes often involve M-H homolysis but new photoprocesses are still being discovered.

Photochemical reactions of metal dihydrides have played a critical role in opening up C-H bond activation of arenes and, especially of alkanes.[3-5] The ability to initiate reactions photochemically provides a route to the synthesis of labile products since the photochemistry may be performed at low temperature. It also offers the opportunity to study fast reaction kinetics and reaction intermediates by time-resolved spectroscopy (especially laser flash photolysis) and by low temperature matrix isolation. These techniques have all been applied to the C-H activation problem. Photochemistry is also a synthetic tool, sometimes with no alternative route as in the synthesis of decamethylrhenocene by M-H homolysis.[6]

Most recently, photochemistry has been used to generate metal dihydride complexes in selected nuclear spin states formed synchronously with a pulsed laser[7] and to study reaction intermediates in nitrogenase.[8] Another important development is the recognition that equilibrated excited states of metal hydride polypyridine complexes can act both as strong acids and strong hydride donors, opening up new photocatalytic reactions.[9-10] The last few years have also seen important progress in the photochemistry of complexes with bridging hydrides.[11-12]

The production of hydrogen by photocatalytic methods is of enormous current interest, but the vast majority of approaches neither involve photochemical reaction of metal hydride complexes directly, nor formation of excited states of metal hydride complexes by photosensitization. The involvement of hydrides in the photocatalytic splitting of water, typically by protonation of an intermediate, is reviewed elsewhere,[13-17] and a very different approach will be taken here. There are exceptions, however, that involve metal hydrides directly that will be concern us here.[18-19] We will also review examples in which photocatalysis with metal hydrides has been used for dehydrogenation of alkanes and alcohols, borylation of arenes and other C-H functionalization reactions.

This review starts with a survey of key photoprocesses separating the complexes into monohydrides, dihydrides, polyhydrides and bridging hydrides. This section incorporates the theory of photodissociation and also includes dihydrogen complexes and photocatalysis. In the

succeeding section, we examine methods for studying mechanisms of photochemistry of metal hydride complexes, concentrating on time-resolved spectroscopy, matrix isolation and NMR methods. Here, we also assess the significance of photochemistry in studying reactive intermediates and catalysis. A systematic survey organized by transition metal group completes the review. For an up-to-date introduction to photochemical principles, the reader is referred to the recent book by Balzani, Ceroni and Juris.[20] Although, we have not found any wide-ranging reviews of the photochemistry of metal hydrides, there are several relevant reviews of narrower areas that include some metal hydride photochemistry.[3-5,16-17,21-25]

2. PHOTOCHEMICAL PROCESSES

In this section, we review the major photoprocesses observed for transition metal hydrides providing one or two key examples of each photoprocess. Metal hydride complexes typically show absorption bands in the UV region, often with somewhat indistinct maxima, leading to difficulties in measurement of quantum yields. There is some evidence of wavelength dependence of relative quantum yields for different pathways. We will highlight examples with useful information on electronic spectra, quantum yields and wavelength-dependent photochemistry in this section. The available evidence, albeit limited in extent, points to dissociative photochemical mechanisms for the vast majority of the reactions. Some decisive exceptions concern the metal hydride polypyridine complexes in which equilibrated excited states are formed before reaction. The isomerization of square planar platinum complexes is also likely to be completely intramolecular. The majority of the examples here involve mononuclear complexes, since there is little recent research on metal hydride clusters. However, we single out complexes with bridging hydride ligands, because of the principles they illustrate.

2.1 Metal monohydride complexes

Several photochemical pathways are known for mono-hydrides involving the M-H bond: metal-hydrogen bond homolysis, reductive elimination of R-H (R = alkyl or silyl), isomerization, excited-state proton transfer, and excited-state hydride transfer. These pathways may compete with photodissociation of other ligands such as CO, or partial decoordination of cyclopentadienyl ligands (Scheme 1).

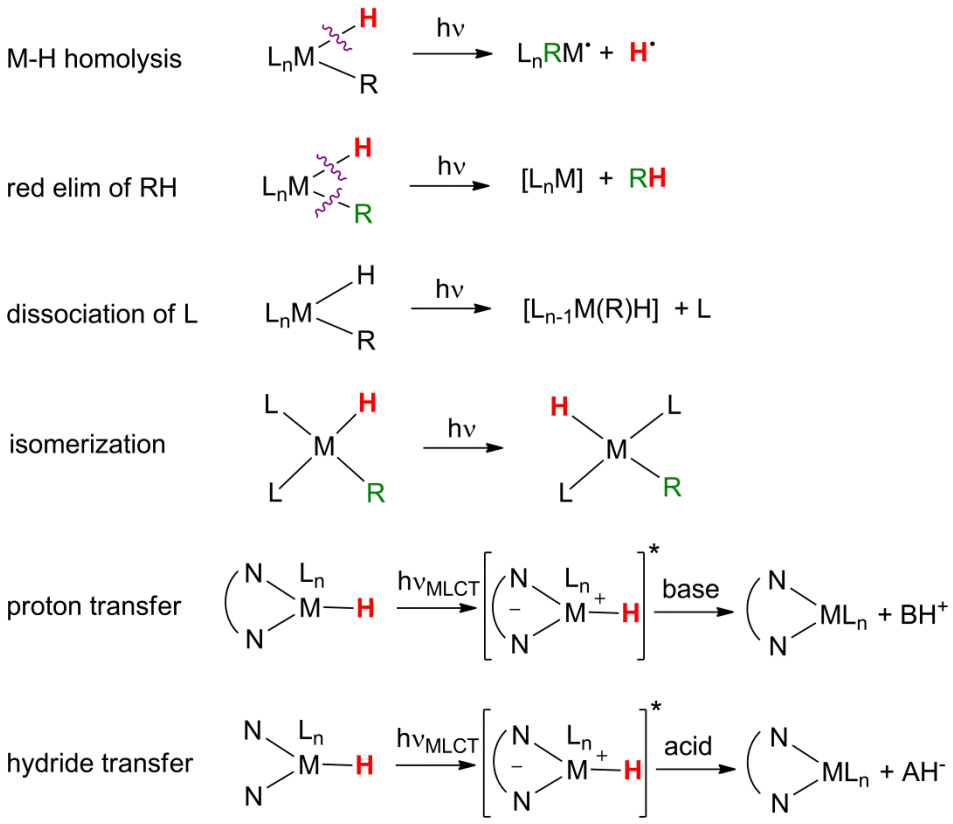

Scheme 1. Photoprocesses of metal monohydride complexes

2.1.1 Homolytic splitting of M-H bond. The homolytic splitting of the metal-hydrogen bond may occur photochemically without the requirement for any radical initiators. An excellent example is provided by the near UV and visible ($\lambda > 290$ nm) photolysis of Cp^*_2ReH in pentane solution leading to the formation of decamethylrhenocene in 60% isolated yield.[6] There is no evidence for any competing photoprocess and this remains the only known access route to decamethylrhenocene (Equation 1).

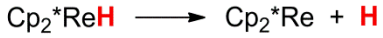

Equation 1

Often, M-H homolysis competes with photodissociation of other ligands: $MnH(CO)_5$ acts as a prototypical example. Initial matrix isolation studies of $MnH(CO)_5$ revealed only CO loss,[26] but later the dissociation of H atoms was demonstrated by trapping the hydrogen atom with CO as the formyl radical allowing the square pyramidal structure of $[Mn(CO)_5]$ to be demonstrated by IR spectroscopy.[27] Use of EPR spectroscopy for detection following photolysis (254 nm) of

$MnH(CO)_5$ in argon matrices allowed the structure of $[Mn(CO)_5]$ to be confirmed independently, the electron distribution of the SOMO to be determined, and the H atom to be detected.[28] The amount of $[Mn(CO)_5]$ produced was increased by 193 nm irradiation in Ar matrices such that $[Mn(CO)_5]$ became the dominant product detected by IR spectroscopy.[29] The electronic spectrum of $MnH(CO)_5$ has been reported experimentally [30] and re-investigated by more modern computational methods with CASSCF methods[31] and including spin-orbit coupling.[32]

The theoretical basis of the photochemistry of $MnH(CO)_5$ has also been investigated extensively. Early calculations[33] have been superseded by calculations using CASSCF methods[34] that led to the conclusion that 193 nm irradiation causes excitation to the c^1E state ($d\pi\rightarrow\pi^*$) which undergoes intersystem crossing and internal conversion to the a^3A_1 ($\sigma\rightarrow\sigma^*$ Mn-H) state. This state lies on the potential energy surface for H-Mn homolysis. Irradiation at 229 nm generates the b^1E state ($d\pi\rightarrow\sigma^*$) which undergoes Mn-CO bond lengthening ultimately yielding Mn-CO cleavage and formation of an excited state of $[MnH(CO)_4]$. This calculation rationalizes the observation of increased yield of $[Mn(CO)_5]$ at short wavelength irradiation. A CASSCF/MRCI and CASPT2 *ab initio* study reinvestigated the electronic structure of $MnH(CO)_5$ identified that population of the A^1E and B^1E states results in CO-dissociation, but did not identify the mechanism of Mn-H homolysis unambiguously.[31] The most recent calculations place the c^1E state at 46820 cm^{-1} (214 nm) and indicate that it has 63% $d\pi\rightarrow\sigma^*$ Mn-H character.[32] It is important to emphasize that such calculations indicate that there is a high density of states at the energies that are irradiated and that the photochemistry must be considered in terms of electronic states, not just population in terms of antibonding orbitals. Moreover, complex crossing between potential energy surfaces is often involved. Nevertheless, dissociation does occur on an M-H antibonding surface.

2.1.2 Reductive elimination of RH (R = Me, $SiEt_3$, OEt, etc.). While thermal reductive elimination of alkanes from metal alkyl hydride complexes is commonplace, the corresponding photochemical reactions are relatively rare. Irradiation of $Cp^*_2ZrH(R)$ (R = alkyl) results in alkane reductive elimination. Crossover and isotopic labeling demonstrated that the reductive elimination occurs by an intramolecular mechanism (Equation 2).[35] The photochemical reaction of *cis-mer*-$[MH(SiEt_3)(CO)_3(PPh_3)]$ (M = Fe, Ru) in alkane glasses at 100 K reveals formation of both CO (40%) and $SiHEt_3$ (60%) as primary photoproducts – only these two photoprocesses are significant. The principle of photochemical reductive elimination can be used to exchange coordinated silyl groups (Equation 3) at room temperature in solution with a quantum yield of 0.6 ± 0.1 at 313 nm. However, loss of CO remains a competing process.[36] The alkoxide hydride

$Cp^*IrH(OEt)(PPh_3)$ undergoes reductive elimination of EtOH on irradiation.[37]

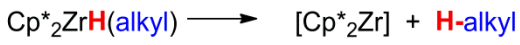

Equation 2

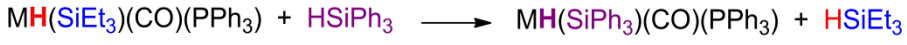

Equation 3

2.1.3. Photoisomerization. Square-planar platinum complexes are well known to undergo photochemical *cis-trans* isomerization and platinum hydrides are no exception. Examples are provided by c*is*-$[PtH(SiR_2R')(PCy_3)_2]$ (R, R' = H, alkyl, aryl) which undergo quantitative isomerization on UV irradiation at room temperature. It is likely that this is an intramolecular process proceeding *via* a tetrahedral transition state as has been postulated for other platinum complexes. [38] Photoisomerization may also occur in other ways: the octahedral complex $[IrH(tpy)(ppy)]^+$ (tpy = terpyridyl, ppy = phenylpyridine) changes configuration,[39] while $IrH(triphos)(C_2H_4)$ undergoes oxidative C-H cleavage to form the vinyl dihydride $IrH_2(CH{=}CH_2)(triphos)$.[40]

2.1.4 Excited state proton transfer and hydride transfer. There are two further photoprocesses that have been discovered much more recently, transfer of a proton from an excited state and transfer of a hydride from an excited state. In each case, we are concerned with metal hydride polypyridine complexes that have equilibrated excited states, as opposed to the dissociative excited states of metal hydrides that are usually formed. As with many polypyridine complexes, $[Cp^*IrH(bpy)]^+$ forms an equilibrated excited state that is emissive. (λ_{em} 708 nm).[9] This cation forms a transient when irradiated in methanol (λ_{ex} 430 nm) that is readily identified as [Cp*Ir(bpy)] and that regenerates the precursor by second order kinetics.[10] The solvent kinetic isotope effect for the regeneration step is remarkably large at 8.2 when methanol is replaced by methanol-d_1. Ultrafast laser experiments (excited at 355 nm) show that the rate of formation of the triplet MLCT state (1.4×10^{10} s^{-1}) is *ca.* 18 times faster than its rate of deprotonation (8.1×10^8 s^{-1}) (Scheme 3).[10] The ground state pK_a is measured as 23.3 compared to the excited state value pK_a* of -12, estimated from the emission spectra, confirming that it can protonate methanol.[9] Remarkably, this complex is also predicted to be a very strong hydride donor, stronger than $[HBEt_3]^-$, resulting from the transfer of charge to bpy in the excited state. Experimentally, $[Cp^*IrH(bpy)]^+$ transfers hydride to several acids in CD_3CN forming H_2; the weakest of these acids is acetic acid (pK_a = 23.5) where the other product is $[Cp^*Ir(OAc)(bpy)]^+$ (Scheme 2). Photoreaction with methylnicotinamide iodide yields the

products of single-hydride transfer or double-hydride transfer according to the conditions.[9] Thus the ability to act both as a strong excited state acid and hydride donor may be compared to the ability of metal polypyridine complexes to act as both strong oxidizers and strong reducers. Several photocatalytic reactions are associated with $[Cp^*IrH(bpy)]^+$ (Section 2.6).

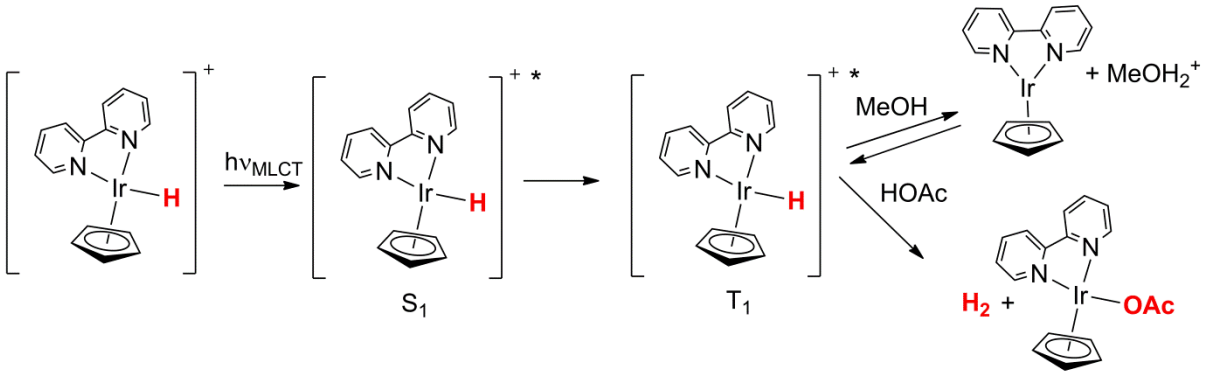

Scheme 2. Excited state proton and hydride transfer from excited triplet state[9] for $[Cp^*IrH(bpy)]^+$

2.2 Metal dihydride complexes

The photoinduced reductive elimination of H_2 from dihydride complexes is by far the commonest photochemical pathway for metal hydrides and competes effectively with the photodissociation of other ligands such as phosphine or CO. All the evidence points to this reaction as a concerted cleavage of the two M-H bonds with concomitant formation of the H-H bond. Three other pathways have been identified: photoinduced electron transfer, photoisomerization, and hydrogen migration. In contrast to the monohydrides, there is no convincing evidence for homolytic cleavage of an M-H bond generating hydrogen atoms. In addition, there are a few examples of formation of charge transfer complexes which exhibit different photochemical pathways. In the examples given in section 2.2.1, photoelimination is the sole process, but this is not generally true, see the case of $Ru(H)_2(PMe_3)_4$ for an example (Scheme 3).[41]

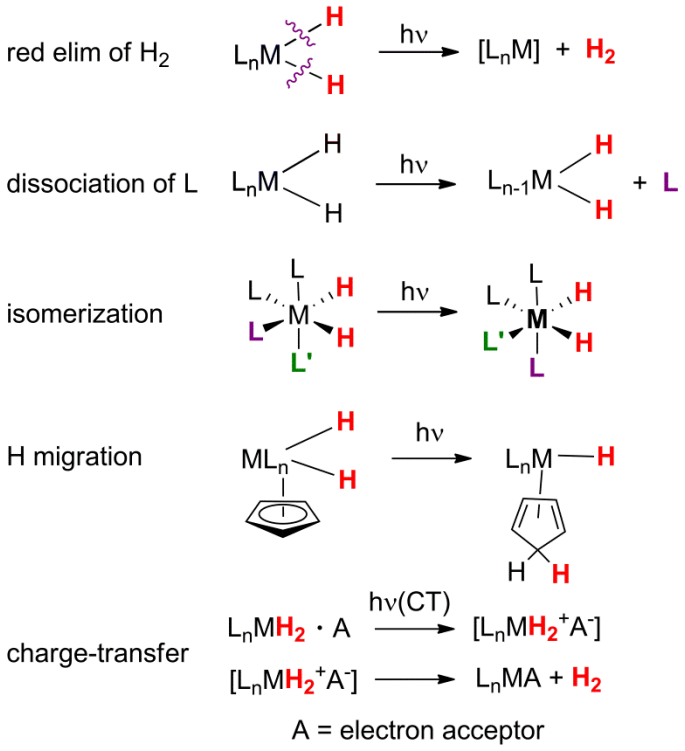

Scheme 3. Photoprocesses of metal dihydride complexes

2.2.1 Reductive elimination of H_2. Irradiation of $Cp_2W(H)_2$ in solution causes loss of H_2 and insertion of $[Cp_2W]$ into C-H or O-H bonds. The discoveries of the insertion reactions into the C-H bonds of benzene and tetramethylsilane[2,42] were significant landmarks in the development of C-H bond activation. The complex $Cp_2W(H)_2$ has a clear absorption maximum in hexane solution at 270 nm (ε = 5000 dm^3 mol^{-1} cm^{-1}) with a shoulder at 325 nm tailing into the visible region; the gas-phase absorption spectrum has also been reported.[43] The photoreaction occurs with a lower limiting quantum yield of *ca.* 0.01 on irradiation at 366 nm.[44] Matrix isolation experiments revealed tungstenocene as the primary photoproduct and showed *via* IR, UV-vis, laser-induced fluorescence and magnetic circular dichroism that it has a parallel sandwich structure with a $^3E_{2g}$ ground state. These early experiments are summarized in reviews.[23,45] Since then, the matrix photochemistry has been investigated in more detail.[46-48] Additional reports have added the photochemical reactions of $Cp_2W(H)_2$ in solution with $HSiCl_3$ $HSiMe_2Cl$, and $HSiMe_3$ to make the corresponding $Cp_2WH(SiR_3)$ complexes.[49-50] Co-irradiation of $Cp_2W(H)_2$ and metal-metal bonded carbonyl complexes such as $[CpNi(CO)]_2$ or $[CpRu(CO)_2]_2$ have been used to generate heterodinuclear complexes. In these reactions with two metal complexes, there is no control of which complex undergoes photochemical reactions and it is

likely that both contribute.[51] The solution photoreactions of $Cp_2W(H)_2$ are shown in Scheme 4; these reactions cannot be achieved by heating $Cp_2W(H)_2$ but many are accessible if $Cp_2WH(CH_3)$ is used as a thermal source of $[Cp_2W]$. The corresponding photochemistry of $Cp_2Mo(H)_2$ is described in Section 4.3.2.

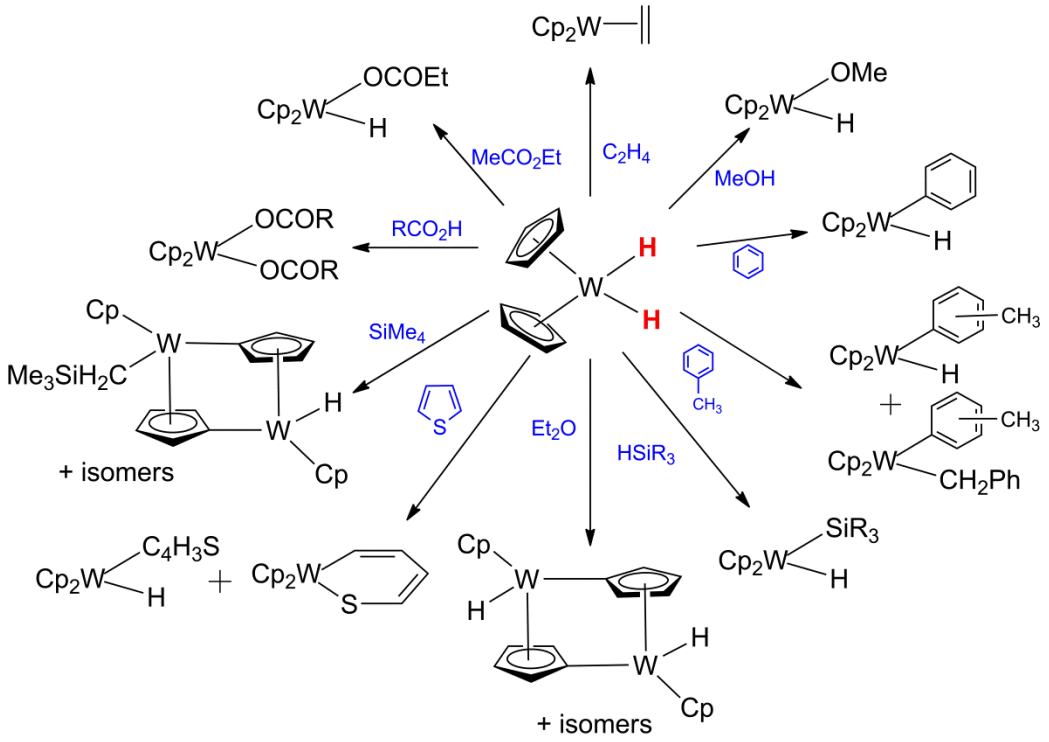

Scheme 4. Solution photochemistry of $Cp_2W(H)_2$

The first report of the solution photochemistry of $Ru(H)_2(dmpe)_2$ and $Ru(H)_2(dppe)_2$ in toluene-d_8 employed mass spectrometry to demonstrate that the dominant photoprocess in these complexes is loss of H_2, revealing H_2 with only *ca.* 3% HD. A similar quantity of HD is formed in a crossover experiment where $Ru(H)_2(dmpe)_2$ and $Ru(D)_2(dmpe)_2$ are irradiated together (313 nm) in solution.[52] Photolysis in an EPR spectrometer at low temperature in the presence of a spin trap also failed to generate a hydrogen spin adduct. Irradiation in benzene solution in the presence of carbon monoxide or ethylene led to loss of H_2 and the formation of the corresponding complexes $Ru(dmpe)_2L$ or $Ru(dppe)_2L$ (L = CO, C_2H_4). In the absence of substrate, the products were identified as $Ru_2(dmpe)_5$ and $RuH(C_6H_4PPhCH_2CH_2PPh_2)(dppe)$, respectively.[52] In understanding these reactions, it is important to note that the *cis*-dihydride isomers dominate over the *trans* isomers ($Ru(H)_2(dmpe)_2$ *ca.* 13:1, $Ru(H)_2(dppe)_2$ 20:1) and that there is probably a slow equilibrium between the isomers. Further photochemical reactions of

$Ru(H)_2(dmpe)_2$ were reported in later studies including C-H, Si-H and B-H activation reactions (Scheme 5).[53-54] Notably, reinvestigation of the reaction with ethylene showed formation of *cis*-$[RuH(C_2H_3)(dmpe)_2]$ in addition to $Ru(dmpe)_2(C_2H_4)$. The UV absorption spectrum of $Ru(H)_2(dmpe)_2$ (colorless when pure) shows a maximum at 210 nm (ε = 4900 $dm^3\ mol^{-1}\ cm^{-1}$) in pentane solution and a shoulder at 260 nm. The quantum yield at 308 nm has been determined by transient actinometry as 0.85 ± 0.1.[55]

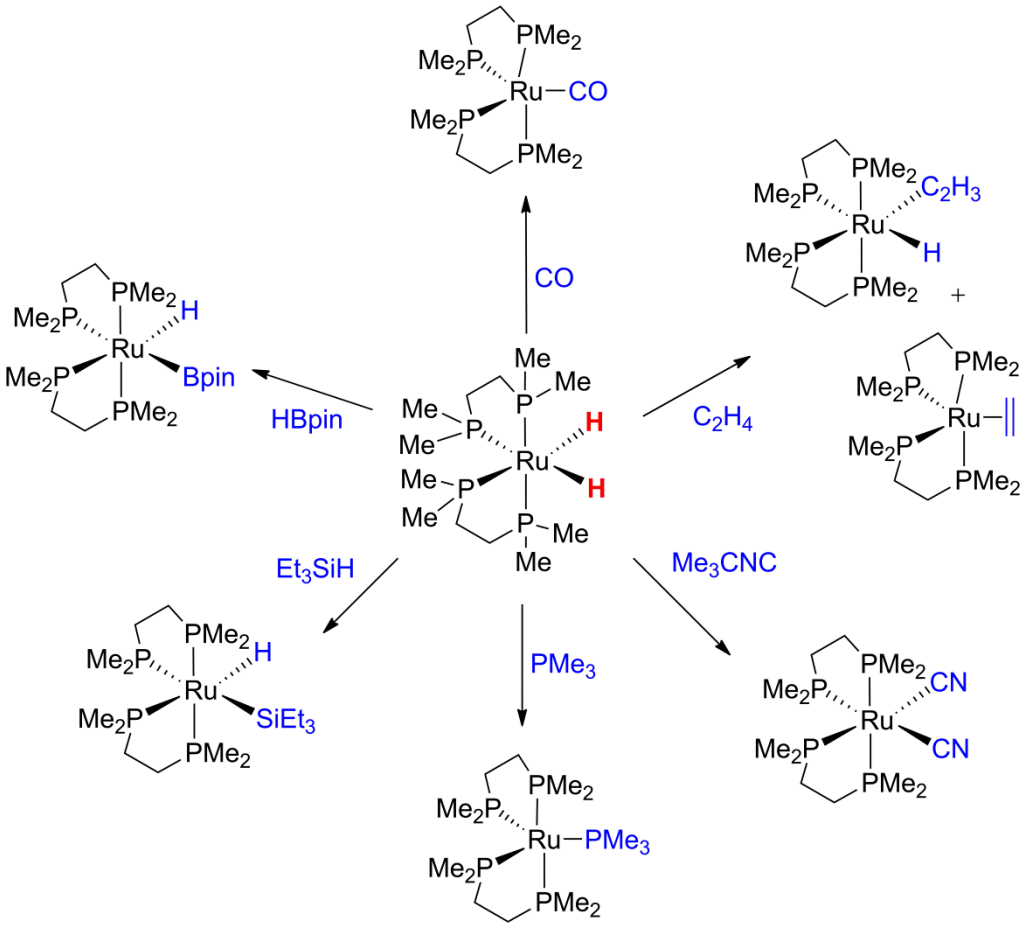

Scheme 5. Solution photoreactions of $Ru(H)_2(dmpe)_2$

The photochemical reactions of $Ru(H)_2(dmpe)_2$ have been investigated by both matrix isolation and laser flash photolysis (time-resolved absorption spectroscopy).[53] UV photolysis in argon or methane matrices causes depletion of the ν(RuH) bands of $Ru(H)_2(dmpe)_2$ in the IR spectrum and growth of characteristic UV-vis absorption bands for $[Ru(dmpe)_2]$, including long wavelength absorptions at 460, 543 and 743 nm (values for Ar matrix). The reactions can be partially reversed by long wavelength irradiation. There is no evidence for activation of methane;

introduction of 1.5% CO results in photochemical conversion of $Ru(H)_2(dmpe)_2$ to $Ru(dmpe)_2(CO)$.

Laser flash photolysis is simplest for a reaction that is driven forwards photochemically and reverses thermally. Such a degenerate reaction is indeed set up by adding sub-atmospheric pressures of H_2 to a solution of $Ru(H)_2(dmpe)_2$ in cyclohexane (Equation 4). The resulting transient absorption spectrum measured 400 ns after the 308 nm flash at 300 K shows a striking match to the spectra observed in methane matrix at 12 K. The transient decays with *pseudo*-first-order kinetics allowing the second-order rate constant to be determined as $(6.8 \pm 0.3) \times 10^9$ $dm^3\ mol^{-1}\ s^{-1}$ by varying the partial pressure of H_2. The kinetic isotope effect is measured as $k_H/k_D = 1.20 \pm 0.08$. The rate constant is very close to the diffusion limit and still represents the fastest recorded rate constant for reaction of H_2 at a transition metal center.[53]

$$RuH_2(dmpe)_2 \underset{k}{\overset{h\nu}{\rightleftharpoons}} [Ru(dmpe)_2] + H_2$$

Equation 4

When laser flash photolysis is performed under an argon atmosphere, the reaction is still largely reversible leading to second order kinetics. Flash photolysis in the presence of a variety of substrates leads to quenching behavior, allowing second order rate constants for reaction with $[Ru(dmpe)_2]$ to be determined which follow the order: H_2 > CO > HBpin > *t*-BuNC > PMe_3 > C_2H_4 ~ $HSiEt_3$ > cyclopentene and span a factor of *ca.* 2000. Activation parameters for several reactions of $[Ru(dmpe)_2]$ are listed in Table 1. When the corresponding experiments are carried out in the absence of substrate, second order kinetics are observed consistent with recombination with H_2 as the major reaction. Indirect evidence for some reaction of $[Ru(dmpe)_2]$ with itself or with $Ru(H)_2(dmpe)_2$ comes from anomalous behavior at higher concentrations and the non-zero intercept in the quenching plots.[53-54] The rise-time of $[Ru(dmpe)_2]$ following irradiation (300 nm) of $Ru(H)_2(dmpe)_2$ under H_2 has been probed by picosecond transient absorption methods and shown to be < 16 ps, the instrumental response (Figure 1). These experiments revealed partial decay of the transient with a rate constant *ca.* 100 times faster than observed in the nanosecond experiments ($k_{obs} = 3 \times 10^9\ s^{-1}$) perhaps due to geminate recombination.[56]

Table 1. Activation parameters for reactions of Group 8 [MP_4] determined by transient absorption spectroscopy

	$\Delta H^{\ddagger}$ kJ/mol	$\Delta S^{\ddagger}$ J/mol/K	$\Delta G^{\ddagger}_{298}$ / kJ/mol	reference
[**Fe**$(dmpe)_2$] + $HSiEt_3$	22 ± 2	-87 ± 6	48 ± 3	[57]
[**Ru**$(dmpe)_2$] + $HSiEt_3$	9 ± 1	-53 ± 4	25 ± 2	[53]
[**Ru**$(depe)_2$] + $HSiEt_3$	11 ± 3	-112 ±4	44 ± 1	[58]
[**Ru**$(dmpm)_2$] + $HSiEt_3$	11 ± 2	-40 ± 5	23 ± 2	[59]
[**Ru**(PP_3)] + $HSiEt_3$	35 ± 2	-18 ± 6	40 ± 4	[60]
[**Ru**(etp)(CO)] + $HSiEt_3$	11 ± 1	-49 ± 4	25.7 ± 0.1	[61]
[**Os**(PP_3)] + $HSiEt_3$	31 ± 5	-27 ± 12	39 ± 6	[60]
[**Ru**(PP_3)] + C_6H_6	39 ± 4	+1 ± 13	38 ± 6	[60]
[**Os**(PP_3)] + C_6H_6	38 ± 3	-7 ± 9	40 ± 4	[60]
[**Os**(PP_3)] + pentane	27 ± 1	-59 ± 4	45 ± 2	[60]

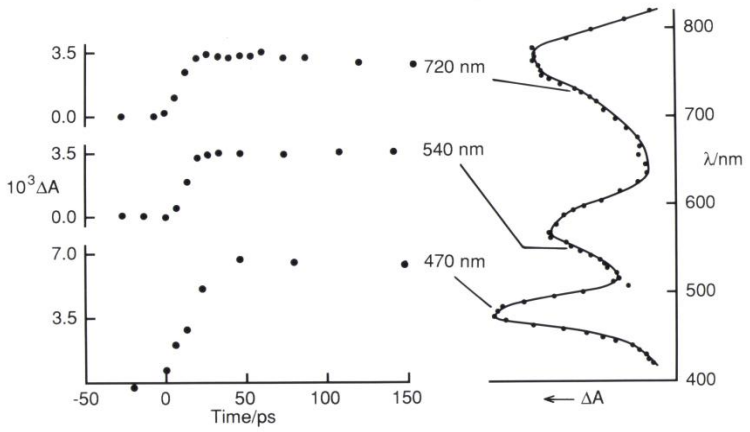

Figure 1. Transient absorption signals following laser flash photolysis of $Ru(H)_2(dmpe)_2$ in cyclohexane solution under 1 atm of H_2 at 300 K monitored at 470, 540, and 720 nm over a 150-ps time scale (left). The signals rise within the response time of 16 ps. The detection wavelengths for the traces (left) are mapped onto the transient UV-vis spectrum of [$Ru(dmpe)_2$] obtained by ns-laser flash photolysis.[56]

When a laser flash is employed to irradiate $Ru(H)_2(dmpe)_2$ under argon and the heat deposition is measured by photoacoustic calorimetry, the enthalpy of reaction of $[Ru(dmpe)_2]$ and H_2 to form $Ru(H)_2(dmpe)_2$ may be determined (Equation 4, back reaction), yielding a value of $\Delta H = -22.7$ kcal/mol allowing the Ru-H bond dissociation enthalpy to be estimated as 63.5 ± 2.0 kcal/mol. The same method can be used with CO and N_2 atmospheres to determine the Ru-CO and Ru-N_2 bond enthalpies as 43 ± 2.0 and 18.8 ± 2.0 kcal/mol, respectively. [55]

Fast kinetic methods have also been used to investigate the photochemistry of $Ru(H)_2(dppe)_2$ showing that transient $[Ru(dppe)_2]$ maybe generated in a similar way to that described for $[Ru(dmpe)_2]$. Replacement of the phosphine methyl substituents by phenyl groups leads to a reduction in the rate constants by a factor of 260 for H_2, rising to a factor of 3700 for ethylene, indicating a great increase in selectivity.[54,58] The transient absorption spectrum of $[Ru(dppe)_2]$ resembles that of $[Ru(dmpe)_2]$.

In a new method development (See Section 3.2), the photochemistry of $Ru(H)_2(dppe)_2$ has been investigated in laser pump - NMR probe experiments in which a single pulse of a laser (355 nm) initiates dissociation of H_2 and a single radio frequency (*rf*) pulse serves to detect the resulting magnetization.[7] In these experiments, *para*-H_2 replaces the usual H_2 atmosphere, resulting in the formation of $Ru(H)_2(dppe)_2$ in selected nuclear spin states, greatly increasing the sensitivity of NMR detection. When the delay time between the laser pulse and the *rf* pulse is varied, oscillations in the magnetization are revealed with an oscillation frequency corresponding to the difference between the two spin-spin coupling constants $|J_{PHtrans} - J_{PHcis}|$. This laser pump - NMR probe method paves the way for studying millisecond or microsecond reaction kinetics with the benefits of highly resolved NMR spectra to identify species unambiguously.

The origin of the rich absorption spectrum of d^8 $[Ru(dmpe)_2]$ has been traced to a square-planar (D_{2h}) structure with a singlet ground state. This characteristic pattern is found in other unconstrained $[RuP_4]$ and $[OsP_4]$ species,[58,62] but is very different from that of constrained species that cannot adopt a square planar structure[63] such as $[Ru(PP_3)]$. It also contrasts with that of $[Fe(dmpe)_2]$ which adopts a triplet ground state.[57] The low energy band of $[Ru(dmpe)_2]$ is assigned to a $4d_{z2} \rightarrow 5p_z$ transition.

The initial photodissociation of H_2 from *cis*-$[Ru(H)_2(dmpe)_2]$ has been modeled with *cis*-$[Ru(H)_2(PH_3)_4]$ and time-dependent DFT calculations.[64] The absorption band is identified with the HOMO-1 to LUMO transition to the S_2 state ($d_{xz} \rightarrow$ combination of d_{x2-z2}, d_{z2} and σ_g of H_2

fragment, C_2 axis defined as *y*). Elimination of H_2 is found to be exothermic and dissociative in both the S_1 and S_2 excited states. Wave-packet analysis shows that elimination of H_2 occurs *via* an avoided crossing on a timescale of 100 fs if the wave packet is allowed to propagate on the potential energy surface after relaxation to the geometry corresponding to the H_2 elimination barrier. This relaxation may itself take a few hundred femtoseconds.

Density functional calculations have also been reported on $[Ru(PH_3)_4]$ as a model for $[Ru(dmpe)_2]$, making extensive comparisons to $[Fe(PH_3)_4]$ and $[Rh(PH_3)_4]^+$.[65] The singlet state of $[Ru(PH_3)_4]$ was calculated to be more stable than the triplet state by *ca.* 12 kcal /mol and the triplet state was calculated to adopt a D_{2d} geometry with P-Ru-P angles of 159°. (There is an interesting comparison to the Ru^0 complex $Ru(CO)_2(P\textit{t}\text{-}Bu_2Me)_2$ that has been isolated and studied computationally and which adopts a C_{2v} structure).[66] Oxidative addition of H_2 was predicted to be exothermic by 34 kcal/mol (evidently an overestimate, see above). The pathway for oxidative addition was calculated to proceed without any barrier *via* an initial end-on approach of H_2. The H-H distance does not elongate and the H_2 does not swing to a sideways orientation until the Ru-H distance is close to its final value. The ΔSCF method was used to calculate the lowest energy transitions of $[Ru(PH_3)_4]$ and $[Rh(PH_3)_4]^+$ and gave energies as 13900 and 26200 cm^{-1}, very accurately reproducing the experimental values for the dmpe compounds of 13800 and 25600 cm^{-1}, respectively. These calculations support the $4d_{z^2} \rightarrow 5p_z$ assignment of the low energy band of $[Ru(dmpe)_2]$.[65]

Details of the photochemistry of related $M(H)_2P_4$ and $M(H)_2P_3(CO)$ complexes (M = Fe, Ru, Os; P = phosphine) are given in Section 4.5.2.

The most thorough theoretical treatments address the photochemical reductive elimination of H_2 from $Fe(H)_2(CO)_4$ and the competing dissociation of CO. The theoretical work is linked to the matrix isolation photochemistry of $Fe(H)_2(CO)_4$ which showed exclusive loss of H_2 and also showed that the reaction could be partially reversed by long-wavelength irradiation.[67] A simplified orbital approach examines the bonding and antibonding orbitals involved in the $Fe(H)_2$ interaction (Scheme 6) and suggests that reaction occurs by population of the orbital which is Fe-H antibonding and H-H bonding, labeled σ_g^* in Scheme 6. According to CASSCF/CCI calculations, the main contributions to the absorption spectrum relevant to H_2 dissociation are $a^1A_1 \rightarrow a^1B_1$ and $a^1A_1 \rightarrow b^1A_1$ transitions which both correspond to d-σ_g^* excitation. The upper states of these transitions are dissociative with respect to H_2 elimination. According to wave-packet analysis, H_2 elimination occurs within 40 fs.[68-69] There is no evidence for intersystem crossing. The dissociation of H_2 is predicted to dominate over CO dissociation throughout the UV absorption region. Although, this sounds simple, there are numerous close-lying states,

such that a multi-configurational approach is necessary to describe the photodissociation dynamics. In more recent work, calculation of the absorption energies have been refined.[70-71]

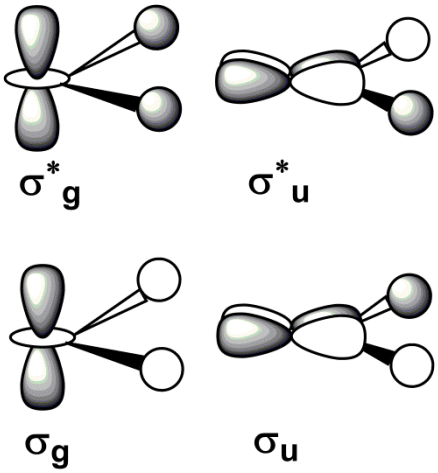

Scheme 6. Simplified bonding and antibonding orbital overlap diagrams for a metal dihydride[69]

2.2.2 Photoisomerization. Photoisomerization of an octahedral metal dihydride complex may occur *via* photoinduced reductive elimination of H_2 or *via* photoinduced loss of another ligand. The example of $Ru(H)_2(NHC)(CO)(PPh_3)_2$ illustrates these processes (Figure 2).[72] The photochemical reaction was studied by *in situ* laser photolysis (325 nm, continuous wave) within the probehead of an NMR spectrometer at 223 K and demonstrates initial conversion of the stable isomer **1** to new isomers **2**, **3**, and **4**. The role of H_2 loss was demonstrated by irradiating under a *para*-H_2 atmosphere resulting in formation of enhanced spectra of **2** and **3**. The competing loss of PPh_3 was evident from a photochemical reaction in the presence of pyridine that yielded a substitution product. A combination of kinetic analysis and DFT calculations revealed the complete pathway for isomerization involving both H_2 and PPh_3 loss.

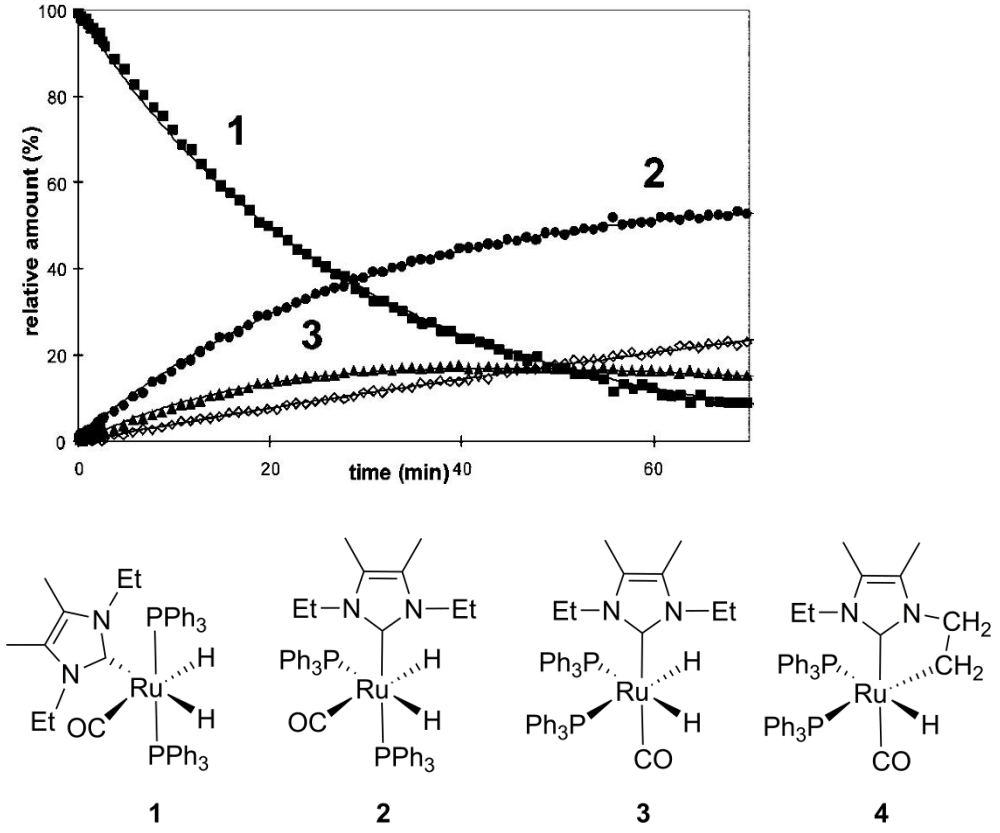

Figure 2. Time profile for conversion of **1** (■) into isomers **2** (•), **3** (▲), and **4** (♦) over 130 min upon photolysis at 223 K (observed points and fitted lines with the dominant pathways indicated).[72]

A particularly interesting example of photoisomerization concerns $CpMn(H)_2$(dfepe) that exists as an equilibrium mixture of the dihydride isomer with *transoid* diphosphine and dihydrogen isomer with *cisoid* diphosphine. Photolysis at 10 °C results in complete conversion to the dihydrogen complex. When left in the dark, the original equilibrium mixture is slowly restored.[73] A related phenomenon has been observed for $CpRe(H)_2(CO)_2$, but neither the distinction between dihydride and dihydrogen isomers, nor the photoisomerization is so complete.[74]

2.2.3 Photoinduced Hydrogen Migration. Photodissociation is not the only photoprocess involving the hydride ligands that has been observed for metal dihydrides. Loss of one or both PPh_3 ligands was observed when $CpRe(H)_2(PPh_3)_2$ was photolyzed and a variety of substitution products were synthesized in the presence of phosphines, THF, C_2H_4. The complex also showed photocatalytic activity (λ > 345 nm irradiating into edge of absorption band at 328 nm) for the conversion of C_2H_4 and benzene into ethylbenzene, ethane, 1-butane and butane.[75] Additionally, it catalyzes photoinduced H/D exchange between deuterated solvents and arene or alkane substrates including methane itself.[76] An extensive series of isotope labeling studies led

to the conclusion that the photochemical mechanism does not involve $[CpRe(H)_2(PPh_3)]$ or $[CpRe(PPh_3)_2]$ as intermediates, but involves metal-to-ring hydrogen migration to form $(\eta^4\text{-}C_5H_6)ReH(PPh_3)_2$. This compound undergoes a further migration to form $[(\eta^3\text{-}C_5H_7)Re(PPh_3)_2]$ which is the active species for H/D exchange.[77]

2.2.3 Photoinduced electron transfer, charge transfer adducts and photosensitization. The first report of the photochemistry of $Ru(H)_2(dmpe)_2$ included the demonstration of the photoreaction with tetracyanoethylene in benzene yielding $Ru(dmpe)_2\{C_2(CN)_3\}(CN)$. The authors detected the $TCNE^-$ radical by EPR and UV-vis spectroscopy and proposed two successive photochemical steps, the first to form $[M(dmpe)_2^+ \cdot TCNE^-]$, the second to convert this charge-transfer adduct to $Ru(dmpe)_2\{C_2(CN)_3\}(CN)$.[52] There was no mention of ground state adducts. Related experiments on $Cp_2W(H)_2$ yielded somewhat different results;[78] ground-state donor acceptor adducts were observed with absorption bands in the region 480 nm (dimethylfumarate, K_{eq} = 0.08 M^{-1}) to 538 nm (maleic anhydride, K_{eq} = 0.2 M^{-1}), where K_{eq} is the formation constant of the adduct. The charge-transfer transition energies correlate with the electron affinity of the activated alkenes. Irradiation of the maleic anhydride adduct into the tail of the CT band (> 550 nm) resulted in formation of the $Cp_2W(\eta^2\text{-}CC\text{-}\{C_2(CO)_2O\}$ together with succinic anhydride. A similar reaction occurred with fumaronitrile. These reactions evidently proceed by a very different photochemical pathway from those described in section 2.2.1 and must involve the excited state of the CT adduct.

The examples described so far absorb predominantly or exclusively in the UV region. It is therefore highly desirable to sensitize metal hydrides by using visible light absorbers. Such photosensitization has been achieved only rarely, but is illustrated by the case of $[Co(H)_2(bpy)(PEt_2Ph)_2]^+$ which has an absorption tailing into the visible and undergoes photoinduced H_2 loss in methanol solution with 405 nm radiation (quantum yield 0.14). Addition of $Fe(bpy)_2(CN)_2$ allows the photolysis to be performed with a similar quantum yield but at much longer wavelength (577 nm).[79] The mechanism does not seem to have been investigated further but may well involve photoinduced electron transfer and hence be related to the charge-transfer photochemistry described above.

An alternative approach is to use photoelectrolysis to deliver the electron to the metal hydride complex. This method is discussed in more detail in the photocatalysis section in the context of the $[Mo(H)_2(O_2CMe)(dppe)_2]^+$ as the electron acceptor.[80]

2.3 Metal polyhydride complexes

Metal polyhydride complexes offer the possibility of either photoinduced H loss or H_2 loss, in addition to photodissociation of other ligands. The tetrahydride, $Mo(H)_4(dppe)_2$, provides a well-studied example of an emissive hydride complex: it absorbs at 380 nm (26000 cm^{-1}) and emits at 580 nm (17300 cm^{-1}) in a 2-MeTHF glass at 77 K with an emission lifetime of 87 μs, leading to the assignment of the emissive state as a spin triplet.[81] The emission yield is enhanced in the deuterated analogue, $Mo(D)_4(dppe)_2$. The photolysis (366 nm) of $Mo(H)_4(dppe)_2$ under N_2 results in conversion to *trans*-$[Mo(N_2)_2(dppe)_2]$ in high yield. Similarly, the corresponding reactions with CO or C_2H_4 gives $Mo(L)_2(dppe)_2$ (L = CO, C_2H_4).[81-82] In the presence of H_2, $Mo(H)_4(dppe)_2$ acts as a photocatalyst for reduction of alkenes. Photolysis under CO_2 takes a different course, yielding the insertion product $MoH(O_2CH)(dppe)_2$,[83] while reaction with alkyl methacrylates yielded seven-coordinate $MoH(\kappa^2\text{-}CHCMeCO_2R)(dppe)_2$ by C-H activation.[84] A related reaction with allyl carboxylates yielded hydrido carboxylate complexes, releasing propene and H_2. These reactions are thought to involve initial coordination of the allyl group.[85] β-dicarbonyl compounds such as 2,4-pentanedione react to form molybdenum hydrido dionato complexes; the authors interpret this as an O-H oxidative addition from the enol form. Photoinduced oxidative addition reactions of N-H bonds with succinimide and N-alkyl acetamide and related compounds were observed, yielding metalacycles.[86-87] In spite of this extensive preparative chemistry (Scheme 7), the photogenerated intermediate $[Mo(H)_2(dppe)_2]$ has not been characterized, and there remains a question of whether this intermediate undergoes a second reductive elimination to form $[Mo(dppe)_2]$ or whether the products result from reaction of $Mo(H)_2(L)(dppe)$ (photochemical or thermal). In contrast to the behavior of $Cp_2W(H)_2$, most of these reactions can also be effected by thermal reaction of $Mo(H)_4(dppe)_2$. They are reviewed in a perspective article.[21] This photoreactivity is also related to some photocatalytic reactions (Section 2.6).

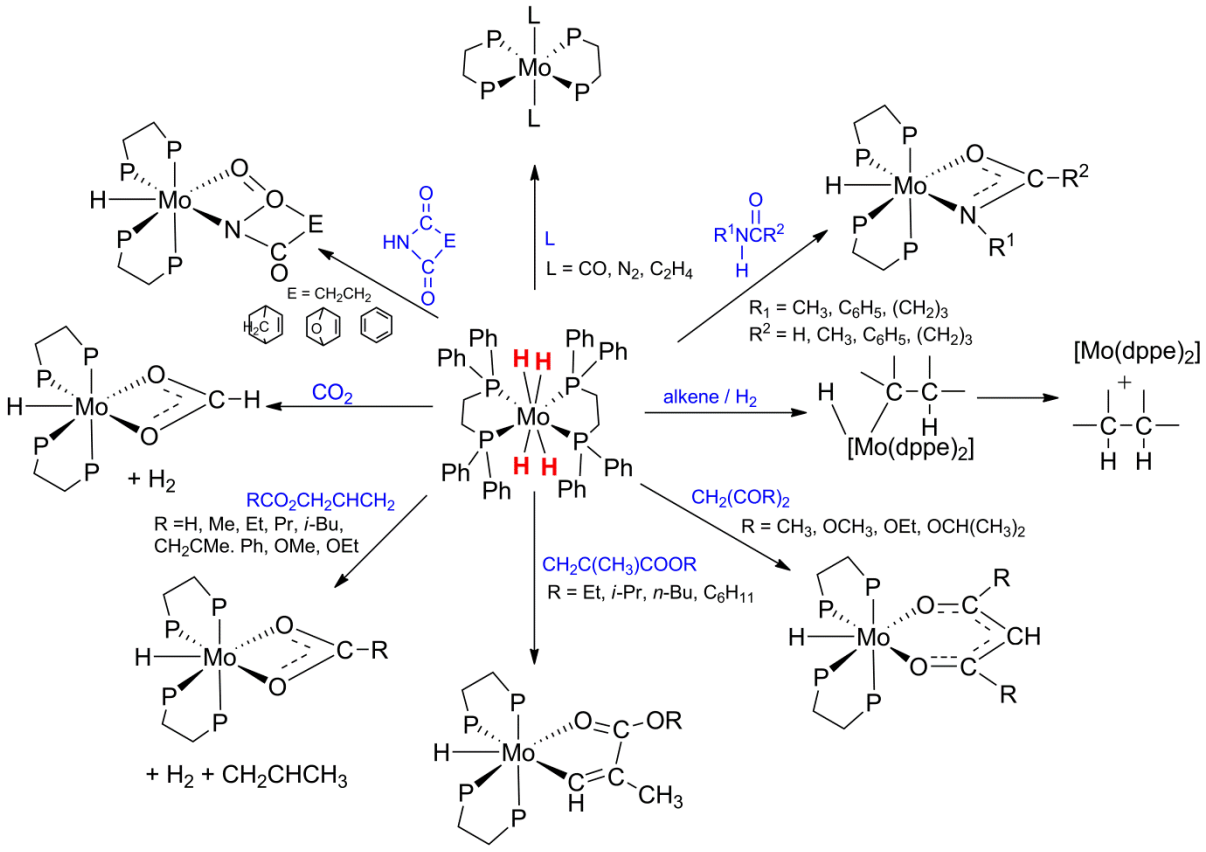

Scheme 7. Solution photochemistry[21] of $Mo(H)_4(dppe)_2$

In a reminder of the possibility of photochemical loss of ligands other than hydrogen, even if chelating, it has recently been demonstrated that irradiation of $W(H)_4(dppe)_2$ under hydrogen results in formation of a photostationary state between $W(H)_4(dppe)_2$ and $W(H)_6(dppe)(\kappa^1\text{-dppe})$.[88]

2.4 Dihydrogen Complexes

The majority of dihydrogen complexes are thermally labile with respect to H_2 loss, meaning that photochemical loss usually becomes significant only at low temperatures. A clear demonstration of photochemical loss of H_2 from a dihydrogen complex came from the reaction of chromium hexacarbonyl in H_2-doped argon matrices at 4-12 K. UV photolysis causes generation of $[Cr(CO)_5]$ which reacts on long-wavelength photolysis to form $Cr(H_2)(CO)_5$. Irradiation at 365 nm into the absorption band of $Cr(H_2)(CO)_5$ caused conversion back to $[Cr(CO)_5]$.[89] Similarly, irradiation of $CpMH(CO)_3$ (M = Mo, W) in H_2-doped argon matrices generates $CpMH(H_2)(CO)_2$ which is itself photosensitive, losing H_2 on 350 nm irradiation.[90] In these reactions the dihydrogen ligand behaves similarly to other 2-electron donor ligands in its photolability under

long wavelength irradiation. Metal dihydrogen complexes may also be generated by metal vapor methods in conjunction with matrix isolation. For example, $Fe(H)_2(H_2)_3$ has been formed by cocondensation of iron atoms with pure hydrogen at 4.5 K and proved to be photolabile.[91] The photochemical loss of H_2 from two $Rh(H_2)(PCP)$ complexes at room temperature has been used to monitor transient spectra and kinetics of [Rh(PCP)] intermediates (Scheme 8). Thus the photodissociation of the (η^2-H_2) ligand can prove useful even though $Rh(H_2)(PCP)$ equilibrates with other ligands very readily.[92] An example of photocatalysis,[93] probably involving photolysis of dihydrogen complexes, is summarized in section 2.6.

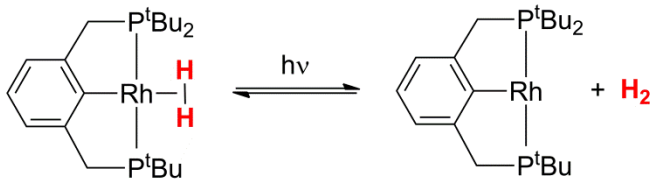

Scheme 8. Photochemical loss of H_2 from the dihydrogen complex[92] $Rh(H_2)(PCP)$

2.5 Bridging metal hydrides

The photochemistry of dinuclear and polynuclear complexes offers approaches to photochemical generation of hydrogen with visible light rather than UV radiation. Recent work has also highlighted the importance of bridging hydrides in bioinorganic chemistry. This section illustrates key principles for bridging hydrides. The first example to be studied was $[Pt_2(H)_2(\mu\text{-}H)(dppm)_2]^+$ which contains two terminal and one bridging hydride supported by two bridging diphosphine ligands.[94] Irradiation in CH_3CN leads to conversion to $Pt_2H(dppm)_2(CH_3CN)$ with a single terminal hydride with a quantum yield of 0.62 at 366 nm. This reaction has a far higher quantum yield than for irradiation of $[Pt_2(H)_2Cl(dppm)_2]^+$ which has one hydride on each platinum. It can be considered as a model for the photochemical H_2 release from dinuclear rhodium complexes containing parallel terminal rhodium-hydride bonds that may be converted to HRh(μ-H)Rh isomers before losing H_2.[95] Irradiation of these $d^8\cdots d^8$ rhodium dimers into their σ-σ^* transition generates predominantly H_2 even in the presence of THF as a trap. Crossover experiments with mixtures of $[Rh_2(H)_2]$ and $[Rh_2(D)_2]$ generate mainly H_2 and D_2 (Scheme 9).

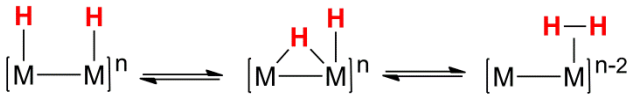

Scheme 9. General scheme for H_2 elimination from a dinuclear metal species[95]

Much more recently, the photochemistry of $(Cp^*Ru)_2(\mu\text{-}H)_4$ has been examined. This complex absorbs at 371 nm (ε = 2200 dm^3 mol^{-1} cm^{-1}) and is photochemically inert in THF, but reacts on irradiation at 365 nm with methyl ketones to form $(Cp^*Ru)_2(\mu\text{-}H)_2(\mu\text{-}\eta^4\text{-}CH_2C(O)CHR)$ + $2H_2$ where the bridging ligand is described as oxatrimethylenemethane.[12] The authors propose that the reaction proceeds *via* an exciplex, though no further evidence is provided. Photoreaction of CO_2-saturated THF yielded the trihydrido formato complex $(Cp^*Ru)_2(\mu\text{-}H)_3(\mu\text{-}\kappa^2\text{-}OCHO)$ (Scheme 10). However, the corresponding reaction of $(Cp''Ru)_2(\mu\text{-}H)_4$ where Cp″ = 1,2,4-C_5H_2t-Bu_3 yielded $(Cp''Ru)_2(\mu\text{-}O)(\mu\text{–}CO)$ with bridging oxo and carbonyl ligands.[11] An interesting feature of these reactions with CO_2 is that there is no H_2 loss, but reaction at the hydride ligands.

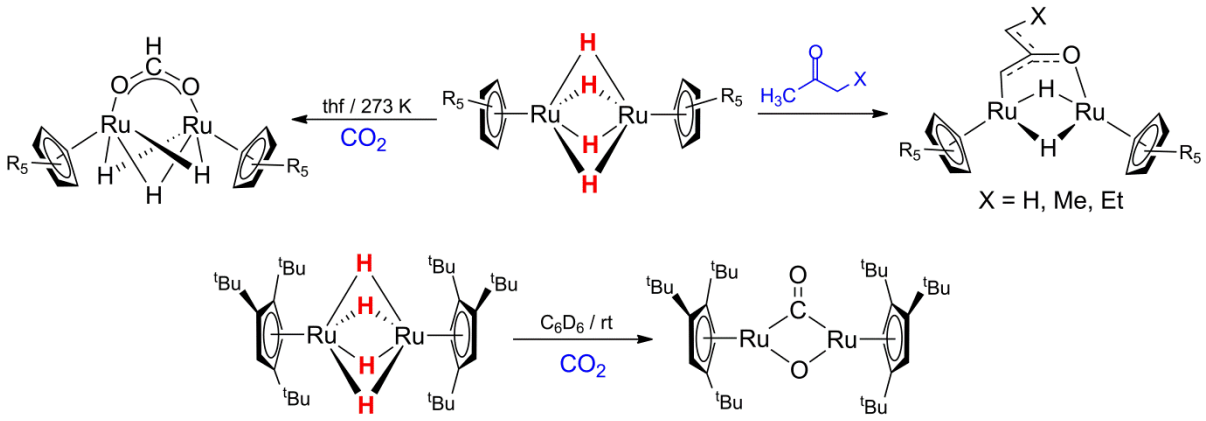

Scheme 10. Photoreactivity[11-12] of $(Cp^*Ru)_2(\mu\text{-}H)_4$

UV irradiation of *trans*-$[Fe_2Cp_2(\mu\text{-}H)(\mu\text{-}PPh_2)(CO)_2]$ showed three photochemical pathways according to the conditions: photoisomerization to the *cis*-form, introduction of a new phosphine ligand by reaction with PR_2H with concomitant P-H cleavage, loss of H_2, and CO substitution. Since isomerization is not suppressed by added CO or PR_2H, the authors postulate isomerization by reversible opening of the hydride bridge. The other pathways of the *trans*-

complex are initiated by CO loss; the photochemistry of the *cis*-complex is dominated by CO loss.[96-97] Related *trans-cis* photoisomerization has been reported for *trans*-[$Fe_2Cp_2(\mu$-H)(μ-PR^*_2)$(CO)_2$] where PR^*_2 is an optically active phosphine.[98-99] More recently, the high-spin Fe(II) complex [(β-diketiminate)Fe(μ-H)]$_2$ was found to reductively eliminate H_2 photochemically in the presence of N_2 to yield [(β-diketiminate)FeNNFe(β-diketiminate)].[100]

Nitrogenase generates dihydrogen at the same time as ammonia. Recently, an intermediate has been generated from a mutant form in which a reduced form of the co-factor is stabilized, that is thought to store two molecules of hydrogen as two bridging hydrides and two protonated bridging sulfur atoms in a 4Fe arrangement (Figure 3). Low temperature (< 20 K) irradiation of this form within an EPR cavity results in reversible elimination of H_2.[8] The photochemical reductive elimination exhibits a large kinetic isotope effect (KIE ~ 10) that is temperature independent, indicating that there is a barrier in this step that is overcome by a tunneling mechanism. The reverse oxidative addition step is induced by heating and shows a KIE of ~5.4 at 193 K. There are no examples of photochemical reductive elimination of H_2 from small molecules that are closely comparable.

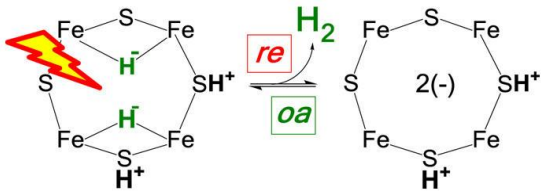

Figure 3. Photochemical reductive elimination of H_2 from co-factor of nitrogenase. [8]

2.6 Photocatalysis

Photocatalysis can encompass many types of catalysis, but here we are principally concerned with the situation in which the light supplies some energy to reactions that would otherwise have positive free energy. There are many photocatalytic processes that involve metal hydride complexes somewhere in the catalytic cycle. However, we will concentrate on examples in which the role of the hydrides is well defined, and preferably that involves direct excitation of a metal hydride complex. A common method of carrying out photocatalysis is to have two components that act as photosensitizer and catalyst, respectively. They may be tied together as a covalently bonded dyad or separate molecules or ions in solution. Several of the examples below involve complexes that act both as light absorber and catalyst.

One of the major goals is, of course, to produce H_2 from water, a process that is very successfully catalyzed by hydrogenases. The mimic of [FeFe}-hydrogenase $[Fe_2(CO)_4(dppv)(\mu\text{-}pdt)(\mu\text{-}H)]BF_4$ (dppv = cis-1,2-$C_2H_2(PPh_2)_2$, pdt = propane dithiolate) generates H_2 on irradiation of CH_2Cl_2 solutions containing $[H(OEt_2)]BF_4$ or HOTf. Addition of octamethylferrocene inhibits catalyst decomposition, but the turnover numbers are under ten.[18]

In an effort to develop a light driven energy conversion catalyst, Heyduk *et al*. reported a two-electron mixed valence Rh compound as photocatalyst for H_2 evolution from the reduction of hydrohalic acid. [101] A few years later the same group showed that an analogous two-electron mixed-valent complex $Rh_2^{0,II}(tfepma)_2(CNAd)_2Cl_2$ (tfepma = $CH_3N[P(OCH_2CF_3)_2]_2$ and CNAd = 1-adamantylisonitrile) could photolytically split HCl with H_2 production continuing for 177 h in THF solution. A rhodium monohydride-chloride dimer formed during the catalytic cycle was the photoactive species that generated H_2 and a dichloride Rh dimer (Scheme 11).[102]

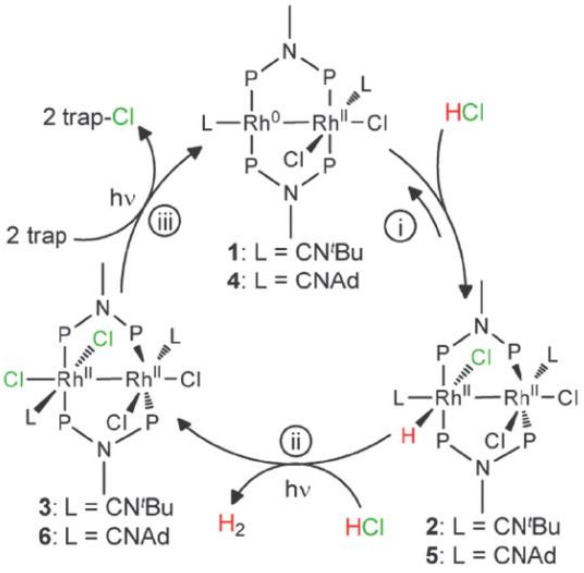

Scheme 11. Photocycle for HCl splitting[102]

An alternative strategy is to use photoelectrocatalysis, such that light is absorbed by the electrode. Following studies of its electrochemistry, $[Mo(H)_2(\kappa^2\text{-}O_2CMe)(dppe)]^+$, was investigated in CH_3CN with added acetic acid with a p-type silicon photoelectrode. Photocatalysis is sustained for more than 65 h giving turnover numbers greater than 120. The maximum efficiency of conversion of photon energy to chemical energy is 2.8%. The proposed mechanism is shown in Figure 4.[80]

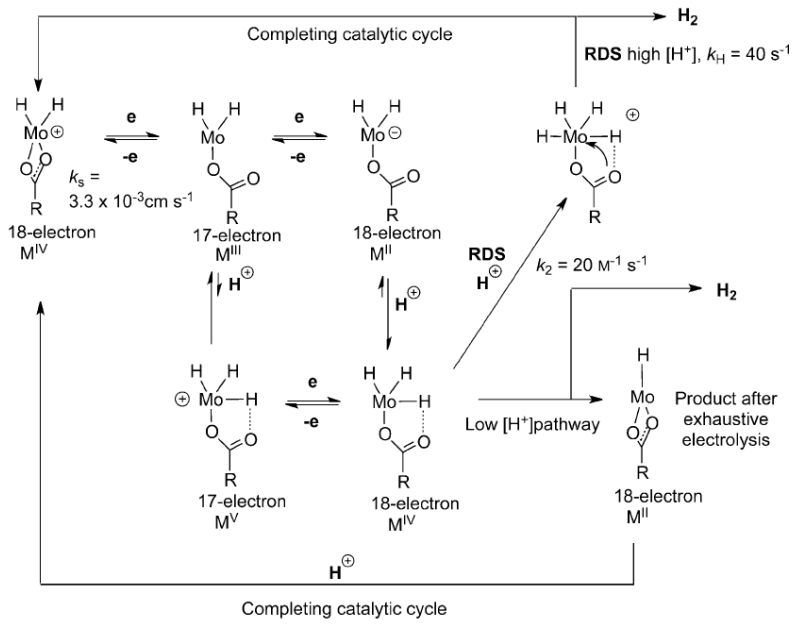

Figure 4. Proposed mechanism of photoelectrocatalysis of H_2 production by $[Mo(H)(O_2CMe)(dppe)]^+$. The dppe ligands are omitted.[80]

The photocatalytic reaction of aqueous formate to CO_2 + H_2 is catalyzed by [Cp*Ir(bpy)Cl]Cl or its 4,4'-bpy$(OMe)_2$ analogue with irradiation by blue light. The catalyst is active over the range pH 5-10 and there is a kinetic isotope effect of 2.6; there is no pressure inhibition up to H_2 pressures of 4 atm. The light absorber is proposed to be the hydride $[Cp^*IrH(bpy)]^+$ and the cycle involves conversion of the hydride to the hydroxide complex by excited state hydride transfer (see Section 2.1.4), thereby releasing H_2. The hydroxide complex is converted to the formate complex that loses CO_2 regenerating the hydride (Figure 5). The optimum results were obtained in a pressure vessel (3 M aqueous sodium formate solution at pH 8, 0.37 mM methoxy catalyst, 296 K, λ_{ex} 443 nm, initial TOF > 50 h^{-1}, TON > 500 over 30 h) giving 5 atm pressure.[103]

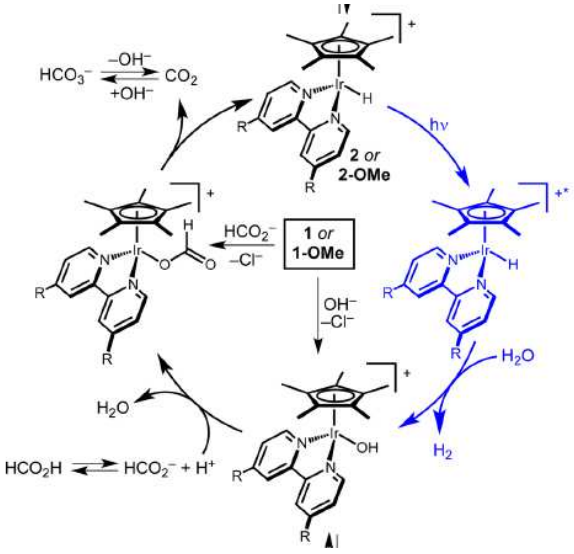

Figure 5 Proposed catalytic cycle for photochemical dehydrogenation of formic acid by $[Cp^*IrH(bpy)]^+$ [103]

Photoelectrocatalytic conversion of water to H_2 was also investigated with [Cp*Ir(bpy)Cl]Cl as catalyst. The reaction was investigated by examining the electrochemistry and the photochemistry in turn. Controlled potential electrolysis generates the hydride $[Cp^*Ir(bpy)H]^+$ (Figure 6); the resulting hydride was photolyzed generating H_2 and the initial iridium chloride cation. Full photoelectrocatalysis involves the iridium hydride acting as light absorber and catalyst, not the electrode. The performance was improved with 4.4.'-bpy$(CO_2H)_2$ giving the following results with 460 nm radiation: rate constant 0.1 s^{-1} at 100 mV overpotential buffered at pH 7. The external quantum efficiency is *ca.* 10%. Again, the catalysis depends on excited state hydricity with a similar photocycle to that for formate reaction.[19]

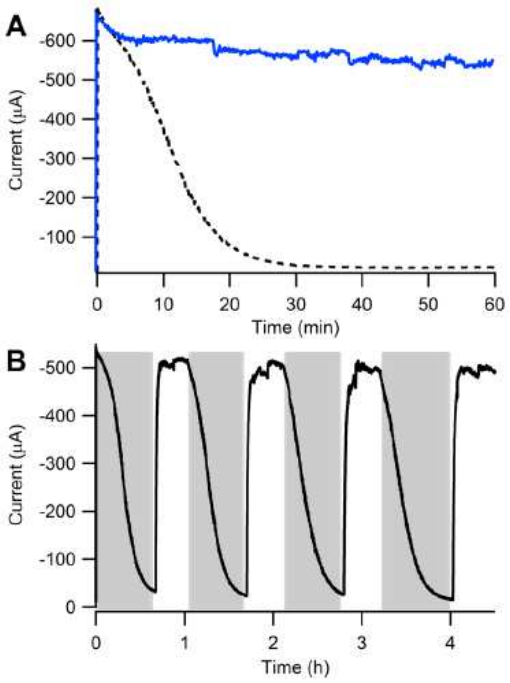

Figure 6. (A) Controlled potential electrolysis at -1 V vs NHE of [Cp*Ir(bpy)Cl]Cl in 0.1 M phosphate buffer at pH 7 in the dark (dashed black) and under 460 nm irradiation (solid blue). (B) Same but at -0.9 V with light off (gray) and light on (white). [19]

There are also a number of catalytic reactions that depend on metal hydrides as absorbers to generate coordinatively unsaturated species for hydrogenation/dehydrogenation, hydrosilation, *etc*. Two recent examples are illustrated here, one for arene borylation and the other for conversion of silanes to silanols. In keeping with the photosensitivity of *cis*-$[Fe(H)_2(dmpe)_2]$, it may also be used as a photocatalyst. The borylation of arenes by HBpin proceeds with 5 mol% catalyst and 350-nm radiation, though the performance of *cis*-$[Fe(Me)_2(dmpe)_2]$ is better. Stoichiometrically, both generate *cis* and *trans* isomers of $FeH(dmpe)_2(Bpin)$. The boryl hydride complex is also photocatalytically active. It seems likely that more than one species acts as light absorber in the catalytic reaction.[104] The dppe complex *cis*-$[Fe(H)_2(dppe)_2]$ was inactive for borylation but showed activity as a precatalyst for the photolytic hydrosilation of aldehydes and ketones.[105]

The rhodium porphyrin complex Rh^{I}(tetrakis(4-methoxyphenyl)porphyrin) reacts photocatalytically in the presence of silanes $SiHR_3$ in THF/H_2O solutions to generate silanols. Since the rhodium iodide complex reacts immediately with silanes to form rhodium hydrides, it is postulated that the photoactive species is [RhH(porphyrin)] which undergoes Rh-H homolysis.

The full photocatalytic mechanism is shown in Scheme 12.[106]

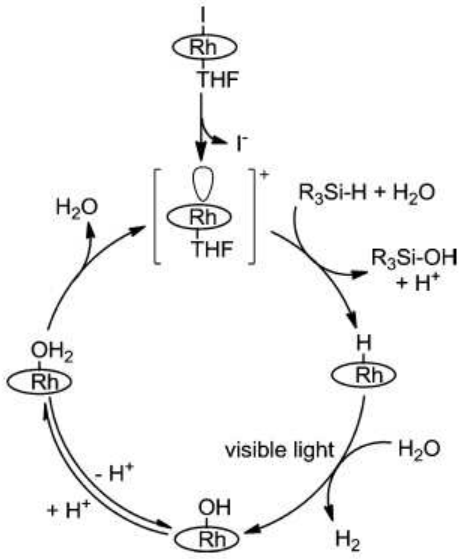

Scheme 12. Proposed mechanism of catalytic hydrolysis of silanes by rhodium porphyrin[106]

3. PHOTOCHEMICAL METHODS FOR REACTIVE INTERMEDIATES AND MECHANISM

Photochemistry is exceptionally well suited to the study of highly reactive molecules and can reveal their electronic and molecular structure as well as their reactivity in far more detail than conventional thermal methods. When a metal dihydride complex is irradiated in the presence of dissolved hydrogen, a reversible degenerate reaction is set up in which the hydrides are destroyed photochemically and reformed thermally. Time-resolved spectroscopy allows detection of reaction intermediates and measurement of the rates of their reaction with H_2. Alternatively, the rate of oxidative addition of other substrates of type E-H may be determined (Scheme 13). The application of such methods to metal hydride photochemistry is of particular relevance to catalytic reactions that involve hydrogenation or hydroformylation and also to reactions involving the oxidative addition of element-hydrogen bonds. The principal detection methods for time-resolved spectroscopy of relevance to metal hydrides are UV-vis and IR spectroscopy, but time-resolved NMR spectroscopy is beginning to make a mark in conjunction with *para*-hydrogen enhancement. Examples of the use of time-resolved spectroscopy on the photochemistry of $Ru(H)_2(dmpe)_2$ have already been described (Section 2.2.1).

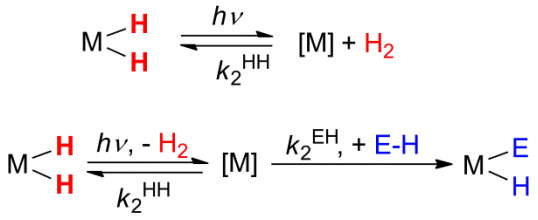

Scheme 13. General scheme for the photoinduced reductive elimination of H_2 and kinetics of H_2 or EH oxidative addition

Matrix isolation methods[24-25,107-110] have seen particular success in two different approaches, the photochemistry of stable metal hydride complexes embedded in low temperature matrices and the formation and photochemical reactivity of very small molecules by co-condensation of metal atoms with hydrogen sources together with noble gases. For some reaction intermediates such as $[Ru(dmpe)_2]$, matrix isolation and time-resolved spectroscopy have proved to be complementary methods (section 2.2.1). For others, matrix photochemistry of metal hydrides is unique; it remains the only method of direct study. Examples include rhenocene[46,48,111] generated by photolysis of Cp_2ReH and $(H)_2Mo{=}(CH_2)$ generated by photolysis of the metal vapor product $HMo(CH_3)$ (see section 4.3).[112]

Photochemistry of stable hydride complexes in matrices has yielded extensive spectroscopic information about reaction intermediates such as $[Cp_2W]$ and $[Ru(dmpe)_2]$ as well as information about the photochemical processes (section 2.2.1).[23-24] The condition for isolation of stable molecules such as $Cp_2W(H)_2$ in matrices is that they may be sublimed or vaporized with minimal decomposition so that they may be co-condensed with noble gases or more reactive matrices such as N_2, CH_4 or CO. They may then be examined by UV-vis, IR, laser induced fluorescence (LIF), resonance Raman, EPR and magnetic circular dichroism (MCD) with only slight perturbation or spectroscopic interference from the matrix material. The matrix is irradiated after deposition with conventional sources or with a low power lasers. Often, the coordinatively unsaturated species generated on initial photolysis exhibits a long wavelength absorption band and will recombine on selective irradiation into this band. Although pure H_2 cannot be condensed under high vacuum at the typical operating temperatures of 8-20 K, substantial proportions of H_2 can be incorporated into an argon matrix. If the temperature is lowered to 4 K, however, pure H_2 can be condensed successfully.[113] Several studies of metal hydride complexes have also been reported using hydrocarbon matrices at 77 K in conjunction with IR spectroscopy for compounds that cannot be sublimed but are soluble in hydrocarbons.[114]

Cocondensation of metal vapor with mixtures of hydrogen sources and noble gases has proved to be an effective method for studying binary metal hydride complexes and small molecules with M-H bonds, including their photochemistry. The metal vapor may be generated by effusion from an oven, or nowadays more often by laser ablation. The hydrogen source may be H_2 itself or alternatives such as methane or hydrogen chloride which give access to species such as $HM(CH_3)$ or HM(Cl), respectively.[112,115] Often, photolysis of the matrix-isolated metal atoms is required to induce reaction in the matrix. Early work has been reviewed previously.[107] The methods are illustrated by the reactions of molybdenum atoms with methane at 8 K (2% in Ar); the products are identified by IR spectroscopy with extensive isotope labeling, assisted by DFT calculations.[112] Long-wavelength photolysis converts the initially generated $HMo(CH_3)$ to $(H)_2Mo{=}(CH_2)$ which is converted in turn to $(H)_3Mo{\equiv}(CH)$; short-wavelength photolysis reverses the process. In many of the papers reviewed here, photochemistry is used simply as a means of grouping bands and assisting in assignment. It is important to note that there is some radiation generated in the laser ablation process, so the initial spectra may have resulted in part from photochemical reactions.

3.1 Spectroscopic methods for time-resolved spectroscopy and matrix isolation

In this section, we illustrate the application of different spectroscopic methods in conjunction with time-resolved spectroscopy and matrix isolation, placing emphasis on opportunities with new and improved techniques, such as time-resolved IR spectroscopy and NMR with *para*-hydrogen enhancement.

3.1.1 IR spectroscopy. Metal hydride stretching vibrations range from *ca.* 2200 cm^{-1} for some terminal platinum hydride complexes[116] to *ca.* 1400 cm^{-1} for some terminal titanium hydrides with much lower frequencies for bridging metal hydrides. Metal hydride stretching frequencies exhibit a very strong dependence on the metal as well as on the ligand environment. The frequencies typically increase from first to second to third row of the transition metals, as illustrated by the M-H stretching frequencies of $HM(CH_3)$: M = V 1534 cm^{-1}, M = Nb 1611 cm^{-1}, M = Ta 1726 cm^{-1}.[117] The increases in M-H stretching frequencies of related $Cp_2M(H)_n$ complexes from left to right as well as down a transition metal group have been noted.[118] Information about ligand effects on the IR spectra of rhodium hydrides has also been collected.[119] There is usually very little difference between symmetric and antisymmetric stretching modes of *cis*-$M(H)_2$ groups. There would be opportunities to parameterize M-H stretching frequencies, especially with improved DFT methods, since little has been done since

1986.[118] Infrared spectra showing M-H stretching bands of metal hydrides have proved important in following the evolution of reactions in low-temperature matrices, but they are often complicated by the presence of multiple conformers or matrix sites.[53,57,120-121]

Matrix IR spectra can also reveal many other aspects of the photoreactions since they can be recorded across the full frequency range, for example showing the vibrations of $(H)_2Mo=(CH_2)$ or the characteristics of a parallel ring metallocene.[112,120] Of particular importance is the sensitivity of CO stretching vibrations of metal carbonyls to change in oxidation state. For example, the ν(CO) band of $CpIr(H)_2(CO)$ appears at 2021.6 cm^{-1} in argon matrices. On photolysis, $CpIr(H)_2(CO)$ undergoes reductive elimination generating [CpIr(CO)] with a ν(CO) band at 1954.4 cm^{-1}, a shift of 67 cm^{-1} resulting from the change from Ir^{III} to Ir^{I}.[122] This complex does not undergo photochemical CO loss at all. In contrast to the behavior in argon matrices, photolysis in methane matrices revealed a product band at 2006.6, shifted only 11 cm^{-1} from the position of $CpIr(H)_2(CO)$ in the same matrix that is readily assigned as $CpIrH(CH_3)(CO)$.

Time-resolved IR spectroscopy has played a part in understanding the photochemistry of metal hydrides in solution, but M-H stretching modes have not been detected because of their low absorption coefficients. Instead, time-resolved IR studies have focused on CO-stretching modes of metal carbonyl hydrides. Ultrafast IR spectroscopy of $Ru(H)_2(PPh_3)_3(CO)$ established that reductive elimination of H_2 occurs within 6 ps of the initial laser pulse, by observing the 98 cm^{-1} shift in the ν(CO) band from 1941 cm^{-1} for the precursor to 1843 cm^{-1} in the $[Ru(PPh_3)_3(CO)]$ transient.[123] The recombination of $[Ru(PPh_3)_3(CO)]$ with H_2 could be followed by time-resolved IR spectroscopy and time-resolved absorption. There have been major improvements in ultrafast IR spectroscopy in recent years as is illustrated by the study of the hydrogenase analogue containing a bridging hydride, $[Fe_2(\mu\text{-}H)(CO)_4(dppv)(\mu\text{-}pdt)]^+$, **1** (dppv = *cis*-1,2-$C_2H_2(PPh_2)_2$, pdt = propane dithiolate). Excitation at 572 nm resulted in formation of a product with three ν(CO) bands that was formed within < 1 ps and exhibited a lifetime of *ca.* 140 ps (Figure 7). This species was distinguished from hot bands of the precursor with the aid of IR pump - IR probe experiments. The product was assigned as a CO-loss species with the aid of DFT calculations.[124] This result was at odds with the observation of photoinduced H_2 loss observed previously.[18] With the improvements in sensitivity of time-resolved IR spectroscopy, it may soon be possible to follow ν(M-H) bands in solution in favorable cases.

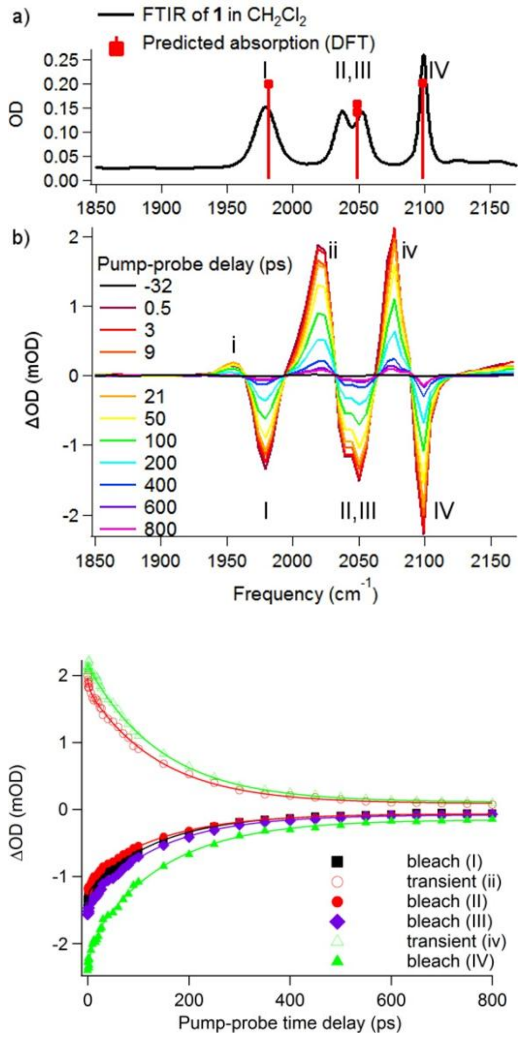

Figure 7. Above a) FTIR spectrum solution of **1** in CH_2Cl_2 (10 mM). Red squares and droplines represent the DFT-calculated absorption frequencies of **1**. (b) TRIR (λ_{ex} 572 nm) difference spectra of **1** at a range of pump–probe delay times (ps). Below: Time dependence of the amplitudes of peaks in TRIR spectra of **1** (λ_{ex} 572 nm). Solid lines display fits of an exponential function.[124]

3.1.2 UV-vis absorption and emission spectroscopy and allied methods. In this section, we are concerned with the use of UV-vis absorption spectroscopy and related techniques for the characterization of reaction intermediates derived from metal hydride complexes. Matrix isolation has the benefit of providing UV-vis spectra, measured with conventional high-resolution spectrometers and access to full IR spectra measured under the same conditions to aid assignment. The method also benefits from access to variable wavelength photochemistry applied to the reaction intermediates. On the other hand, it is not possible to determine the kinetics of reaction of the intermediates and moreover, matrix isolation

does not stabilize excited states. In time-resolved absorption studies, both the spectra and kinetics of the reaction intermediates and excited states are accessible. The kinetics are determined continuously (Figure 9) and the spectra are derived point-by-point or vice versa. In practice, it has only proved possible to detect electronic excited states of metal hydrides in exceptional cases such as $Mo(H)_4(dppe)_2$ (Section 2.3.2) and $Cp^*IrH(bpy)^+$ (Section 2.1.4) because most excited states undergo dissociation within the instrumental response time.

The major absorption features of most metal mononuclear metal hydride complexes lie in the UV-vis part of the spectrum. In contrast, many coordinatively unsaturated intermediates exhibit rich visible absorption bands. This point is illustrated by the spectra of $Os(H)_2(dmpe)_2$ which is colorless and exhibits broad, featureless UV spectra. On the other hand, the matrix photoproduct $[Os(dmpe)_2]$ shows several absorption bands in the visible and one band in the near-IR at 798 nm. The transient absorption spectrum of $[Os(dmpe)_2]$ measured in solution at 294 K 100 ns after the laser flash is remarkably similar to the methane matrix spectra measured at 12 K (Figure 8) demonstrating the complementarity of the methods. The visible absorption peaks can be used to measure reaction kinetics as illustrated in Figure 10. In the absence of matrix spectra, evidence for the nature of the reaction intermediate may be obtained by using multiple precursors as illustrated by the transient photochemistry of $Rh(H_2)(PCP)$ and related complexes (Scheme 8).[92] Ultrafast transient absorption spectroscopy has been used very effectively to monitor the formation of the triplet excited state of $[Cp^*IrH(bpy)]^+$ and its subsequent deprotonation.[10]

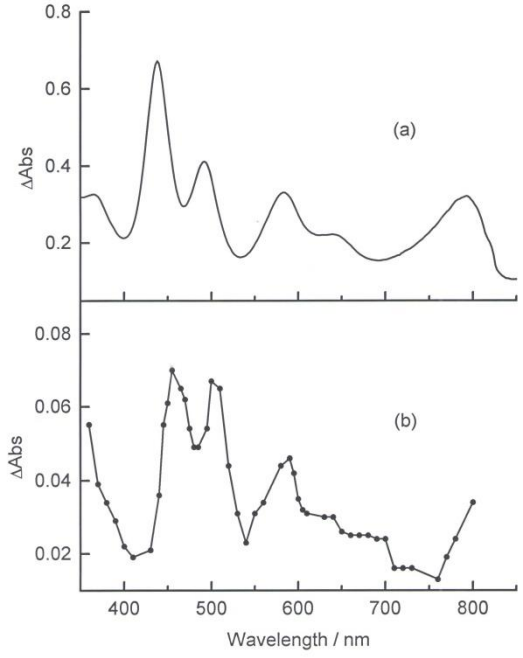

Figure 8. Visible spectra of $[Os(dmpe)_2]$[56] (a) in CH_4 matrix at 12 K; b) in cyclohexane solution at 294 K by transient absorption spectroscopy measured 100 ns after laser flash (λ_{ex} 266 nm).

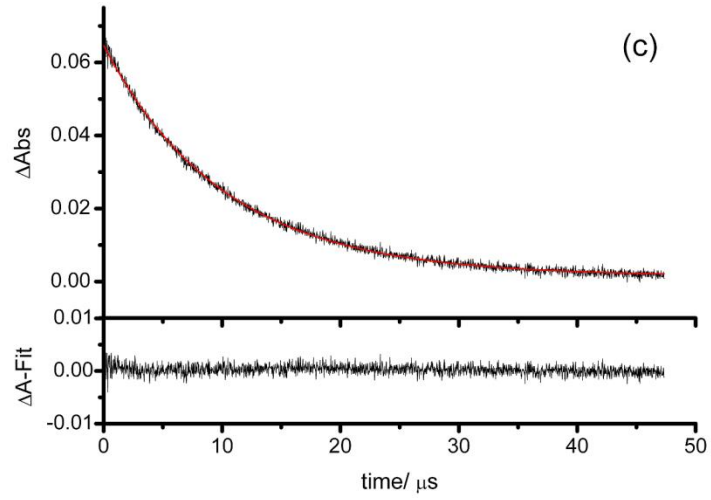

Figure 9. Transient decay after photolysis of $Ru(H)_2(BPE)_2$ recorded at 500 nm.[125]

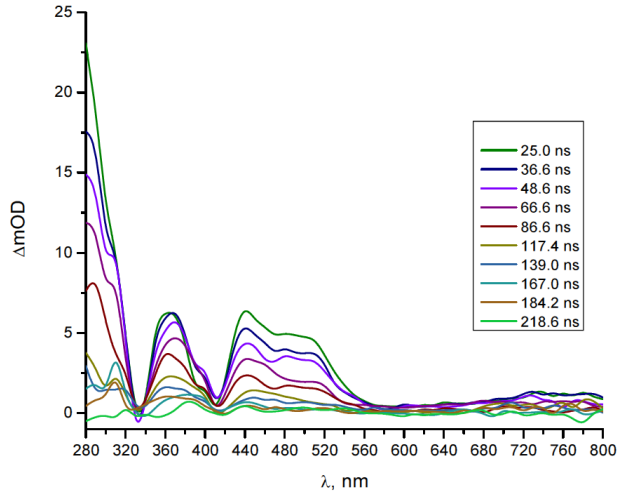

Figure 10. UV-vis transient absorption spectra obtained at specified time delays after 355 nm laser flash photolysis of $Rh(H_2)(PCP)$ in n-heptane under H_2 at 298 K (see also Scheme 8).[92]

Matrix isolation also allows the measurement of emission and magnetic circular dichroism. The low temperature combined with the low dielectric host can lead to exceptionally sharp absorption and emission spectra for matrix-isolated molecules, as exemplified by

rhenocene. The photolysis of Cp_2ReH in argon or nitrogen matrices leads to Re-H homolysis and formation of [Cp_2Re] which exhibits very prominent emission spectrum due to ligand-to-metal-charge-transfer with emission lifetime of *ca.* 72 ± 1 ns in solid nitrogen (Figure 11). Both the fluorescence spectrum and the corresponding excitation spectrum are fully vibrationally resolved with progressions in the symmetric Cp-Re-Cp stretching mode.[48] The magnetic properties of the same molecules were determined by MCD in nitrogen matrices, leading to a value of $g_{||}$ of 5.3 ± 0.4, consistent with a $^2E_1$ ground state.[46]

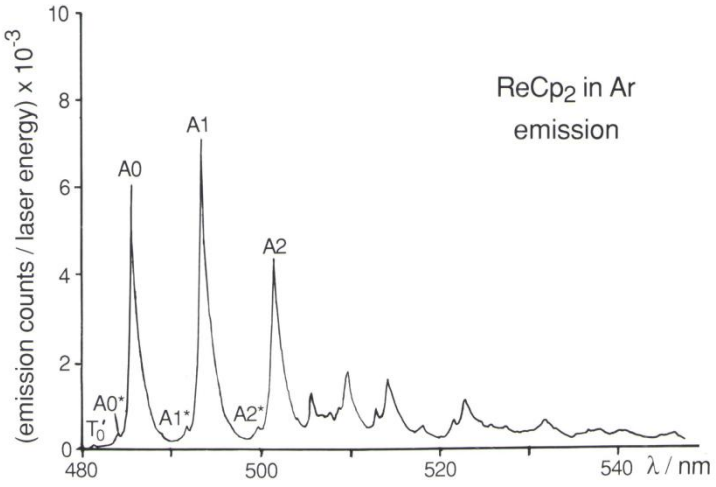

Figure 11. Laser-induced fluorescence spectrum of [Cp_2Re] obtained following UV photolysis of Cp_2ReH in an argon matrix at 12 K excited with λ_{exc} = 470.0 nm. A0, A1, A2 refer to members of the vibrational progression in ν(Cp-Re-Cp).[48]

3.2 NMR spectroscopy and para-hydrogen enhancement

The photochemical hydrogen cycle (Scheme 13) lends itself to the use of ^{1}H NMR spectroscopy for the study of metal hydrides. Dissolved dihydrogen itself may be detected by NMR spectroscopy (δ 4.45 in C_6D_6) and readily distinguished from HD by the prominent coupling (J_{HD} = 42 Hz). Photochemical reactions may be followed effectively by use of *in situ* methods where the sample is irradiated within the probehead either by white light from an arc lamp or by monochromatic laser irradiation. Examples include the photoisomerization of $Ru(H_2)(CO)(NHC)(PPh_3)_2$ (Section 2.2.2)[72] or the generation of a photostationary state between $W(H)_4(dppe)_2$ and $W(H)_6(dppe)(\kappa^1\text{-dppe})$ by low temperature irradiation under H_2.[88] The photochemical kinetics of reaction of $Tp'Rh(H)_2(PMe_3)$ with HBpin and with $PhSiH_3$ were

determined by laser photolysis within the probe, demonstrating that the reaction is zero order with respect to substrate concentration.[126] Competition reactions with two substrates revealed the relative rate of reaction of the [Tp'Rh(PMe_3)] intermediate with different substrates.

The ^{1}H NMR spectra obtained through the photochemical hydrogen cycle can be enhanced by the use of *para*-hydrogen if certain conditions are met. *Para*-hydrogen is the antisymmetric nuclear spin isomer of H_2 (nuclear spin function $\alpha\beta - \beta\alpha$) which is a nuclear spin singlet and therefore NMR-silent. Nevertheless, if it undergoes oxidative addition to a metal complex in a concerted manner to generate a metal dihydride such that the two hydride nuclei are chemically or magnetically inequivalent, the spectrum may be strongly enhanced. The "hyperpolarized" NMR spectrum formed in this way typically shows an absorption-emission (or emission-absorption) profile as a consequence of the overpopulation of the nuclear spin states formed in the addition process. This *para*-hydrogen induced polarization (PHIP) effect may be optimized by use of a 45° *rf* pulse leading to signal enhancements of several thousand. The enhancement may also be transmitted through to organic hydrogenation products. It may last long enough to obtain COSY spectra and the polarization may be transmitted through to heteronuclei. This approach has been demonstrated in several examples including the photoisomerization of $Ru(H)_2(CO)(NHC)(PPh_3)_2$ (Figure 2). Here photolysis *in situ* under *para*-H_2 results in the immediate formation of two new isomers with enhanced hydride resonances, one with chemically inequivalent hydrides and the other with magnetically inequivalent hydride resonances.[72] In another striking example, *in situ* laser irradiation of $Ru(H)_2$(Duphos)$_2$ in the presence of *para*-H_2 results in strong enhancement of the hydride resonances of the magnetically inequivalent hydrides and also simplification of the spectrum resulting from the overpopulation of selected energy levels (Figure 12). Transfer of polarization to phosphorus enhances the signal from the ^{31}P nuclei *trans* to hydride.[125] This PHIP enhancement is characteristic of concerted oxidative addition of H_2. However, the absence of PHIP enhancement should not be taken as evidence of a non-concerted pathway since the enhancement may be prevented by rapid nuclear spin relaxation associated with an electronic triplet state intermediate found for iron complexes or a dihydrogen complex as intermediate. There are several examples of photodissociation of CO or N_2 under *para*-H_2 from metal carbonyls and metal dinitrogen complexes generating hydride complexes with enhanced NMR signals.[88,112,127] It is not yet clear whether these reactions also involve photochemical hydrogen-cycling through light absorption by the dihydride complexes.

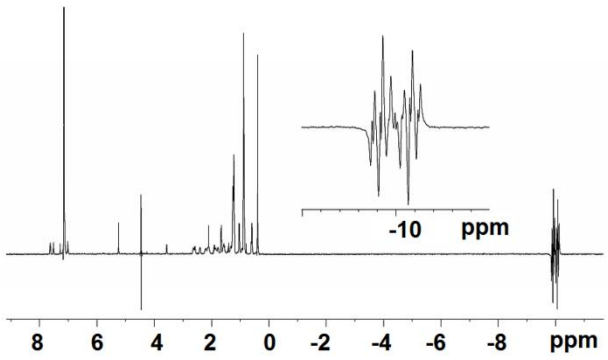

Figure 12. ^{1}H NMR spectrum of $Ru(H)_2(Duphos)_2$ in C_6D_6 obtained at 295 K during photolysis under *para*-H_2 atmosphere. The inset shows the hydride region with emission-absorption profile characteristic of PHIP.[125]

Most recently, the photochemistry of $Ru(H)_2(dppe)_2$ in solution under a *para*-H_2 atmosphere has been investigated in laser pump - NMR probe experiments (Figure 13, above) in which a single pulse of a laser (355 nm) initiates dissociation of H_2.[7] Photodissociation of H_2 and reaction with *para*-H_2 result in the formation of $Ru(H)_2(dppe)_2$ in selected nuclear spin states, greatly increasing the sensitivity of NMR detection. Indeed, $Ru(H)_2(dppe)_2$ is now detected with a single 90° *rf* pulse showing a very simplified spectrum in the hydride region with a greatly enhanced signal. Use of variable delays between the laser pulse and the *rf* pulse on the millisecond timescale reveals oscillations in the magnetization with an oscillation frequency of 83 ± 5 Hz corresponding to the difference between the P-H spin-spin coupling constants $|J_{PHtrans} - J_{PHcis}|$ (Figure 13, below). Such oscillations have not been observed previously because the phase coherence of the spin states is lost. This method demonstrates that it is possible to use a laser pulse to generate NMR coherence, rather than one of the usual *rf* pulse sequences. Moreover, it demonstrates the connection between the oscillations in the *x-y* coherence and the coupling constants in a molecule exhibiting magnetically equivalent hydrides.

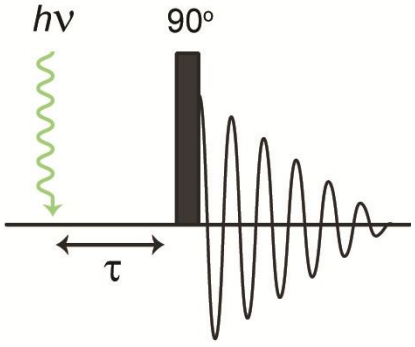

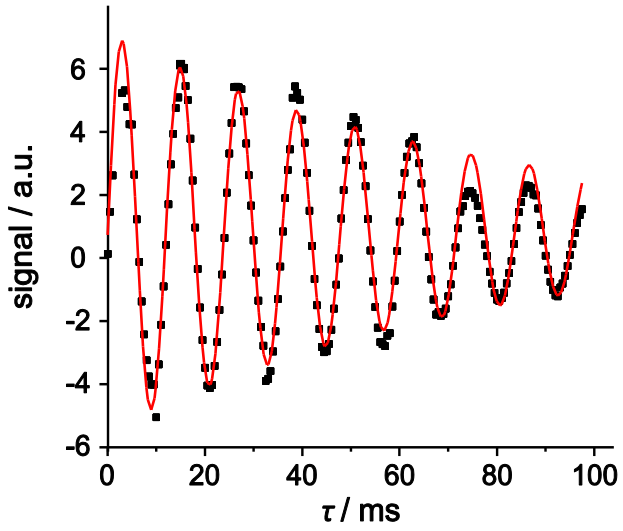

Figure 13. Above: NMR pump-probe sequence used in the PHIP study. Below: Integral of the hyperpolarized hydride signal of $Ru(H)_2(dppe)_2$ in a series of ^1H pump-probe NMR experiments acquired with increasing values of the pump-probe delay. Red line is a fit to a decaying sine-wave of 83.7 ± 0.1 Hz.[7]

4. Metal hydride photochemistry by transition metal group

In this section, we summarize a full range of metal hydride photochemistry, ordered primarily by transition metal group. The majority of the examples are to be found in Groups 6-9 and for these groups, we subdivide into mono-, di- and poly-hydrides. In most sections, we arrange the examples by element within the group.

4.1 Group 4 metals. Very few examples of photoactive complexes are reported for Ti, Zr and Hf hydride species. Titanium atoms cocondensed with H_2 in Ar matrices formed the hydride species $Ti(H)_2$ and $Ti(H)_4$ under visible light which decomposed under UV irradiation.[128] When the laser ablation method was employed with methane, $TiH(CH_3)$ was formed which isomerized to $(CH_2)=Ti(H)_2$ on near UV irradiation and was identified by isotopic labeling in conjunction with DFT calculations; the reaction was reversed with visible radiation.[129] Related experiments were reported on $(CH_2)=Zr(H)_2$ and $(CH_2)=Hf(H)_2$.[130-131] Matrix isolation IR spectroscopy identified $Ti(O)(CH_4)$ as the product of cocondensing TiO with methane. This rearranged to $TiH(CH_3)(O)$ photochemically; the latter was capable of isomerization under UV light to yield the $TiH(CH_2)(OH)$ carbene complex. When a CH_4 molecule added spontaneously to the $TiH(CH_2)(OH)$ complex, a dimethyl $TiH(CH_3)_2(OH)$ was formed that could also be obtained *via* UV photorearrangement of the $TiH(O)(CH_3)(CH_4)$ species.[132]

The first complexes of Group 4 to be investigated photochemically were $Cp^*_2Zr(H)_2$ and

$Cp^*_2ZrH(R)$ (R = alkyl or aryl); the dihydride underwent slow H_2 photoejection with near UV radiation and the fragment formed inserted into the C-H bond of benzene. Similar reactivity is shown by the alkyl hydride analogue but in this case alkane reductive elimination was observed upon irradiation. The quantum yield of $Cp^*_2ZrH(alkyl)$ was higher than that of $Cp^*_2Zr(H)_2$. Crossover and isotopic labeling demonstrated that the reductive elimination occurs by an intramolecular mechanism.[35] Photolysis of $Cp^*_2ZrH(aryl)$ was exploited in a preparative way to form the zirconocene dinitrogen complex $[\{(\eta^5\text{-}C_5Me_4H)_2Zr\}_2(\mu^2,\eta^2,\eta^2\text{-}N_2)]$ through arene reductive elimination.[133]

4.2 Group 5 metals. The photochemistry of group 5 is also very limited. Investigations of the metal atom chemistry have been carried out on the three metals in the presence of CH_4 in excess argon. All of the metals formed hydride complexes by CH_4 activation; the Nb and Ta products were found to convert to higher order products of the formula $(CH_3)_2M(H)_2$ upon further photolysis.[117]

Both $Cp_2Nb(H)_3$ and $Cp_2Ta(H)_3$ complexes were irradiated in aromatic solvents and found to yield the photogenerated intermediates $[Cp_2MH]$ (M = Nb, Ta) as a consequence of H_2 photoejection.[134] The monohydrides $Cp_2MH(CO)$ (M = Nb, Ta) were also investigated photochemically and were found to follow the same reactivity. The unsaturated species displayed reactivity towards CO, H_2 or PEt_3 to yield the substitution products and also proved able to insert into aromatic C-H bonds and catalyze H/D exchange. The PEt_3 substitution product was obtained just with the second row metals (Nb) but not with third row ones (Ta). Similar behavior was observed for group 6 (Section 4.3).[134] Low temperature matrices (Ar, N_2) studies followed; the identity of the transient Cp_2MH (M = Nb, Ta) formed from H_2 loss as a primary photoprocess was confirmed by IR and UV-vis spectroscopy for photoreactions starting both from the trihydride and the carbonyl-hydride species. In the latter case, a small amount of the $17e^-$ complex $[Cp_2M(CO)]$ was also observed suggesting that a minor amount of M-H homolysis took place.[135]

More recently the $(Me_2Si)_2(\eta^5\text{-}C_5H_4)_2Nb(H)_3$ was prepared and found to be very unstable both in solution and in solid state. However irradiation in benzene-d_6 converted it to the dimeric analogue $[(Me_2Si)_2\{\mu\text{-}(\eta^1\text{:}\eta^5\text{-}C_5H_3)\}(\eta^5\text{-}C_5H_4)NbH]_2$; H_2 photoelimination was proposed as primary photoprocess.[136]

4.3 Group 6 metals.

The hydrides of the group 6 metals provided several of the paradigms, especially for autocatalytic M-H homolysis, for H_2 elimination from $Cp_2M(H)_2$ (M= Mo, W), and for the *ansa*

effect.

4.3.1 Group 6 Monohydrides. The main photochemical process in the solution photochemistry of the anionic $[M_2(\mu\text{-}H)(CO)_{10}]^-$ was shown to be CO loss and the M–H–M bonding network was not involved in the photochemistry.[137] The $CrH(CO)_5^-$ anion was reported to produce the radical $Cr(CO)_5^-$ as a damage product of γ-radiation suggesting M–H bond homolysis.[138] The photochemistry of $CpCrH(CO)_3$ was studied in gas matrices at 12 K and CO photoejection postulated as the initial step of the photoreaction at wavelength between 290 and 370 nm; reversibility was observed on irradiation at λ greater than 370 nm. Photolysis in CO matrices led to the formation of the HCO radical indicating Cr-H cleavage under these conditions. Solution photochemistry at room temperature formed the dimer $[Cp_2Cr(CO)_2]_2$ along with CO and H_2 production.[139] The irradiation of $(\eta^5\text{-}C_5H_4PPh_2)CrH(CO)_3$ with broadband photolysis was employed as a preparative method to obtain the dimer $[(\mu,\eta^5\text{–}C_5H_4PPh_2)Cr(CO)_2]_2$ but competition between decarbonylation and dehydrogenation afforded a mixture of products.[140]

The molybdenum hydride $CpMoH(CO)_3$ showed the same behavior in matrix photochemistry as the Cr analogue but it proved less photoactive in solution photochemistry. The major product after prolonged photolysis was characterized as $[CpMo(CO)_3]_2$ derived from dehydrogenation, a minor product arisen from decarbonylation was also detected.[139,141] Further investigations on the same complex in C_2H_4-doped CH_4 matrices were performed to obtain insights into the hydroformylation mechanism. The $16e^-$-intermediate $CpMo(CO)_2H$ was observed together with the *cis* and *trans* isomers of the ethylene adduct; secondary photolysis of this species led to the olefin insertion to form $CpMo(CO)_2(C_2H_5)$.[141-142] Photolysis of $CpMoH(CO)_3$ and $(\eta^5\text{-}C_5R_5)MoH(CO)_3$ (R = H, Me) in H_2-containing matrices yielded *cis* and *trans* isomers of $(\eta^5\text{-}C_5R_5)MoH(H_2)(CO)_2$ identified by IR analysis. All the steps to the formation of these products showed reversibility on changing the photolysis wavelength.[90] When D_2 was employed, H/D exchange was observed for the Cp complex through an isotopic shift of the $CpMoD(CO)_2$ bands.[143] The photochemical synthesis of the Mo dimer $[(\mu,\eta^5\text{–}C_5H_4PPh_2)Mo(CO)_2]_2$ from $(\eta^5\text{-}C_5H_4PPh_2)MoH(CO)_3$ proceeded cleanly.[140] The photoreaction of $Cp^*MoH(\eta^6\text{-}C_5Me_4CH_2)$ is described together with that of $Cp^*_2Mo(H)_2$ below.

Experiments on the reactions of Mo atoms in matrices with CH_4 in excess Ar formed the hydride species $(CH_3)MoH$, $(CH_2)=Mo(H)_2$ and $(CH)=Mo(H)_3$. These compounds were found to reversibly interconvert by α-H transfer when irradiated with visible or UV light.[144] Photoreversibility was also determined for methylidene and methylidyne complexes of the type

(CH_2)=MoHX and (CH)=$Mo(H)_2X$ (X = F, Cl, Br, I) formed in similar experiments in the presence of methyl halides.[145] The reactivity of molybdenum atoms toward hydrogen is discussed under group 6 polyhydrides.

The tungsten monohydride $CpWH(CO)_3$ undergoes CO substitution by PBu_3 by UV irradiation (311 nm) without dimerization with quantum yields up to at least 30. A radical chain initiated by W-H bond homolysis was given as the primary mechanism; the $17e^-$ radical substitutes much faster than the $18e^-$ complex yielding $CpW(CO)_2(PBu_3)$ which abstracts H from $CpWH(CO)_3$. The quantum yield becomes much higher on addition of a few percent of $[CpW(CO)_3]_2$ reaching values of at least 1000.[146] Following this first publication, numerous investigations on the photochemical behaviour of this complex were undertaken in Ar, N_2 and CH_4 matrices containing $CpWH(CO)_3$ and $Cp^*WH(CO)_3$, the intermediate formed from CO loss was trapped. Addition of two-electron donor ligands (L) to the matrices led to $CpWH(CO)_2L$. As observed for Cr and Mo, CO matrix photochemistry led to the identification of the HCO radical indicating W–H bond cleavage.[141-142] Solution photochemistry of tungsten complexes proved to be the least efficient of the group; in addition to the products obtained for the Cr and Mo analogues, a dinuclear complex $[CpW(CO)_2(\mu\text{-}H)]_2$ was formed.[139,141] Solution photochemistry in the presence of ethylene also proved to be very similar, the olefin adduct *trans*-$[CpWH(CO)_2(C_2H_4)]$ was found photoactive and converted to the *cis* form before affording the insertion product $CpW(CO)_2(C_2H_5)$. Similar behavior was observed in ethylene-doped matrices.[141] Different results from the molybdenum analogues were obtained when H_2-matrices were investigated, both Cp and Cp* complexes afforded the dihydrogen adduct postulated to form *via* the CO loss intermediate $[CpWH(CO)_2]$, but unlike $CpWH(H_2)(CO)_2$ did not photoeject H_2 upon further photolysis but instead oxidatively added H_2 to yield $CpW(H)_3(CO)$.[90] $Cp_2WH(CH_3)$ also proved photoactive, ejecting CH_4 upon broadband photolysis in low temperature Ar-matrices to form $[Cp_2W]$.[120] The photoreaction of $Cp^*WH(\eta^6\text{-}C_5Me_4CH_2)$ is described together with that of $Cp^*_2W(H)_2$ below. The bimetallic species $Cp^*(CO)_2W(\mu\text{-}SiMe_2)(\mu\text{-}H)Re(CO)_2Cp^*$ was used to prepare silene-bridged W-Re complexes through photoinitiation.[147] More recently the dimeric compound $Cp_2W_2(H)(\mu\text{-}PCy_2)(CO)_2$ exhibited photoactivity in the presence of various metal carbonyl complexes (metal = Ru, Cr, Mo, W) to yield heterometallic compounds with either W_2M or W_2M_2 metal cores.[148]

Reactions of methyl halides with W atoms generated (CH_2)=WHX and $(CH)\equiv W(H)_2X$ that showed photoreversibility by the use of either visible or UV light as mentioned earlier for the Mo analogues.[145]

4.3.2 Group 6 Dihydrides and dihydrogen complexes. There are no examples of

chromium dihydride complexes investigated photochemically, but there are examples of photochemistry of dihydrogen adducts. The dihydrogen complex $Cr(H_2)(CO)_5$ was formed from UV photolysis of $Cr(CO)_6$ in H_2-doped Xe matrices. The reaction proved reversible under visible light irradiation (Section 2.4). Short wavelength photolysis led to CO loss and formation of $Cr(H_2)_2(CO)_4$.[89] Cocondensation of Cr metal and H_2 in Kr and Ar matrices produced the dihydrogen adduct $Cr(H_2)$. When H_2 was in excess, the latter was converted to the trihydride $Cr(H)_3$ with photolysis (520 - 580 nm).[149]

The scenario for molybdenum and tungsten is much richer than for chromium and there are close parallels in the behavior of the two elements. It is dominated by the photochemistry of $Cp_2M(H)_2$ (M = Mo, W) and their derivatives. The absorption spectrum of $Cp_2Mo(H)_2$ in solution shows bands at 270 and 310 nm. The gas phase electronic absorption spectrum of $Cp_2Mo(H)_2$ gave clearly defined Rydberg band confirming that the HOMO is non-bonding.[43] The photoactivity of $Cp_2Mo(H)_2$ led to H_2 elimination in the primary photochemical step (quantum yield at 366 nm 0.1 ± 0.02) to yield the transient unsaturated species $[Cp_2Mo]$ that was trapped in the presence of CO, C_2H_2, and PR_3 to form the respective adducts.[44,150] The photochemical reaction in C_6H_6 led to dimerization,[151] while irradiation in the presence of thiophene formed the C-H activated product Cp_2MoH(2-thienyl), selectively.[152] Reactions in the presence of hydridosilanes produced the silyl hydride complexes $Cp_2MoH(SiR_3)$ in very good yields through a reductive elimination/oxidative addition process; similar behavior was observed for the Cp* analogue.[49-50] Thus, molybdenocene inserts into Si-H bonds but the only C-H bonds that prove reactive are those of thiophene and its own precursor $Cp_2Mo(H)_2$. The reactions in the presence of activated alkenes formed a series of electron donor acceptor complexes with charge-transfer bands in the visible region. Irradiation into the charge-transfer band led to products; for example $Cp_2MoH(CHCNCH_2CN)$ was formed on photolysis at > 550 nm with fumaronitrile.[78] A more detailed explanation of this mechanism is given in section 2.2.4. The formation of clusters was achieved by photolysis of the $Cp_2Mo(H)_2$ in the presence of metal carbonyl dimers, a series of homo and heterometallic complexes were isolated and characterized.[51]

UV photolysis of $Cp_2Mo(H)_2$ in an argon matrix at 10 K led to the formation of the metallocene $[Cp_2Mo]$, characterized by IR and UV/vis spectroscopy. The photoelimination of H_2 was described as concerted due to lack of detection of the HCO radical in CO matrices.[120,153] Photogeneration of the metallocene in matrices was exploited to generate the $[Cp_2Mo]$ fragment for optical determination of magnetization behavior – like $[Cp_2W]$, it has a triplet ground state[46] Molybdenocene exhibits an LMCT absorption (origin at 420 nm) and laser induced fluorescence from the same electronic state.[111] Uv-vis transient photochemistry agreed with the matrix

investigations; a transient species was detected which decayed in *ca.* 10 μs by reaction with CO or the parent complex and was assigned to $[Cp_2Mo]$.[154]

Photolysis of $Cp^*_2Mo(H)_2$ in pentane caused loss of H_2 and intramolecular C-H bond activation to form $Cp^*MoH(\eta^6\text{-}C_5Me_4CH_2)$, which in turn lost H_2 again to form $Cp^*Mo\{\eta^7\text{-}C_5Me_3(CH_2)_2\}$. The first product can be considered as having a tetramethylfulvene ligand or a "tucked-in" tetramethylcyclopentadienyl group with one coordinated alkyl ligand, while the second may be described an allyldiene or as doubly tucked-in (Scheme 14).[155] The irradiation of Cp'_2MoH_2 ($Cp' = \eta^5\text{-}C_5H_4CH_3$) in H_2O–CH_3CN mixture afforded Cp'_2MoO and H_2 gas (2 eq.) quantitatively. The mechanism was proposed to start with H_2 reductive elimination to form the unsaturated fragment which could then undergo H_2O activation and release the second equivalent of H_2.[156] The *ansa*-bridged molybdenocene dihydride $(\eta^5\text{-}C_5H_4)CMe_2(\eta^5\text{-}C_5H_4)Mo(H)_2$ proved photoactive when irradiated in C_6H_6 solutions yielding the phenyl hydride product (Scheme 15). Thus, this *ansa*-bridged molybdenocene is capable of activating benzene C-H bonds whereas molybdenocene is not.[157] An investigation of the selectivity between the activation of C-H *versus* C-chalcogen bonds of furan, thiophene and selenophene bonds was reported exploiting the photochemical ability of *ansa*-$[Me_2Si(C_5Me_4)_2]Mo(H)_2$ to eliminate H_2 to form the *ansa*-metallocene. The reactivity towards the different substrates was found to be quite diverse: C-S insertion with thiophene, C-H insertion at both positions with furan but only at the 3-position with benzofuran, C-Se insertion with selenophene (Scheme 15)[158-159] These experiments illustrate the strong effects of the *ansa* geometry. The metallocene 1,1 disilamolybdenocenophane was synthesized by the photochemical reaction of the dihydride analogue and H_2 reductive elimination with intramolecular Si-Si oxidative addition (Scheme 15).[160-161]

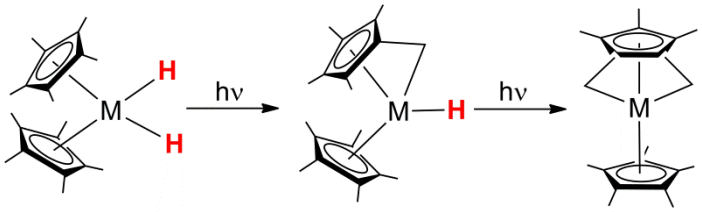

Scheme 14. Photolysis of $Cp^*_2M(H)_2$ (M = Mo, W, Re^+)

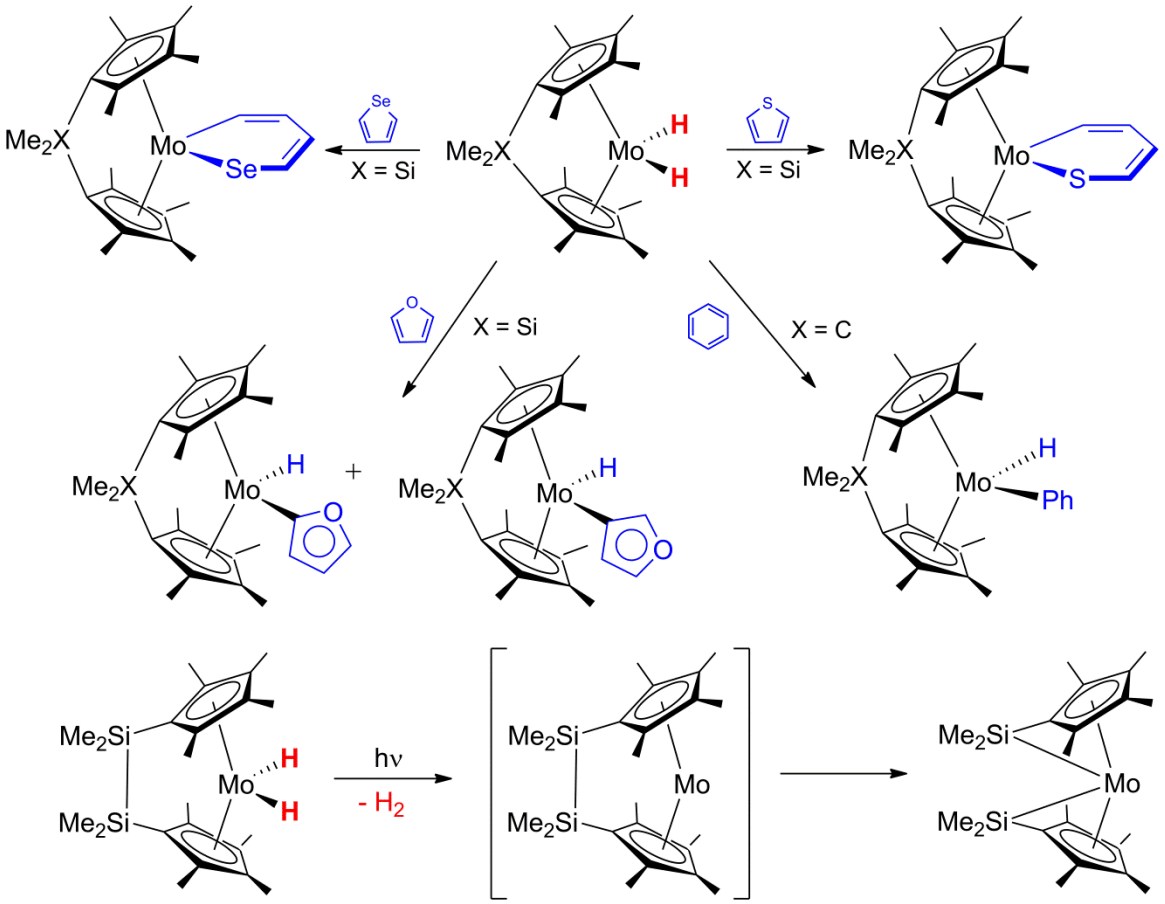

Scheme 15. Photoreactivity of *ansa*-molybdenocene complexes

Dinuclear-dihydride complexes have also been subject of photochemical investigations; [{CpMoH}$_2$(μ-η^5-C_5H_4-η^5-C_5H_4] converted into *cis*- and *trans*-[{Mo(η^5-C_5H_5)H}$_2$(μ-σ:η^5-C_5H_4)$_2$] and eventually yielded the [{Mo(η-C_5H_5)}$_2$(μ-σ:η^5-C_5H_4)$_2$]. A mechanism was proposed for the generation of this latter where the first photochemical step induced a ring shift from η^5 to η^3, followed by hydride migration reminiscent of Scheme 3 allowing photoinduced H_2 elimination and ring shift back to η^5 coordination to afford the final product.[162] The cyclopentadienyl bridged complex [MoH(CO)$_3$]$_2$(η^5-η^5-$C_5H_4CH_2C_5H_4$) was stable in solution if kept in the dark but reported to lose hydrogen if exposed to ambient light.[163] More recently, the quadruply bonded complex [$Mo_2(H)_2${HC(N-2,6-^{i}Pr$_2$C$_6$H$_3$)$_2$}$_2$(THF)$_2$] was also found photoactive in arene solution, yielding products with η^2-η^2 bridging arenes. Free H_2 was detected confirming H_2 photoelimination as the primary photochemical step.[164]

The photochemistry of $Cp_2W(H)_2$ is summarized in section 2.2.1 and Scheme 4 and

therefore a brief résumé will be given here. Photolysis of $Cp_2W(H)_2$ at 366 nm forms the transient tungstenocene by H_2 elimination with much lower quantum yield than the molybdenum analogue. Tungstenocene has never been observed in solution, only in matrices. It is capable of activating C-H bonds of arenes,[2,165-166] and Me_4Si[42,166] but not alkanes. The same fragment was able to insert into MeOH to yield $Cp_2WH(OMe)$ and $Cp_2W(Me)(OMe)$ in a 1:5 ratio,[167] With thiophene, C-S bond cleavage was achieved as a primary photoproduct, prolonged irradiation converted the latter into the C-H insertion product Cp_2WH(2-thienyl).[152] A number of mono and bis-silyl complexes of W were obtained in good yields by photolysis at 350 nm of $Cp_2W(H)_2$ in hydridosilanes; Cp* derivatives were also prepared by the same method.[49-50] In the absence of substrates, dimers are formed resulting from activation of C-H bonds of the cyclopentadienyl groups.[151] The reaction of $Cp_2W(H)_2$ in the presence of M-M bonded complexes led to the formation of heterometallic clusters, but the presence of CO groups in the reagents made it unclear whether the photochemistry proceeds by H_2 reductive elimination from the tungsten precursor or CO loss from one of the dimers.[51] The photochemistry of the charge-transfer adducts of $Cp_2W(H)_2$ was summarized in section 2.2.3.[78]

Studies of the photochemistry of $Cp_2W(H)_2$ in low temperature matrices[120,153] confirmed the formation of the $[Cp_2W]$ fragment by H_2 photoinduced concerted elimination; laser induced fluorescence[111] and magnetic circular dichroism[168] (see section 2.2.1 for details).

Irradiation of $Cp^*_2W(H)_2$ in pentane proceeded by loss of H_2 in two steps like the molybdenum analogue to generate $Cp^*WH(\eta^6\text{-}C_5Me_4CH_2)$ and $Cp^*W\{\eta^7\text{-}C_5Me_3(CH_2)_2\}$. When starting with $Cp^*_2W(D)_2$ no deuterium is incorporated into the solvent, consistent with $[Cp^*_2W]$ as the intermediate in the first stage of reaction.[155] The *ansa*-bridged tungsten dihydride $(\eta\text{-}C_5H_4)CMe_2(\eta\text{-}C_5H_4)W(H)_2$ is not photosensitive, unlike its molybdenum analogue.[157] The adduct $(i\text{-}C_3H_7C_5H_4)_2W(H)_2$-9,10-phenanthrenequinone was found to display a long wavelength charge-transfer absorption at λ_{max} = 530 nm; irradiation into this band was claimed to result in H_2 transfer to the diol but no evidence was presented.[169]

4.3.3 Group 6 Polyhydrides. In this section, we will treat analogous molybdenum and tungsten compounds together because of their close relationship.

$Mo(H)_4$ was formed from the photochemical reaction of cocondensed H_2 and Mo atoms in Kr and Ar matrices at 12 K with $\lambda > 400$ nm; photoreversibility was obtained on irradiating at shorter wavelengths (320 nm – 380 nm) where $Mo(H)_4$ liberated H_2 and regenerated the dihydride species.[149] The same type of experiments were also performed with H_2-doped noble gas matrices at 3.5 K and MoH, $Mo(H)_2$, $Mo(H)_4$, $Mo(H)_6$ were obtained and found to interconvert photochemically.[170] The structures of $Mo(H)_2$, $Mo(H)_4$, and $Mo(H)_6$ are assigned as belonging to

C_{2v}, T_d and C_{3v} (trigonal prismatic) point groups, respectively, on the basis of the spectra and DFT calculations. Reaction of W atoms with H_2 in Ne matrices generated WH, $W(H)_2$, $W(H)_3$, $W(H)_4$ and $W(H)_6$ that were distinguished by wavelength-dependent photochemistry in addition to annealing, H_2 concentration and isotopic shifts.[171] Observation of six fundamental vibrations, including four W-H stretching bands, provided good evidence for the C_{3v} trigonal prismatic structure of $W(H)_6$, consistent with the early predictions for d^0 ML_6.[172] Co-condensation of tungsten atoms with pure H_2 generated a species assigned as $W(H)_4(H_2)_4$ which was partially destroyed by UV photolysis.[173]

The reactivity and features of $Mo(H)_4(dppe)_2$ have been already discussed in section 2.3.[21,81-82] Studies on $W(H)_4(dppe)_2$ took place in parallel with the molybdenum ones. The complex exhibited visible light emission if photoexcited at 77 K in 2-methyltetrahydrofuran, emission lifetime (absorption λ_{max} 400nm, emission λ_{max} 590 nm, lifetime *ca.* 13 μs, compared to 87 μs for the Mo analogue). Stoichiometric reduction of alkenes was achieved when $M(H)_4(dppe)_2$ (M = Mo, W) was irradiated in the presence of such substrates; this process became catalytic when H_2 was added in excess.[81] Hydrogen loss was the sole photochemical process observed until very recently when H_2 addition and phosphine dechelation to form $W(H)_6(dppe)(\kappa^1\text{-dppe})$ was reported. In this investigation, *para*-H_2 was employed to improve NMR sensitivity (section 3.2).[88] Photocatalytic reduction of molecular nitrogen to ammonia and hydrazine has been demonstrated with $W(H)_4(dppe)_2$, $W(H)_4(PPh_2Me)_4$ and $W(H)_4(etp)(PPh_3)$ as catalysts; light in this case was responsible for the hydride ion elimination which creates a free vacant site for the dinitrogen to coordinate.[174] Studies on $W(H)_4(PRPh_2)_4$ (R = CD_3, C_2D_5) also established H_2 loss as the primary photochemical step, the unsaturated species formed underwent intramolecular C-D insertion to form a metal carbon bond with subsequent HD photoelimination.[175] Finally, the clusters $[\{(Cp''Y)_4(\mu\text{-}H)_7\}(\mu\text{-}H)_4MCp^*(PMe_3)]$ (M = Mo, W, Cp'' = C_5Me_4H) were found to undergo PMe_3 loss under UV irradiation.[176]

4.4 Group 7 metals. The photochemistry of group 7 metals has been particularly valuable for M-H homolysis of monohydrides and for the photochemical interplay of dihydride with dihydrogen complexes.

4.4.1 Group 7 monohydrides. Hydrido manganese pentacarbonyl was the first hydride complex to be investigated photochemically, but the original 1969 publication on photolysis in Ar matrices at 15 K only recognized CO loss to form $MnH(CO)_4$.[26] Many studies followed that uncovered more insights into the photoreactivity. Use of CO matrices at 10-20 K revealed that

Mn-H bond homolysis was also obtained to yield HCO and the [$Mn(CO)_5$] fragment.[27,177] This result was validated by Ar-matrix EPR where both $Mn(CO)_5$ and the H radical were detected; the analysis of the hyperfine splitting constants of Mn led to the conclusion that the lone electron occupies a metal centered orbital ($3d_z^2$) mixed with the $4p_z$ and 4s.[28] In a complementary experiment, γ-irradiation of $MnH(CO)_5$ in krypton generated $KrMn(CO)_5$ revealed through Kr-superhyperfine coupling.[178] Prolonged irradiation in Ar matrices at 193 nm proceeded along both the photochemical pathways but the quantum yield for the homolysis process was much lower than that for CO photoejection. A photoisomerization was detected under these conditions where [$MnH(CO)_4$] could rearrange from a C_s geometry to a C_{4v}.[29] DFT calculations computed the C_s structure to be the most stable and the C_{4v} structure only 3 kcal/mol higher in energy.[179] The theoretical work on the photochemistry of $MnH(CO)_5$ is described in section 2.1. In a more preparative approach, the photochemistry of $MnH(CO)_5$ was exploited to synthesize new species; photolysis in impregnated polyethylene films under a pressure of CO generated $Mn_2(CO)_{10}$ and H_2.[180] $MnH(CO)_5$ underwent multiple CO photodissociation to form the phosphine substituted product in the presence of excess phosphine.[181] *Cis*-[$MnH(CO)_4(PPh_3)$] was found to be active in the photocatalytic hydrogenation and isomerization of alkenes,[182] while a series of disilanyl Mn-compounds of the formula $Cp^*MnH(SiR_2SiR_2H)(CO)_2$ underwent photochemical decomposition by reductive elimination of disilane; interestingly, $Cp^*MnH(SiPh_2SiPh_2H)(CO)_2$ showed some H_2 evolution ascribed to 1,2-H_2 elimination.[183] The charge-transfer photochemistry of $MnH(CO)_3$(diazabutadiene) has been compared computationally to that of its alkyl and rhenium analogues.[184]

The scenario for the photochemistry of rhenium monohydrides is slightly more diverse. Earlier studies focused on the photochemistry of Cp_2ReH and Cp_2^*ReH in Ar and CO matrices. Cp_2ReH produced the rhenocene fragment, HCO and a mono-carbonyl species, deuteration experiments confirmed that the Re-H bond was cleaved homolytically.[185] Later results identified a competing photochemical pathway which involved partial ring de-coordination plus concomitant ligand addition to yield $CpReH(\eta^3\text{-}Cp)(L)$ (L = CO, N_2).[186] Rhenocene was generated photochemically in Ar matrices allowing magnetic circular dichroism and laser-induced fluorescence investigations to be undertaken (see Section 3.1.2).[187] Photolysis of Cp_2^*ReH could be carried out on a preparative scale (section 2.1); matrix investigations of [Cp_2^*Re] were compared to those for [Cp_2Re].[6,48] The low lying excited states for $ReH(CO)_5$ were calculated and assigned to the MLCT 5d to π^*_{CO} excitations, with significant differences from its first row analogue.[188] Rhenium monohydrides containing carbonyl ligands have also been of use in photochemistry, a series of $ReH(CO)_{5-y}L_y$ (L = $P(OEt)_3$,$PPh(OEt)_2$, $PPh_2(OEt)$ or

$PPh_2(OMe)$) were prepared from photolysis of $ReH(CO)_5$ in the presence of phosphites; in these cases, CO acted as the photolabile ligand.[189] Similarly, *cis, mer*-$[ReH(CO)_2(PPh(OMe)_2)_3]$ was prepared photochemically from $ReH(CO)_3(L)$ (L = $PPh_2OCH_2CH_2OPPh_2$) with excess phosphonite.[190] Photolysis of $Cp^*(CO)_2W(\mu\text{-}SiMe_2)(\mu\text{-}H)Re(CO)_2Cp^*$ afforded an isomeric mixture of hetero-bimetallic complexes $Cp^*(CO)_2HW(\mu\text{-}\eta^1,\eta^2\text{-}SiMeCH_2)ReH(CO)_2Cp^*$.[147] The complexes with a bridging hydride and a bridging pyridyl $Re_2(CO)_7(L)(\mu\text{-}H)(\mu\text{-}pyR)$ (L = CO, 4-benzoylpyridine, pyR= pyridyl, 4-benzoylpyridyl) provide rare examples of metal carbonyl hydrides designed to possess long-lived emissive triplet excited states. Detailed absorption, emission and transient absorption spectra are reported. Extensive studies of excited state reactivity toward amines and phosphines are consistent with quenching by electron transfer to the complexes, while reactivity with methylpyridinium salts results from electron transfer in the opposite direction.[191]

4.7.2 Group 7 dihydrides and dihydrogen complexes. When we move the search into dihydrides, examples of photoactive species of group 7 are scarcer. The photochemical behavior of the dihydride cations, $[Cp^*_2Re(H)_2]^+$ parallels that of the neutral analogues of molybdenum and tungsten (Scheme 14).[155] The dihydride $CpMn(H)_2$(dfepe) was found to exist in a thermal equilibrium with its dihydrogen analogue; full conversion to the dihydrogen adduct was observed if the solution mixture was photolyzed (see section 2.2.2).[73] Studies of *trans*-$[Cp^*Re(H)_2(CO)_2]$ in cyclohexane solution at 298 K under an atmosphere of H_2, methane, or argon or in liquid Xe at 200 K under H_2 showed that it photoisomerizes to the *cisoid*-analogue. There was no incorporation of deuterium under a D_2 atmosphere. Matrix photochemistry at 12 K in the presence of ^{13}CO established that photoisomerization took place intramolecularly, prolonged photolysis afforded fragments both from H_2 and CO loss.[192] The Cp analogue, $CpRe(H)_2(CO)_2$ exists as a 98:2 equilibrium mixture of *transoid* and *cisoid* isomers. However, the *cisoid* species may be generated as the kinetic product of reaction and itself may have dihydrogen and dihydride isomers. Photolysis of *trans*-$[CpRe(H)_2(CO)_2]$ in methylcyclohexane glasses at 77 K leads to a photostationary state with a 40:60 *transoid* : *cisoid* mixture that reverts slowly to the *transoid* complex on melting.[74] The photochemistry of $CpRe(H)_2(PPh_3)_2$ is described in sections 2.2.3.[75,77,193]

4.4.3 Group 7 polyhydrides. Polyhydride species have also offered examples in photochemistry, both for Mn and Re metal centers. The clusters $M(H)_3(CO)_{12}$ (M = Mn, Re) were investigated under UV irradiation. The photoreaction of the Re complex in degassed solutions yielded the dimer $Re_2(H)_2(CO)_8$ quantitatively; if a CO atmosphere was added $ReH(CO)_5$ was detected in addition. The reaction of the manganese analogue proceeded less cleanly than the

Re one. The photochemical mechanism was partially elucidated.[194] $Re(H)_3(dppe)_2$ complex afforded an example of cleaner photochemistry, H_2 photoejection to form the unsaturated complex $ReH(dppe)_2$ was determined as the primary photoprocess and the transient was trapped by the use of CO, N_2 and C_2H_4.[195] Furthermore, the rhenium fragment was found capable of CO_2 insertion and intramolecular C-H activation of phenyls.[196] The same type of photochemistry was established for $Mn(H)_3(dmpe)_2$,[197] A similar photochemical path was followed when the bidentate phosphine was replaced with the monodentate one PMe_2Ph, whereas phosphine loss appeared to be the major photochemical step in studies of $Re(H)_5L_3$ (L = PMe_2Ph, $PMePh_2$, PPh_3).[198] The tetrahydride $CpRe(H)_4(P–Ph_3)$ showed preferential loss of H_2 upon photolysis while PPh_3 loss occurred thermally.[75] The tetranuclear cluster $Re_4(\mu\text{-}H)_4(CO)_{16}$ reacted photochemically to yield the unsaturated dimer $Re_2(\mu\text{-}H)_2(CO)_{8,}$[199] and the heteronuclear compound $Pt_2Re_2(CO)_7(P^tBu_3)_2(\mu\text{-}H)_4$ photoejected H_2 at room temperature.[200]

4.5 Group 8 metals

Iron, ruthenium, and osmium belong to one of the richest groups in examples of photoactive metal hydrides. The majority of the studies involve dihydrides with *cis* geometry at the metal center. Reductive elimination of H_2 is usually the primary photochemical process but dissociation of a different ligand has also been reported. These studies have enabled detailed comparison of how reactivity varies with the structure of the transient $16e^-$ intermediate. The group also offers some of the best examples of photochemistry of bridging hydrides.

4.5.1 Group 8 Monohydrides. Little is reported about the photochemistry of iron monohydride complexes. The photochemistry of $FeHCo_3(CO)_{12}$ and $FeHCo_3(CO)_{10}(PPh_3)_2$ was explored in the context of declusterification but proved to be inconclusive.[201] The monohydride bridging dimers $Cp_2Fe_2(\mu\text{-}H)(\mu\text{-}PR_2)(CO)_2$.[96,98-99] are discussed in section 2.5.

The biomimic of the active site of [Fe-Fe]-hydrogenases $[Fe_2(\mu\text{-}H)(pdt)(CO)_4(dppv)]^+$ (dppv = *cis*-1,2-$C_2H_2(PPh_2)_2$) was discovered as an effective photocatalyst for the H_2 evolution reaction affording four turnovers in the presence of triflic acid.[18] However, the primary photoprocess was demonstrated to be CO loss (see section 3.1.1).[124]

As with iron, the photochemistry of ruthenium monohydride species is far less investigated than that of the dihydrides. It often proceeds through the loss of a two electron donor ligand, mostly CO, followed by catalytic activity shown by the unsaturated metal-hydride intermediate formed. $RuHCl(CO)(PPh_3)_3$ was reported to lose CO under ultraviolet irradiation to form $[RuHCl(PPh_3)_3]$, a potent hydrogenation catalyst, with concomitant formation of

$RuHCl(CO)_2(PPh_3)_2$.[202] Interestingly, the dicarbonyl analogue $RuHCl(CO)_2(PPh_3)_2$ did not show any photoinduced ligand-elimination reaction but underwent reversible photoisomerization according to UV and IR spectra.[203] Irradiation of $CpRuH(CO)_2$ in frozen nujol yielded [CpRuH(CO)], again displaying CO photodissociation.[114] Surprisingly, it was observed that triethylsilane reductive elimination competes with CO photorelease in $RuH(SiEt_3)(CO)_3(PPh_3)$ where the authors postulated an excited state similar to that of $Ru\text{-}H_2$ species due to the similarity to the oxidative addition reaction. The viability of changing the R group on the silane offered an additional way to tune the reactivity in comparison to molecular H_2 (see section 2.1.2).[36]

Irradiation of $CpOsH(CO)_2$ in the presence of H_2 delivered the photoproduct $CpOs(H)_3(CO)$ formed from CO loss.[204] In agreement with these observations, the photolysis of $CpOsH(CO)_2$ in frozen nujol yielded the CO loss transient and a species that was speculated to be either the $[CpOs(CO)_2]$ radical or a compound where the hydrogen atom had migrated onto the Cp ring.[114] Photolysis of the mesitylene complex $(\eta^6\text{-}C_6H_3Me_3)OsH(CO)(CH_3)$ in an argon matrix resulted in loss of methane identified by its IR bands and formation of $[(\eta^6\text{-}C_6H_3Me_3)Os(CO)]$ (see below for the photochemistry of the dihydride complex).[205] The stannylene complex $Cp^*OsH\{SnH(trip)\}(P\textit{i}Pr_3)$ (trip = 2,4,6-triisopropylphenyl) was reported to convert slowly to the metallostannylene complex $Cp^*Os(H)_2\{Sn(trip)\}(P\textit{i}Pr_3)$ under ambient light through a radical mechanism.[206] The 2-trihydrofuranyl complex $OsH(PP_3)(C_4H_7O)$ (PP_3 = $P(CH_2CH_2PPh_2)_3$) reacts photochemically to loose tetrahydrofuran and form the product of cyclometalation of one of the phenyl rings of PP_3 (see section 4.5.2 for $Os(H)_2(PP_3)$).[60]

4.5.2 Group 8 Dihydrides. Iron dihydride complexes have attracted the photochemical community since the early 1980s both for fundamental mechanistic studies and applications in the activation of strong bonds. The main skeleton of photoactive Fe species involves either an Fe-carbonyl or an Fe-phosphine scaffold where the two *cis*-hydrides are the photolabile ligands. Sweany first reported the matrix isolation of $Fe(H)_2(CO)_4$ and formation of $[Fe(CO)_4]$ which arose from photoinduced H_2 reductive elimination from the parent complex $Fe(H)_2(CO)_4$; CO loss was not observed. The reverse reaction, H_2 oxidative addition was also induced photochemically in matrices.[67] The theoretical description of the photochemical reaction is described in section 2.2.1.

Iron phosphine dihydride complexes have proved more effective in small molecule activation than iron carbonyl dihydrides. $Fe(H)_2(drpe)_2$ (drpe = dmpe, depe, dppe) are well known as good activators of sp^2 C-H bonds of alkenes,[207-208] the much stronger sp^3 C-H bonds of alkanes,[209] and C-S bonds of thiophenes[210] (Scheme 16). The activation of such strong bonds

was achieved at low temperature and involved photolysis of the dihydride parent complex to reductively eliminate molecular hydrogen and form the unsaturated intermediate capable of insertion into the C-X bonds (X = H, S). The activation of the C-H bonds of methane in liquefied xenon through photolysis of $Fe(H)_2(dmpe)_2$ was also reported.[211] Elimination of H_2 from this complex was found to be predominately intramolecular on the basis of lack of deuterium scrambling.[52] Intramolecular C-H activation to form a metalacycle was detected in the presence of bulkier phosphine ligands.[212] $Fe(H)_2(dppe)_2$ showed activity as a precatalyst for the photolytic hydrosilation of aldehydes and ketones.[105] The dmpe analogue, $Fe(H)_2(dmpe)_2$, showed photochemical activity in dechlorination reactions of chlorinated ethylenes.[213] The kinetics and actinometry of the hydrodechlorination of trichloroethylene and dichloroethylene with $Fe(H)_2(dmpe)_2$ in excess were investigated in detail (Figure 14). More importantly, $Fe(H)_2(dmpe)_2$ is an active photocatalyst for the C-H borylation of arenes (see section 2.6).[104]

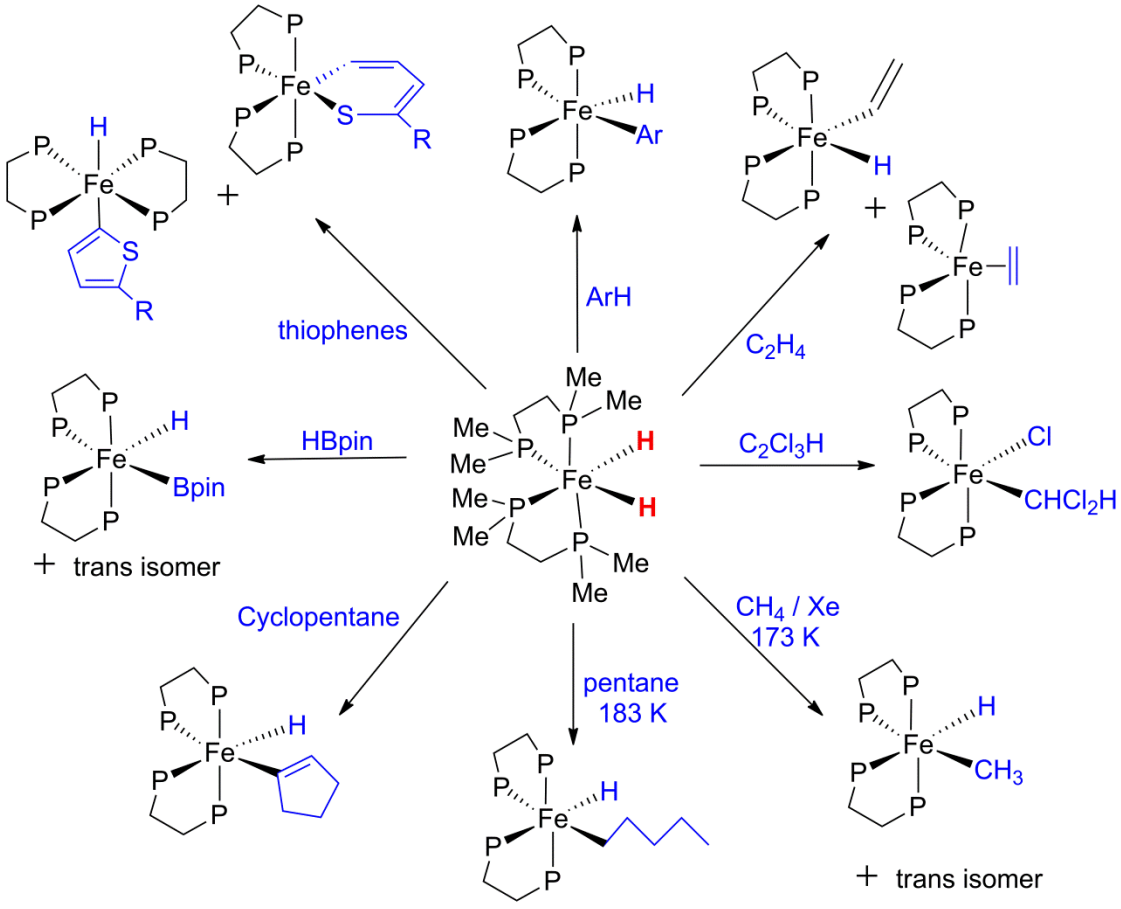

Scheme 16. Photoreactivity of $Fe(H)_2(dmpe)_2$ in solution

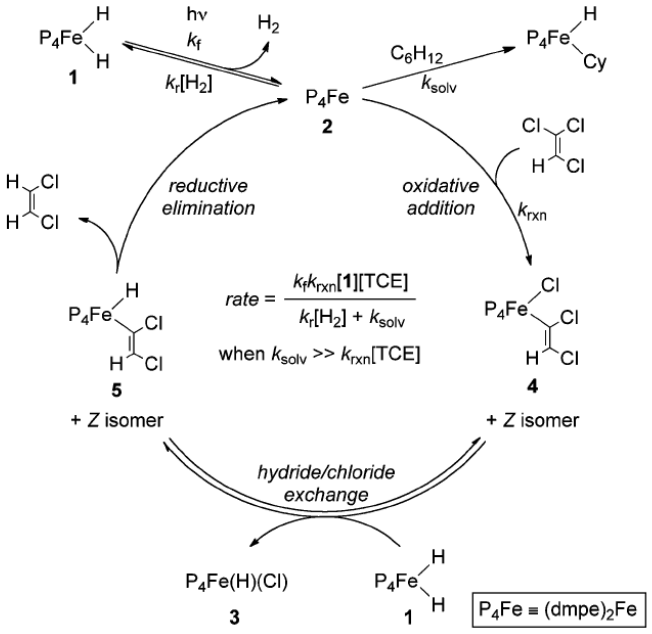

Figure 14. Proposed mechanism and corresponding rate law for the photochemical conversion of trichloroethylene to *cis*-dichloroethylene. [213]

Clearer insights into the photochemical process were obtained by transient UV-vis spectroscopy and low temperature matrix photochemistry. The $[Fe(dmpe)_2]$ intermediate was observed directly by both methods and its reactivity examined. The key finding was the formation of a single unsaturated transient $[Fe(dmpe)_2]$ that differed significantly from the Ru analogue in its spectroscopic features and reactivity (see below and Figure 15).

Although both $[Fe(dmpe)_2]$ and $[Ru(dmpe)_2]$ react with CO with a second order rate constant close to the diffusion limit, the reactivity towards hydrogen was found to be very different. The rate constant for reaction of $[Fe(dmpe)_2]$ with H_2 was a factor of 7500 smaller than that of $[Ru(dmpe)_2]$ one and reacts with arenes and alkanes unlike $[Ru(dmpe)_2]$. The UV-vis absorption spectrum was also markedly different, with the long wavelength visible absorption bands absent from the spectrum of $[Fe(dmpe)_2]$, leaving only a near UV band. These differences were rationalized in terms of a different geometry for the two species and a C_{2v} geometry with a triplet ground state was suggested for $[Fe(dmpe)_2]$ by analogy with $[Fe(CO)_4]$.[57] Rate constants were also reported for the coordination or oxidative addition reactions of $[Fe(dmpe)_2]$ with benzene, toluene, alkenes, nitrogen and triethylsilane. Notably, $[Fe(dmpe)_2]$ exhibits little kinetic discrimination.[57] The enthalpies of activation for the reactions with triethylsilane (Table 1) highlight the differences between Fe and Ru. There is also a contrast in the reactivity in low temperature matrices since $[Fe(dmpe)_2]$ reacts with methane to form

$FeH(CH_3)(dmpe)_2$ whereas no corresponding reaction is observed for $[Ru(dmpe)_2]$.

Density functional calculations predicted a more stable singlet configuration for the Ru complex with a D_{2d} geometry while the Fe species was computed to be slightly more stable in its triplet state with a C_{2v} geometry.[65] Later calculations confirmed that Fe^0P_4 complexes have a C_{2v} geometry with a triplet ground state. The triplet singlet energy gap changes in the order $[Fe(PH_3)_4] > [Fe(dpe)_2] > [Fe(dmpe)_2]$. In the case of $[Fe(dmpe)_2]$, the triplet state was calculated to be more stable than the singlet by 52.5 kJ/mol. The reaction with hydrogen was analyzed by the minimum energy crossing point method, accounting for the slower rate of reaction of $[Fe(dmpe)_2]$ with H_2 compared to $[Ru(dmpe)_2]$.[214-215]

Irradiation of iron atoms in molecular H_2/noble gas matrices at 12 K generated $Fe(H)_2$.[216-218] The results suggested that H_2 oxidative addition to the metal center had a small degree of H-H stretching in an early transition state and no activation barrier to insertion. The process followed a "simple" concerted insertion into the Fe metal. The insertion product was investigated by 440 nm-photoexcitation at 12 K and found to be converted back to Fe atoms; the reverse reaction was described as a concerted reductive elimination with no activation barrier (Scheme 17). Both H_2 insertion and its microscopic reverse were reported to happen with no detectable formation of FeH or $Fe(H)_x$ ($x > 3$) or hydrogen atom abstraction products. This work represented the first example of ligand-free H_2 reductive elimination from a metal center. Studies of the kinetic isotope effect (KIE) for oxidative addition at low temperature in Xe yielded a k_H/k_D isotope ratio of 5.6. Although this seems large, it translates into a k_H/k_D ratio of around 1.1 at ambient temperature indicating a small degree of H-H stretching and low activation barrier for insertion.[216-217] Later studies of Fe in H_2/Ar and Fe/Kr reported laser induced fluorescence excitation spectra and IR spectra. The authors suggest that $Fe(H)_2$ is formed from an $Fe(H_2)$ exciplex with broadened and shifted absorptions. Isotopic substitution indicates an H-Fe-H angle exceeding 170° and enables measurement of KIEs for forward and reverse reactions. The KIE for the formation of $Fe(H)_2$ was measured as 7 in Ar but 86 in Kr and the KIE for the reverse reaction was *ca.* 3 in both matrices.[218] Later studies with laser ablation sources of Fe are barely concerned with the photochemistry.[219]

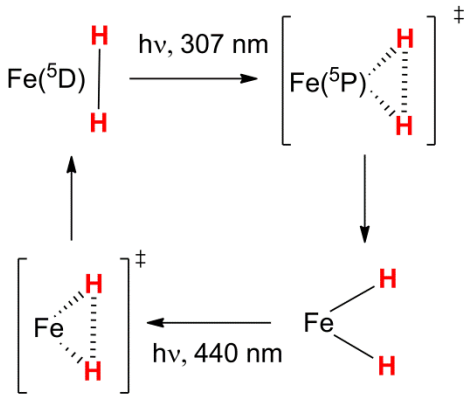

Scheme 17. Photochemistry of Fe + H_2 in matrices

The photoreactions of the high-spin Fe(II) complex with bridging hydride ligands[100] [(β-diketiminate)Fe(μ-H)]$_2$ and the photochemistry of nitrogenase[8] are covered in section 2.5.

Ruthenium dihydride complexes also show a vast variety of examples in photochemistry. Unlike its monohydride analogues, $Ru(H)_2(CO)(PPh_3)_3$ undergoes H_2 reductive elimination when exposed to ultraviolet irradiation. Photoelimination of CO did not occur as confirmed by the GC analysis of the gases produced. The transient was trapped when it was exposed to a CO atmosphere during photolysis where $[Ru(CO)_3(PPh_3)_3]$ was the only product formed.[203] The transient photochemistry (Scheme 18) for this complex was investigated twenty years later by laser flash photolysis in benzene solution. The transient $[Ru(CO)(PPh_3)_3]$ reacted with an H_2 atmosphere to regenerate the dihydride species with a second order rate constant of $k_2 = (8.4 \pm 0.4) \times 10^7$ dm^3 mol^{-1} s^{-1}. More notably, it was found by time resolved IR experiments that H_2 reductive elimination was complete within 6 ps implying that any geometry reorganisation and bond breaking/making around the Ru center had to take place within this time (see section 3.1).[123] The dissociative photochemistry of this complex was also demonstrated by quantum dynamics calculations.[64]

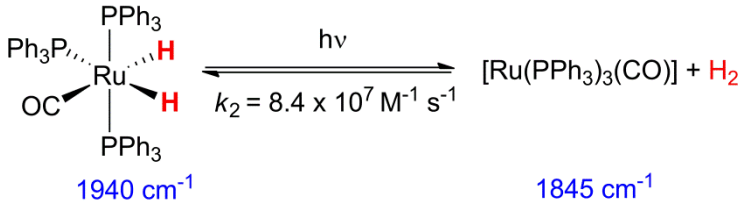

Scheme 18. Photochemical H_2 reductive elimination from $Ru(H)_2(CO)(PPh_3)_3$ and reverse reaction

A further example with a carbonyl ligand studied by steady state and transient absorption spectroscopy is $Ru(H)_2(CO)(etp)$ (etp = $PhP(CH_2CH_2PPh_2)_2$). The reactivity is exclusively derived from H_2 reductive elimination and shows little discrimination between incoming substrates (see also Table 1).[61] Substitution of a PPh_3 ligand with an NHC-carbene led to a drastic change in the reactivity; *in situ* photolysis and the use of *para*- H_2 established that photoisomerization took place after both H_2 and PPh_3 dissociation had happened (see section 2.2.2).[72] $Ru(H)_2(CO)_2(PMe_3)_2$ was also subject to photochemical investigation in low temperature Ar, CH_4 and Xe matrices. It also loses hydrogen to form the $16e^-$ unsaturated species, the reversibility of the reaction on long wavelength (λ > 360 nm) photolysis identified $[S\cdots Ru(CO)_2(PMe_3)_2]$ (S = Ar, CH_4, Xe) as the sole coordinatively unsaturated species.[220]

Initial studies of the photochemistry of $Ru(H)_2(PMe_3)_4$ only revealed photochemical PMe_3 loss.[97,221] However, more extensive investigation demonstrated the competition of two photochemical pathways[41] in contrast to $Ru(H)_2(CO)_2(PMe_3)_2$. Studies by matrix isolation, and time-resolved spectroscopy, together with NMR studies of the products showed that both $[Ru(PMe_3)_4]$ and $[Ru(H)_2(PMe_3)_3]$ are formed as transients, highlighting how the parent complex could either reductively eliminate H_2 or lose the $2e^-$-donor ligand PMe_3. The transient absorption band in the near UV observed by flash photolysis is closely matched by the matrix spectra and is assigned to $[Ru(PMe_3)_4]$. Insertion products deriving from both unsaturated species were observed in the presence of Ph_2SiH_2 with initial relative quantum yields of 1:4.5 for H_2 loss relative to PMe_3 loss. (Scheme 19).[41] The triphenylphosphine analogue $Ru(H)_2(PPh_3)_4$ and the N_2 substituted species $Ru(H)_2(N_2)(PPh_3)_3$ were investigated photochemically for H_2 production from ethanol but the photochemical process was not identified conclusively.[222] The photochemistry of $(\eta^6\text{-}C_6H_6)Ru(H)_2(PR_3)$ (R = Me, ^{i}Pr) and $(\eta^6\text{-}C_6H_6)Ru(H)_2(PHPh_2)$ appeared to be less complicated: H_2 loss was the only photoactivated pathway to the unsaturated species that proved capable of inserting into C-H bonds of arenes.[223-224]

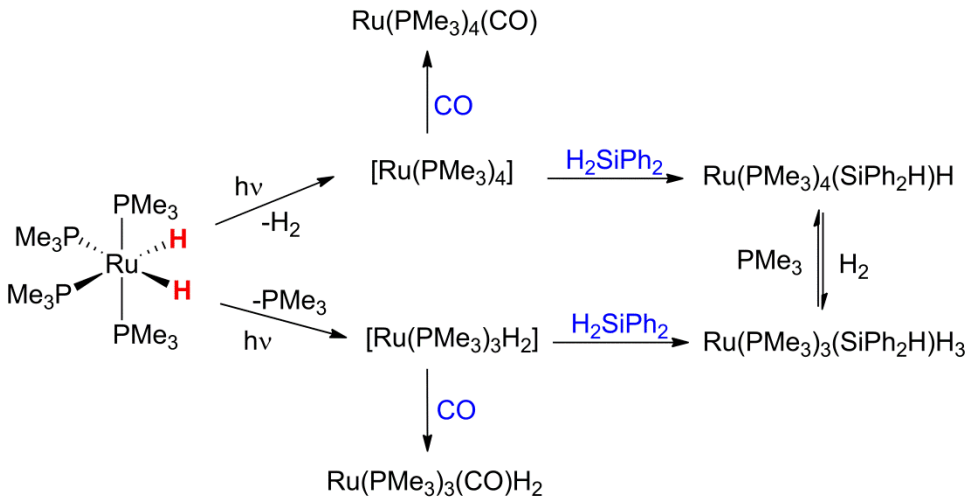

Scheme 19. Photoreactivity of $Ru(H)_2(PMe_3)_4$ displaying both H_2 reductive elimination and PMe_3 loss

Bergamini *et al.* first reported the photoactivity of the $Ru(H)_2(drpe)_2$ (drpe = dmpe, dppe) type of complexes together with the Fe analogues. For both sets of complexes, molecular hydrogen elimination through a concerted process was found to be the sole photoprocess.[52] Details of the photochemistry and transient spectroscopy of these two complexes[7,53-55,58] are discussed in Section 2.2.1. Unexpectedly, $[Ru(dmpe)_2]$ displayed very different reactivity and spectroscopic features from its Fe analogue (Figure 15). Similar complexes of the type $Ru(H)_2(drpe)_2$ (drpe = depe, dfepe, dmpm – see list of abbreviations) were also studied by transient spectroscopy.[58-59] $Ru(depe)_2$ exhibited very similar features in its UV-vis spectra to those observed for the dmpe and dppe analogues with three major UV-vis bands. One of the bands falls at long wavelength (600-800 nm) and is assigned to an $M(d_z^2)$-$M(p_z)$ transition. These features, in addition to comparison of the spectra to that of $[Rh(dppe)_2]^+$, confirmed the square planar geometry around the metal center. The $[Ru(defpe)_2]$ transient displayed a three band UV-vis spectrum more shifted towards the blue part of the spectrum as a result of either a slight distortion from the planar structure, or a stabilizing interaction of the F atom with the Ru center. Each of the effects was considered to be minor in distorting the square planar geometry as confirmed by the survival of the multiband UV-vis spectrum. The absorption spectrum of $[Ru(dmpm)_2]$ is also much less well resolved and blue-shifted as result of the reduction in the size of the ring.[59] The reactivity of the complexes tested with different substrates (H_2, CO, C_2H_4, silanes, boranes) showed a sensitivity to the change of the phosphine substituent and increased in the order $[Ru(dfepe)_2] < [Ru(dppe)_2] < [Ru(depe)_2] \sim [Ru(dmpm)_2] < [Ru(dmpe)_2]$ spanning a

factor of 34000 for reaction with H_2 and 418000 for reaction with CO.[54,58] The reactivity toward $SiHEt_3$ was used as a further standard for comparison between these complexes (Table 1). Of these complexes, only [Ru(dmpm)$_2$] inserts into the C-H bonds of benzene as had been shown earlier.[225] However the kinetics of the transient's reaction with benzene were complex and interpreted in terms of a rapid pre-equilibrium step between [Ru(dmpm)$_2$] and the arene complex Ru(η^2-C_6H_6)(dmpm)$_2$. The latter undergoes oxidative cleavage of benzene relatively slowly, leading to the phenyl hydride species. In line with these results, Ru(H)$_2$(dfmpe)$_2$ reductively eliminated H_2 if irradiated under a D_2 atmosphere to form the dideuteride analogue but showed no further reactivity towards organic C-H bonds.[226] Recently, the well-understood photochemistry of the Ru(H)$_2$(dppe)$_2$ was exploited in studies aimed to develop a new time resolved method based on a laser-pump and NMR-probe set-up (See section 3.2). *Para*-H_2 was employed to overcome the NMR insensitivity.[7] It would be interesting to relate the reactivity of [Ru(dppe)$_2$] to the photocatalytic experiments with [$RuCl_2(C_6H_6)]_2$ + excess dppe (see below).[93]

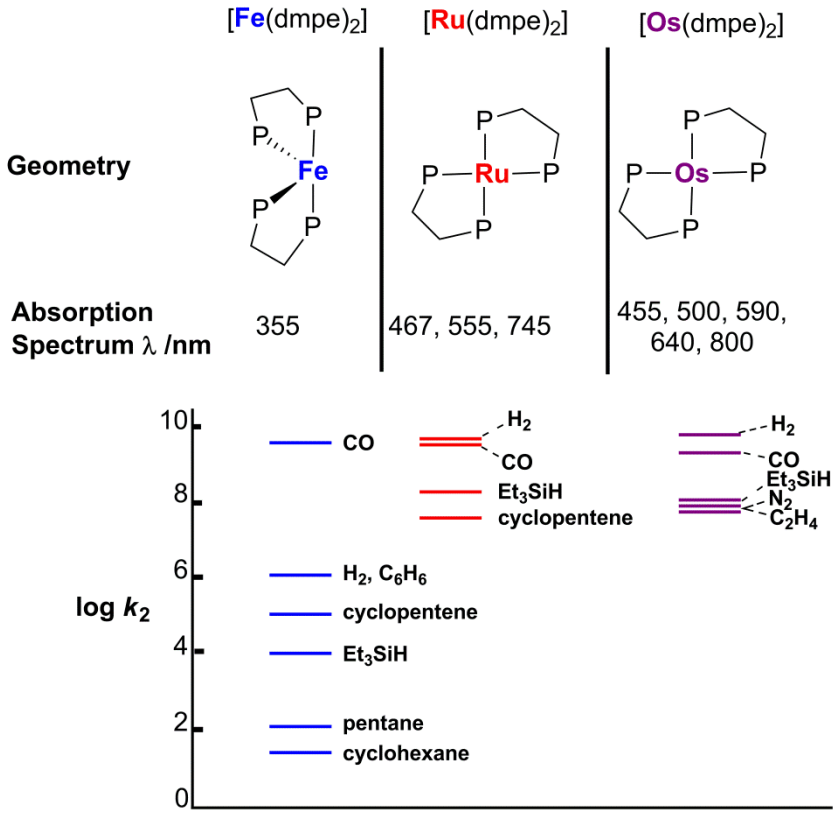

Figure 15. Comparison between spectral features and rates of reactions for group 8 metal MP_4 intermediates.

The photochemistry of an analogous class of Ru dihydride complexes bearing the chiral phosphines Me-BPE and Me-Duphos was also investigated. Once again, the primary photoprocess was H_2 concerted reductive elimination demonstrated by transient time resolved spectroscopy. The concerted nature of this process and the H_2 oxidative re-addition to the metal center was additionally established through the observation of a *para*-hydrogen enhancement of the NMR spectrum acquired after the solution was photolyzed inside the NMR probe under a *para*-H_2 atmosphere (Figure 12) (see section 3.2). Very low temperature (180 K) photolysis *in situ* performed under D_2 atmosphere generated H_2 but no HD. However, repetition of the experiment at 273 K resulted in the formation of a minor amount of HD, suggesting that a secondary photoprocess could compete where the chelating phosphine unhooked from the Ru center with the subsequent formation of a [Ru(κ^1-Duphos)(Duphos)$(H)_2(\eta^2$-$D_2)$]. This type of complexes can undergo H/D exchange rapidly; chelate ring closing will then eliminate HD and form a Ru-hydride/deuteride complex. Kinetic studies for their reactivity towards a variety of substrates were carried out; [Ru$(BPE)_2$] reacted with H_2 with a similar rate constant to that of [Ru$(dppe)_2$], but [Ru$(Duphos)_2$] reacted considerably more slowly and this was explained by a blocking actions of the methyl groups on the phospholane rings.[125]

The effect of introducing a more constrained unit on the Ru center such us PP_3 = $P(CH_2CH_2PPh_2)_3$ was also of interest.[60,227] The tetradentate ligand prevented the transient from adopting a square planar D_{2h} geometry and offers two additional possible arrangements: pyramidal C_{3v} or butterfly C_s. Steady state photolysis experiments showed that, unlike the complexes with bidentate ligands, [Ru(PP_3)] undergoes cyclometalation on irradiation in THF under argon, but forms a stable dinitrogen complex under an N_2 atmosphere. Photolysis in benzene-doped THF yielded the metal phenyl hydride complex, while similar experiments with thiophene in THF yield the 2-thienyl hydride. As expected, laser flash photolysis demonstrated that the complex showed quite different UV-vis spectra for its transient (a single broad absorption maximum at 390 nm) from those of [Ru$(drpe)_2$] because of the enforced change in structure. The reactivity of [Ru(PP_3)] towards H_2 was found to be much slower than that of [Ru$(dmpe)_2$] and [Ru$(dppe)_2$]. On the other hand, [Ru(PP_3)] showed a wider range of reactions, including rapid C-H activation with benzene in cyclohexane (rate constant (1.3 ± 0.1) x 10^6 M^{-1} s^{-1} with KIE 1.5 ± 0.2, compare [Fe$(dmpe)_2$] + benzene (9.6 ± 0.4) x 10^5 M^{-1} s^{-1}, see also Table 1); however, there was little kinetic discrimination between substrates. The reactivity toward THF is shown in Scheme 20. The two-stage kinetics of reaction of transient [Ru(PP_3)] toward thiophene has also been reported.[227] In the most satisfactory model of the reactivity, it was

postulated that [Ru(PP$_3$)] adopts a structure with an agostic phenyl group.[60]

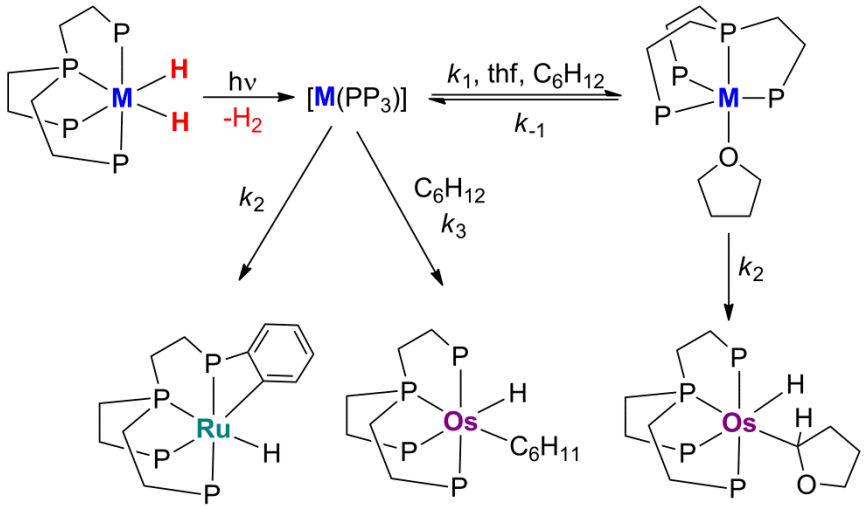

Scheme 20. Comparison of [Ru(PP$_3$)] and [Os(PP$_3$)] transient photochemistry in THF

The use of [RuCl$_2$(C$_6$H$_6$)]$_2$ in the presence of a variety of phosphine ligands for the photocatalytic decomposition (380-780 nm) of formic acid·triethylamine (5:2) to hydrogen was reported. The most successful phosphines were PPh$_3$ and dppe giving TON of 1650 and 2800 respectively after 3 h irradiation using 320 ppm Ru. Control experiments in the dark gave far less H$_2$. The catalysts work in a temperature range from 0 to 45 ºC. This is a very different reaction from those described in Section 2.6 because it does not require the photon energy (it is described as photoassisted). Indeed the catalyst can be activated photochemically and the reaction then proceeds in the dark. One of the photoactive species is proposed to be a Ru(H$_2$)(OCHO)(PR$_3$)$_n$ complex.[93] Improved performance was obtained with Fe$_3$(CO)$_{12}$/phenanthroline/PPh$_3$. An analogous cycle is proposed but evidence for hydrides, of concern for our purpose, is limited. [228]

Photoactive osmium dihydride complexes are slightly more numerous than the monohydride complexes. The first report of a photochemical reaction that involved an Os(H)$_2$ moiety aimed to prepare clusters; Os$_3$(H)$_2$(CO)$_{10}$ was irradiated in the presence of Fe(CO)$_5$ or Ru$_3$(CO)$_{12}$ to form a hetero-tetra-nuclear species as a consequence of CO photoelimination. The bridging dihydrides of the starting complex remained intact in the product suggesting no reactivity towards irradiation.[229] Bergamini *et al.* explored the photochemistry of the Os(H)$_2$(dmpe)$_2$ and Os(H)$_2$(dppe)$_2$, analogues of the Fe and Ru mentioned previously. No substantial differences were found in the photochemical behavior at that time.[52] The photochemistry of Os(H)$_2$(dmpe)$_2$, explored by low temperature matrix photochemistry, laser

flash photolysis and steady state studies of the photolysis products, showed a strong analogy to the [Ru(dmpe)$_2$] analogue (see section 3.1.2).[62] Notably, [Os(dmpe)$_2$] has the lowest energy UV-vis transition of all the M^0P_4 complexes at 798 nm (Ar matrix). Unlike [Ru(dmpe)$_2$], it undergoes C-H oxidative addition with benzene to form OsH(Ph)(dmpe)$_2$ and with ethylene to form *cis*- and *trans*-[OsH(CH=CH$_2$)(dmpe)$_2$] without forming Os(dmpe)$_2$(C_2H_4).

The piano-stool complex (η^6-C_6H_6)Os(H)$_2$(CO) was investigated photochemically with respect to the C-H activation of saturated and aromatic hydrocarbons. The formation of the reactive species was achieved by photoelimination of H_2 with no mention of CO loss.[230] The mesitylene analogue (η^6-$C_6H_3Me_3$)Os(H)$_2$(CO) was employed for matrix photochemistry and proved to undergo H_2 reductive elimination to yield the unsaturated fragment [(η^6-$C_6H_3Me_3$)Os(CO)] upon photolysis in an Ar matrix and to form (η^6-$C_6H_3Me_3$)OsH(CH_3)(CO) in a methane matrix (see section 4.5.1).[205]

The photochemistry of Os(H)$_2$(PP_3) was studied by steady state methods and by time-resolved absorption.[60,63,227] Transient absorption methods on Os(H)$_2$(PP_3) complexes in the presence of hydrocarbons demonstrated that it activates the C-H bonds of primary alkanes and methane itself (rate constant (2.6 ± 0.4) x 10^5 M^{-1} s^{-1}). The transient [Os(PP_3)] appears also to react with cyclohexane, but much more slowly, thus showing kinetic selectivity for alkane C-H bonds CH_4 > 1° > 2°, but the rate constant for benzene exceeds those for all alkanes. The alkyl products were not observed by NMR spectroscopy, principally because of the low solubility of the complex in alkanes. However, C-H activation products were identified by NMR spectroscopy with THF, benzene and thiophene. The transient kinetics for reaction with THF and with thiophene are complicated by initial coordination of the substrate through oxygen or sulfur, respectively (Scheme 20). Unlike [Ru(PP_3)] no quenching could be observed with H_2 probably because of the competing reaction with cyclohexane. Although [Os(PP_3)] was quenched by N_2, no dinitrogen complex could be isolated, whereas Ru(PP_3)(N_2) was isolated as a reaction product. Intramolecular photochemical C-H activation was not observed for Os(H)$_2$(PP_3), unlike the Ru analogue: evidently the barrier for cyclometalation at Os was higher than for C-H activation of alkanes, whereas the reverse is true of [Ru(PP_3)]. The authors postulate that the structure of [Os(PP_3)] predisposes it to C-H activation through the enforced C_{3v} or C_s structure with the additional possibility of the agostic phenyl group.[60,63,227]

4.5.3 Group 8 Polyhydrides. Iron, ruthenium and osmium atoms formed by laser ablation have been cocondensed with pure H_2 or with Ne/H_2 mixtures at 4.5 K allowing examination of a series of binary hydrides and hydride dihydrogen complexes. The monohydride FeH reacted with H_2 in solid neon and pure hydrogen to form FeH(H_2)$_x$, the Fe(H)$_2$

molecule was also observed experimentally and found capable of forming the weakly bound $Fe(H)_2(H_2)_3$ supercomplex. There is a reversible photochemical cycle linking $Fe(H)_2$ and $Fe(H)_2(H_2)_3$ [91] The behavior of Ru is similar to that of Fe with the difference that the $Ru(H)_2$ was not detected due to the large activation energy needed for atomic insertion with one H_2 molecule. The reactive RuH species formed in first place reacts with hydrogen to form $Ru(H)(H_2)$ rather than a trihydrido species. Although, photochemical reactions are reported, the photochemical reaction sequence is unclear.[91] The reactive OsH species combines with H_2 to form the complex $OsH(H_2)$ instead of the trihydride $Os(H)_3$ and $OsH(H_2)_x$ is also formed.[91]

The cluster $Ru_4(H)_4(CO)_{12}$ was found to be active in catalytic isomerization and hydrogenation of alkenes when irradiated and it was suggested that photoejected CO was responsible for the formation of the reactive complex $[Ru_4(H)_4(CO)_{11}]$.[231] The isolation of the intermediate came later by matrix photochemistry at low temperature confirming clean loss of CO.[232]

Most of the reactions of $[Cp^*Ru]_2(\mu\text{-}H)_4$ and its analogues are described in Section 2.4. It also reacted photochemically with $CpNi(CO)_2$, $CpCo(CO)_2$ and $[CpFe(CO)_2]_2$ to yield heterobimetallic clusters with different geometries. Although no mention is made of the primary photoprocess by the authors, elimination of H_2 from the tetrahydrido Ru-species is required for the observed product to be formed.[11-12,233]

The only example of a polyhydride of osmium involved in a photochemical reaction is the photochemical reductive elimination of H_2 from $Cp^*Os(H)_3(CO)$ to form the dimer $[Cp^*Os(CO)]_2(\mu\text{-}H)_2$.[204]

4.6 Group 9 metals

Group 9 metal-hydride photochemistry has played a critical role in the development of C-H bond activation and also includes some rare examples of photochemistry in aqueous solution and examples of equilibrated excited states.

4.6.1 Group 9 monohydrides. The first cobalt monohydride complex reported to undergo photoreactivity was $CoH(CO)_4$; the transient $[Co(CO)_4]$ formed upon photolysis was trapped in both Ar and CO matrices and arose from metal-hydrogen bond homolysis proposed as a primary photoprocess (Equation 5).[234] A few years later, CO photoelimination was also detected for the same complex along with M-H bond homolysis; the relative quantum yields for M-H vs M-CO cleavage were estimated as 1:8 with 254 nm irradiation (Equation 5).[235] The first calculations of electronic structure suggested that the dominant electronic transition responsible

for photoactivity had mixed LF and MLCT character.[33] The photodissociation dynamics[236] for $CoH(CO)_4$ and simulation of the intersystem crossing process[237] were computed. Finally, wave-packet dynamics established that competition in multiple photoprocesses had a time dependence on the sequence of the elementary events occurring between the initial absorption and the formation of the photoproducts. The Co-H homolysis can occur *via* population of the ^1E ($d \rightarrow \sigma^*_{Co-H}$) state as well as from triplet states (albeit, more slowly).[69] The fragment $[CoH(CO)_3]$ formed after CO loss also showed photochemical reactivity in H_2-containing matrices forming the hydride(dihydrogen) species $CoH(H_2)(CO)_3$; the latter proved to be inert to irradiation.[238-239]

$$HCo(CO)_4 \xrightarrow{h\nu} H^{\bullet} + Co(CO)_4$$
$$HCo(CO)_4 \xrightarrow{h\nu} HCo(CO)_3 + CO$$

Equation 5

Cobalt complexes have been used extensively in photocatalytic systems for hydrogen production from water. These photosensitized reactions are thought to involve photoinduced electron transfer to cobalt and formation of cobalt hydrides by reaction with acid, but the hydrides are rarely observed directly. For details, the reader is referred to reviews.[13-14]

More direct participation of monohydrides in the photochemical process is offered by Rh-monohydrides. The first report published in 1979 showed how ultraviolet irradiation of $[RhH(NH_3)_4(OH_2)]^{2+}$ in the presence of O_2 resulted in the formation of a hydroperoxide rhodium species. The photoinitiation produces a H radical and $[Rh(NH_3)_4]^{2+}$ which acts as the chain carrier.[240] In a related example, UV photolysis of an aqueous solution of *trans*-$[RhH(14\text{-}aneN_4)]^{2+}$ (irradiating at 254 nm into absorption maximum at 288 nm) causes Rh-H homolysis generating hydrogen atoms and Rh^{II} products *trans*-$[Rh(H_2O)(14\text{-}aneN_4)]^{2+}$ and *trans*-$[Rh(OO)(14\text{-}aneN_4)]^{2+}$ under Ar and O_2, respectively.[241] The Rh^{II} products are detected by EPR spectroscopy and the H atoms may detected by trapping. The 18-electron complex $RhH(CO)(PPh_3)_3$ was capable of enhanced hydrogenation of olefins under photocatalytic conditions.[242] and the triisopropylphosphine analogue $RhH(CO)(P^iPr_3)_2$ displayed photoreactivity in H_2 production in the presence of MeOH *via* the photoelimination of CO.[222,243] The photocatalytic reactions of a rhodium porphyrin to generate silanols and of mixed valence Rh_2 complexes to generate H_2 are summarized in Section 2.6.[101-102,106]

Rhodium complexes are popular catalysts for photocatalytic reduction of protons to hydrogen. Typically, a photosensitizer transfers an electron to a rhodium complex which subsequently picks up a proton to form a rhodium hydride. Such catalysts are the subject of a

recent review.[15]

There are few examples of iridium monohydrides that undergo photochemical reaction. Clean and rapid EtOH elimination was observed on irradiation of the alkoxide hydride $Cp^*IrH(OEt)(PPh_3)$; the unsaturated fragment formed in the reaction proved capable of inserting into C-H bonds of arenes inter and intramolecularly.[37] The tridentate phosphine complexes $IrH(triphos)(C_2H_4)$ and $IrH(triphos)(CH_2{=}CHPh)$ undergo photoisomerization to form Ir^{III} vinyl dihydride complexes, that are themselves photoactive (see below).[40] In related reactions, photolysis of $CpIr(C_2H_4)_2$ in argon matrices resulted in two photoisomerization steps, first to $CpIrH(CH{=}CH_2)(C_2H_4)$ and subsequently to the vinylidene complex, $CpIr(H)_2(C{=}CH_2)$.[47] Only the first step has been observed in solution. Different behaviour was observed for $IrH(CO)_2$(xantphos); despite having a large bite angle phosphine, the introduction of CO ligands led to the photodissociation of the carbonyl as the primary photochemical step, observed by photolysis under hydrogen.[244]

The ability of $[Cp^*IrH(bpy)]^+$ to undergo excited state proton transfer and hydride transfer was discussed in section 2.1.4.[9-10] This complex, and derivatives with other polypyridine ligands, have also been used extensively for photocatalysis and photoelectrocatalysis, see section 2.6.[19,103,245] Pioneering studies of $[Cp^*IrH(NN)]^+$ (NN = bpy, phen and several substituted derivatives of bpy) as photocatalyst for the water gas shift reaction were reported.[245] The photochemical step was identified as protonation of the hydride and several reaction intermediates were identified spectroscopically. The activation energy was reduced by introduction of an electron withdrawing group on the bipyridine. The global quantum yield for $[Cp^*IrCl(bpy\text{-}4,4'\text{-}(CO_2H)_2]^+$ with irradiation at 410 nm was 0.13.[245] A related derivative with terpyridyl (tpy) and phenylpyridine (ppy) ligands, $[IrH(tpy)(ppy)]^+$ is formed in two isomers with hydride *trans* to N or C that exhibit very different properties in ground and excited states. The N-*trans*-H isomer is emissive and is quenched by triethylamine by electron transfer, whereas the C-*trans*-H isomer is non-emissive and is not quenched in this way. Their excited state spectra are appreciably different, as determined by transient absorption spectroscopy. Steady-state photolysis of the C-*trans*-H isomer in CD_3CN results in proton transfer and formation of Ir(tpy)(ppy) and, over longer periods, the N-*trans*-H isomer. Both isomers act as photocatalysts for CO_2 reduction in the presence of triethanolamine to generate CO with similar turnover numbers. It is postulated that the reaction with CO_2 occurs *via* a common square pyramidal intermediate [Ir(tpy)(ppy)] with a vacancy *trans* to C.[39]

4.6.2 Group 9 dihydrides and dihydrogen complexes. Examples of cobalt dihydride complexes involved in photochemistry are scarce. In the earliest experiments on hydride

photochemistry, the cationic complexes $[Co(H)_2(NN)(PR_3)_2]^+$ (NN = 2,2'-bipyridine *or* 1,10-phenanthroline, $R_3 = Bu_3$, Pr_3, Et_3, Et_2Ph) exhibit photoinduced reductive elimination of H_2 under vacuum which is reversed thermally by restoring a hydrogen atmosphere; photolysis of the dideuteride under H_2 generates the dihydride (Scheme 21).[1,79] Later, $[Co(H)_2(bpy)(PEt_2Ph)_2]^+$ was shown to undergo sensitized photoelimination of H_2 with visible-light in the presence of $Fe(bpy)_2(CN)_2$ (see section 2.2.3).[79]

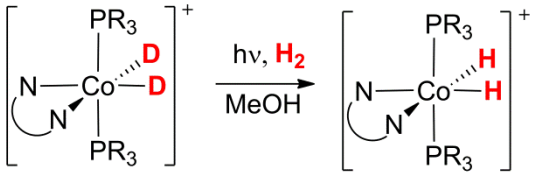

$PR_3 = PEt_2Ph$, $\phi_{408} = 0.14$

Scheme 21. Photochemical elimination of D_2 from $[Co(H)_2(bpy)(PEt_2Ph)_2]^+$ under H_2 atmosphere to form the dihydride-Co analogue

Rhodium dihydride complexes are easily accessible and have been investigated far more extensively; most of the examples have a skeleton involving a phosphine as a spectator ligand. The photochemistry of $Cp^*Rh(H)_2(PMe_3)$ was reported in seminal studies,[4,76,246-250] that demonstrated loss of H_2 and C-H activation of arenes and alkanes (Scheme 21). For example, the photolysis in liquid propane at low temperature yields the propyl hydride complex. Similarly, reaction with cyclopropane generates the cyclopropyl hydride, but the latter rearranges intramolecularly to the rhodacyclobutane on warming. The rhodium dihydride exhibits substantial selectivity for primary over secondary alkanes. Careful isotope studies revealed evidence of intramolecular rearrangements of the rhodium alkyl complexes *via* η^2-alkane complexes. This mechanism also allows for products of activation of secondary C-H bonds to isomerize to the preferred primary alkyl product. Strong support for the role of alkane complexes has been obtained in the intervening period.[249,251] The intramolecular competition between the benzylic and aryl protons of toluene at 228 K reveals the kinetic selectivity for aryl protons. On photoreaction with 1,3,5-$C_6H_3D_3$, the intramolecular kinetic isotope effect for arene C-H activation was measured as 1.4 ± 0.1, whereas the intermolecular competition between C_6H_6 and C_6D_6 gave a value of 1.05 ± 0.06. The competition between benzene and cyclopentane at 238 K demonstrated a 5.4:1 kinetic selectivity for benzene C-H activation. These observations proved that C-H activation of arenes did not proceed directly but proceeded *via* an intermediate,

postulated as $CpRh(PMe_3)(\eta^2\text{-}C_6H_6)$ and led, with further measurements to a complete free energy diagram for the alkane/arene competition at $[Cp^*Rh(PMe_3)]$.[4] A more recent photochemical study of the same complex, $Cp^*Rh(H)_2(PMe_3)$, in neat CH_3CN, demonstrated the kinetic C-H activation product to be $Cp^*RhH(CH_2CN)(PMe_3)$; thermal conversion to the C-C activated complex was detected at higher temperatures (Scheme 22). [252]

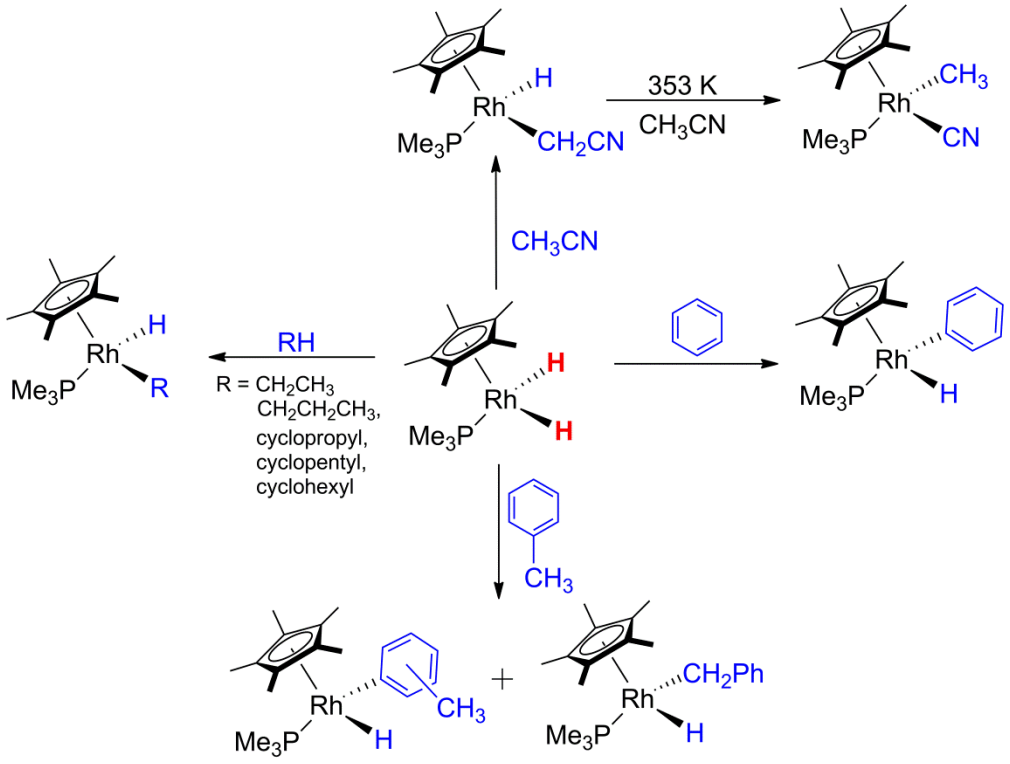

Scheme 22. Photochemistry of $Cp^*Rh(H)_2(PMe_3)$

Studies in low temperature matrices revealed that a $16e^-$ transient with a characteristic UV-vis absorption band was formed when $CpRh(H)_2(PMe_3)$ complex was irradiated; H_2 reductive elimination, the primary photochemical process, could be partially reversed by long wavelength photolysis. Furthermore the transient showed reactivity in CH_4-, CO- and N_2-doped matrices to produce the insertion/coordination products.[121]

The substitution of the Cp* with the bulkier Tp' ligand led to three dihydride complexes that undergo photoejection of H_2 to form coordinatively unsaturated species capable of inserting into C-H bonds of arenes, $Tp'Rh(H)_2(L)$ (L = PMe_3, PMe_2Ph, $CNCH_2CMe_3$).[253-254] In addition to the phenyl hydride complex, irradiation of $Tp'Rh(H)_2(PMe_2Ph)$ yields the cyclometalated complex

Tp'RhH($PMe_2C_6H_4$). The selectivity for C-H activation over C-F activation and for the C-H bonds ortho to fluorine is revealed by photolysis of Tp'Rh$(H)_2$(L) (L = PMe_3, PMe_2Ph) in fluoroarenes. This selectivity originates in the increased Rh-C bond dissociation energy which correlates with the C-H bond dissociation energy (Figure 16**)**.[254] Like Cp*$RhH_2(PMe_3)$, the photoreactions of Tp'Rh$(H)_2$(L) (L = PMe_3, PMe_2Ph), results in C-H bond activation of CH_3CN.[255] More recently, Tp'Rh$(H)_2(PMe_3)$ was employed in investigations on intramolecular and intermolecular selectivity between C-H and "hetero-bonds" (hetero = C-F, Si-H, B-H).[126] Notably, C-F bond activation is observed with pentafluoropyridine, but neither C-F bond activation nor arene coordination occurs with hexafluorobenzene allowing the latter to be used as an inert solvent. There is strong intramolecular selectivity for the Si-H bond over C-H bonds in SiH_2Et_2 but lower selectivity in SiH_3Ph. The lack of dependence of the photochemical conversion on [substrate] demonstrated that this is a dissociative reaction. Irradiation with a laser within the NMR probe of C_6F_6 solutions containing two substrates allowed the intermolecular selectivity to be determined (see Section 3.2). It is commonly assumed that thermal reactions of methyl hydride complexes are comparable to photochemical reactions of dihydride reactions in generating a coordinatively unsaturated intermediate. A comparison between photochemical and thermal reactivity, using Tp'RhH(CH_3)(PMe_3) as a thermal precursor in the presence of a variety of substrates was undertaken and the kinetics studied. Interestingly, it was found that the two complexes followed different mechanisms despite forming the same final products (Figure 17).[126]

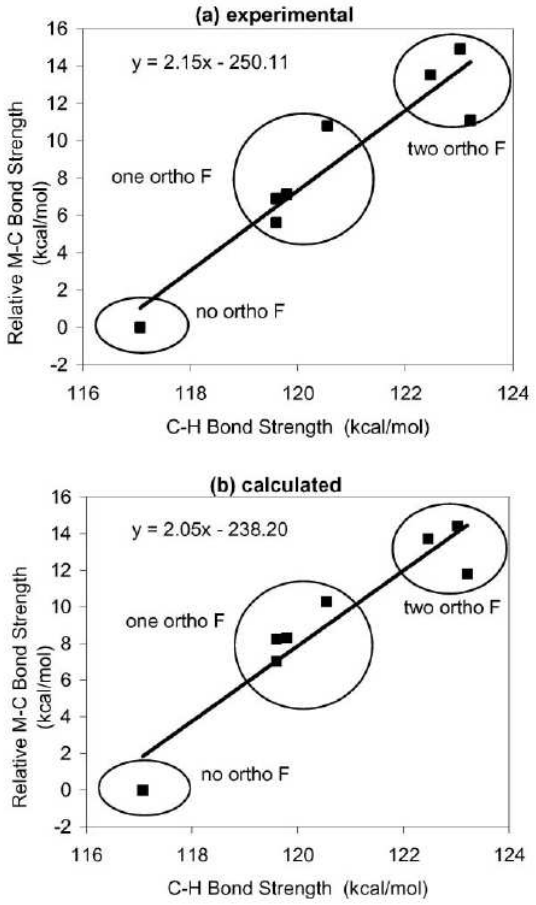

Figure 16. Plot of relative Rh–Ar^F bond strength *vs.* calculated C–H bond strength (kcal/mol); Experimental result (a) and DFT calculated result (b).[254]

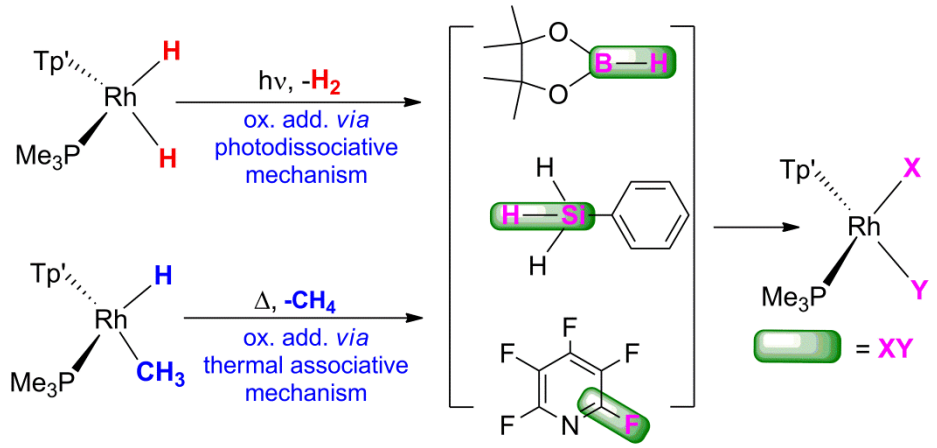

Figure 17. Reactivity of Tp'RhH(CH_3)(PMe_3) and Tp'RhH(CH_3)(PMe_3).[126]

The triphenylphosphine complex $Rh(H)_2(Cl)(PPh_3)_3$ exhibits concerted reductive elimination of dihydrogen under irradiation to give Wilkinson's complex $[RhCl(PPh_3)_3]$, as shown by flash photolysis [256] This reactivity contrasted strongly with that of the iridium analogue (see below). Photocatalytic dehydrogenation of cyclohexane was observed on irradiation of $Rh(H)_2(Cl)(PCy_3)_2$ or of $Rh(Cl)(PCy_3)_2$ with optimum activity with $\lambda > 270$ nm photolysis and the same wavelength dependence for both complexes. A catalytic cycle was postulated in which cyclohexane attacks $Rh(Cl)(PCy_3)_2$ to form the cyclohexyl hydride; thermal β-elimination yields the cyclic alkene and $Rh(H)_2(Cl)(PCy_3)_2$ before photoelimination of H_2 regenerates the reactive intermediate.[257]

The photoreactivity of $[CpM(CO)_2]_2$ with $Cp^*Rh(H)_2(SiEt_3)_2$ was exploited in the synthesis of trinuclear complexes, the fragment formed by H_2 elimination was capable of inserting into $[CpM(CO)_2]_2$ (M = Co, Ru, Ni, Fe) dimers to yield different types of metal clusters.[233] No evidence was provided that the rhodium complex was the light absorber rather than the metal carbonyl. Finally, the dimeric dihydride *syn*-$[Rh^{II,II}ClH_2(tfepma)_3]$ (tfepma = bis[bis(trifluoroethoxy)phosphinomethylamine, $MeN(P[OCH_2CF_3]_2)_2$) was shown to eliminate H_2 photochemically to form a short lived blue product along with a stoichiometric amount of H_2. Although there is one hydride ligand on each metal, photoreaction of a mixture of Rh_2D_2 and Rh_2H_2 gives predominantly H_2 and D_2. The blue intermediate is thought to be $[Rh_2^{I,I}(tfepma)_3Cl_2]$. This process was a step in a more complicated photocycle for the production of H_2 in homogeneous solutions of hydrohalic acids.[95] The photochemical reactions of the dihydrogen complex $Rh(H_2)(PCP)$ have been described earlier (section 2.4).[92]

The first Ir-dihydride reported to undergo photochemical H_2 elimination was the Vaska`s-H_2 adduct $Ir(H)_2Cl(CO)(PPh_3)_2$; the photochemical reaction yielded the Ir^I square planar complex. Similar behavior was observed for the dihydride iodide analogue and for the dihydrides formed from H_2 addition to the cations $[Ir(dppe)_2]^+$ and $[Ir(dppv)_2]^+$.[258] The replacement of CO with PPh_3 afforded $Ir(H)_2(Cl)(PPh_3)_3$ and resulted in very similar photochemistry (quantum yield for loss of H_2 0.56 ± 0.3); cyclometalation of the PPh_3 ligand was also observed in this case (Scheme 23) and the sequence could be reversed photochemically under H_2. Photolysis of a mixture of $Ir(H)_2(Cl)(PPh_3)_3$ and $Ir(D)_2(Cl)(PPh_3)_3$ gave only H_2 and D_2.[259] Laser flash photolysis investigations (with a 20 μs xenon arc flash lamp) on both Vaska`s dihydride and the *tris*-PPh_3 analogue resulted in the observation of a common intermediate assigned to $[IrCl(PPh_3)_2]$ formed from CO or PPh_3 loss respectively. It was postulated that H_2 elimination would follow after the dissociation of those ligands.[256] A more modern approach with time-resolved IR spectroscopy on $IrCl(CO)(PPh_3)_2$ did not support this interpretation, but there

has been no re-examination of the dihydride complexes.[260]

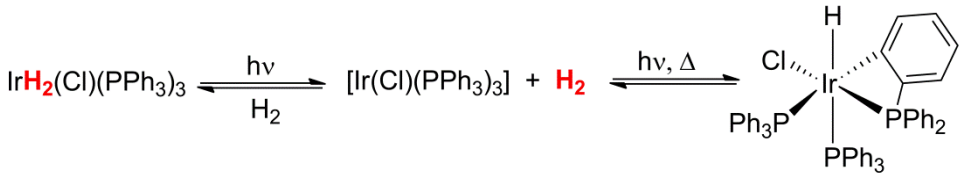

Scheme 23. Photoreaction of $Ir(H)_2(Cl)(PPh_3)_2$ and intramolecular insertion into the C-H bond of the phosphine phenyl group

The photochemical reactivity of $Cp^*Ir(H)_2(PMe_3)$ toward alkanes, in particular cyclohexane and neopentane, heralded the age of C-H bond activation of alkanes. Like the rhodium analogues investigated slightly later, this molecule eliminates H_2 under irradiation to form a very reactive $16e^-$ fragment that acts as the intermediate in these reactions.[261-263] The kinetic selectivity of the intermediate for benzene over cyclohexane is (3.5 ± 0.1):1, compared to *ca.* (9.1 ± 0.6):1 for the rhodium analogue. The reaction of $Cp^*IrH(Cl)(PMe_3)$ with strong base appears to give the same intermediate as obtained by photolysis of $Cp^*Ir(H)_2(PMe_3)$. However, the kinetic selectivities and kinetic isotope effects are significantly different, probably because the salt that is eliminated stays bound to iridium.[264] The reactions of $(\eta^5\text{-Ind})Ir(H)_2(PMe_3)$ with alkanes and benzene are similar to those of $Cp^*Ir(H)_2(PMe_3)$.[265] Although both $Cp^*Ir(H)_2(PPh_3)$ and $Cp^*Ir(H)_2(PMe_3)$ proved capable of inserting into the C-H bonds of benzene, only the PMe_3 complex attacks alkanes. When the reaction was run in CH_3CN, the PPh_3 complex reacted to form a cyclometalated product.

Photochemistry of $CpIr(H)_2(PMe_3)$ in Ar matrices allowed detection of the $16e^-$ transient confirming H_2 photoelimination as the primary process; the highly reactive fragment $[CpIr(PMe_3)]$ inserted into the C-H bond of methane to form an Ir-methyl hydride species.[121] The analogue with phosphine replaced by CO, $CpIr(H)_2(CO)$ once again undergoes H_2 reductive elimination as the primary and only photoprocess in 12 K matrix photochemistry. Again this complex acts as a C-H activator in methane matrices yielding $CpIrH(CH_3)(CO)$. A more complicated situation was found in solution photochemistry where H/D scrambling during neopentane activation at 298 K disagreed with H_2 loss as the sole pathway.[122,266] In a more unusual study, the same complex was impregnated into zeolite materials and photolyzed in the presence of D_2, HBr, CO, C_6H_6 and alkanes. In contrast to solution photochemistry, no reactivity was detected in the presence of arenes and alkanes.[267]

An important step in the application of photochemical C-H activation was the photocatalytic dehydrogenation (λ_{ex} = 254 nm) of linear and cyclic alkanes using the complex

$Ir(H)_2(\kappa^2\text{-}O_2CCF_3)(PAr_3)_2$ in the presence of CH_2=CH*t*-Bu as hydrogen acceptor. The reaction still proceeded when the hydrogen acceptor was omitted, but with reduced turnover number. The unsaturated reactive species formed *via* H_2 reductive photoelimination is postulated to react with the alkane; the resulting alkyl hydride undergoes β-elimination to regenerate $Ir(H)_2(\kappa^2\text{-}O_2CCF_3)(PAr_3)_2$.[268-269]

The photochemical reactivity of Tp'$Ir(H)_2$(cyclooctene) with phosphites was also investigated; cyclooctene was shown to be the photolabile ligand with H_2 still bound to the metal center in the products. The initially formed [Tp'$Ir(H)_2$] intermediate undergoes a complex series of reactions with incoming ligands and with benzene solvent.[270] The vinyl complex $Ir(H)_2$(CH=CHPh)(triphos) is isomerized photochemically to two isomers of IrH(triphos)(η^2-CH_2=CHPh); the H_2-loss product $Ir(H)_2$(C≡CPh)(triphos) is also formed. The latter undergoes photoisomerization to IrH(triphos)(η^2-CH=CPh) probably *via* a vinylidene complex. The photochemistry of $Ir(H)_2(C_2H_5)$(triphos) was less clean, producing several metal products and gases due to secondary photolysis of the species formed in solution.[40]

4.6.3 Group 9 polyhydrides. Examples of trihydrides of group 9 involved in photochemical reactions are scarce. $Rh(H)_3$(triphos) reacted photochemically to eliminate H_2 and form transient [RhH(triphos)] which reacts rapidly with HBpin to form $Rh(H)_2$(Bpin)(triphos);[54] the Ir analogue also showed photoactivity in C_6H_6 to form the metal(hydride)phenyl species and H_2 gas.[40] Finally, the irradiation of *mer* and *fac*-$[Ir(H)_3(PPh_3)_3]$ led to H_2 loss and cyclometalation. If the same complex was photolyzed under a hydrogen atmosphere, $Ir(H)_5(PPh_3)_2$ was the product detected suggesting that H_2 loss was inhibited under these conditions, allowing loss of PPh_3 to be observed.[259]

4.7 Group 10 metals

Examples of photoactive compounds become very rare as we move to the right of group 9. To our knowledge there are no palladium hydrides which have been investigated photochemically and we have found only one example for nickel where a $Ni(H_2)(CO)_3$ complex underwent photodissociation of H_2 in H_2/Ar matrices.[271] Platinum offers a few more examples of photoactive mono and dihydrides. The d^8 square planar monohydride *trans*-$[PtH(CH_2CN)(PPh_3)_2]$ was observed to isomerize to the *cis*-analogue on photolysis in a glass at 77 K, which underwent reductive elimination on warming. Solution photolysis (λ_{ex} 313 or 334 nm) caused reductive elimination of acetonitrile and formation of $[Pt(PPh_3)_2]_2$. Crossover experiments indicated that the reductive elimination proceeds without loss of phosphine.[272] Complexes c*is*-$[PtH(SnPh_3)(PCy_3)_2]$, c*is*-$[PtH(SiR_2R')(PCy_3)_2]$ (R, R' = H, alkyl, phenyl, $OSiMe_3$, etc.), and *cis*-

$[PtH(4\text{-}C_5NF_4)(PCy_3)_2]$ also isomerized to the *trans*-form under photolytic conditions.[54,273-274] The photochemistry of the dinuclear complexes $[Pt_2(H)_2(\mu\text{-}H)(dppm)_2]^+$ and $[Pt_2(H)_2(\mu\text{-}Cl)(dppm)_2]^+$ was summarized in section 2.5.[94] The related $[\{PtMe(dppm)\}(\mu\text{-}H)]PF_6$ undergoes photochemical reductive elimination of methane.[275]

Dissociation of H_2 as a primary photochemical step was also detected for a class of square planar $Pt(H)_2(PP)$ complexes (PP = $(t\text{-}Bu)_2P(CH_2)_2P(t\text{-}Bu)_2$, $(t\text{-}Bu)_2P(CH_2)_3P(t\text{-}Bu)_2$, $(t\text{-}Bu)(Ph)P(CH_2)_2P(Ph)(t\text{-}Bu)$); the reactive $14e^-$ intermediate formed was capable of inserting into the C-H bonds of benzene to form PtH(Ph)(PP).[276] Finally, photoejection of H_2 from the cluster $Pt_2Re_2(CO)_7(Pt\text{-}Bu_3)_2(\mu\text{-}H)_4$ took place at room temperature, the same reactivity was achieved thermally at 97° C.[200]

4.8 Group 11 metals

Group 11 is even poorer in examples than group 10. Studies of atom photochemistry in cryogenic matrices were first reported for Cu; the fragmentation of $(CH_3)CuH$ when irradiated yielded Cu, CH_3, CuH, $CuCH_3$ and H.[217] Similar studies were performed on all the group 11 elements with the laser-ablation method of generating the atoms; methane activation afforded the C-H activated products which were observed to fragment under further excitation.[277]

The two additional examples found are of metal clusters capable of H_2 ejection through light initiation; $[Cu_{20}H_{11}(S_2P(O^iPr)_2)_9]$ was reported to release H_2 upon sunlight irradiation[278] and $[Ag_3(H)_2(dppm)]^+$ showed similar behavior upon laser-induced dissociation of the mass-selected ion in the mass spectrometer; deuteration experiments confirmed that the H_2 came from hydride reductive elimination and not from the protons on the ligands.[279]

5. CONCLUSIONS AND OUTLOOK

Our survey of metal hydride photochemistry has revealed numerous examples of metal mono and dihydrides that are photosensitive. The photochemical pathways exhibited by these two classes are strikingly different (Scheme 1 and Scheme 3). Whereas *cis*-dihydride complexes are highly likely to be photoactive with respect to H_2 reductive elimination, the photochemical behavior of monohydride complexes is less predictable. They may undergo one of several processes including M-H homolysis or, for alkyl and silyl hydride complexes, reductive elimination. Photodissociation of other ligands competes with processes involving M-H bonds in many examples but by no means in all. For example, H_2-elimination is the only process in $Ru(H)_2(CO)(etp)$ and $CpIr(H)_2(CO)$. Likewise, reductive elimination of alkanes is the only process for $Cp^*_2ZrH(alkyl)$. The selectivity of photoreaction, of great importance in synthetic

chemistry, has been explored in detail in some examples, such as $Tp'Rh(H)_2(PMe_3)$. It is often assumed that *thermal* elimination of alkanes from alkyl hydrides is equivalent to *photochemical* elimination of H_2 from dihydrides – there is evidence that this is an oversimplification and the pathways differ significantly. The photochemistry of metal polyhydrides and complexes with bridging hydrides is underexplored, but there are exciting developments for bridging hydrides, that are relevant to bioinorganic chemistry. Photochemistry of paramagnetic metal hydrides has barely been explored outside the matrix environment. Another approach with opportunities for more investigation is the formation of charge-transfer complexes that are photosensitive at much longer wavelengths than their constituent components. Applications of dissociative photochemistry in photocatalysis have been published since the early years of metal hydride photochemistry, but will become more important as understanding of how to generate activity with visible radiation advances.

The photoprocesses mentioned so far are likely to involve dissociative excited states, but the ultrafast transient experiments that might prove this are few and far between. There is more information on quantum yields, but measurements are hampered by the lack of distinctive absorption bands for the metal hydride and its product in many examples. On the other hand, transient absorption methods have been exploited extensively for group 8 metal dihydrides to determine the spectra, structure and reactivity of the transient reactive intermediates. With improvements in the technique, it should be possible to make more use of time-resolved infrared spectroscopy.

Luminescent metal hydride complexes are a rarity: we found examples containing pyridine or polypyridine ligands together with a pair of tetrahydrides $MH_4(dppe)_2$ (M = Mo, W). These complexes must have equilibrated excited states with potential for new reactions as demonstrated by the extraordinary excited state acidity and hydricity of $[Cp^*(H)(bpy)]^+$. Although photocatalysis with this ion was first demonstrated many years ago, its great potential in this area is only now becoming clear.

AUTHOR INFORMATION

Corresponding authors

*E-mail: robin.perutz@york.ac.uk

*E-mail: barbara.procacci@york.ac.uk

Notes

The authors declare no competing financial interests.

Biographies

Robin Perutz has devoted most of his career to transition metal photochemistry. After undergraduate studies in Cambridge he studied for his PhD, partly in Cambridge and partly in Newcastle-upon-Tyne under the supervision of J. J. Turner investigating metal carbonyl photochemistry in matrices. After postdoctoral work in Mülheim, he took up fixed term positions in Edinburgh and Oxford. It was in Oxford that he was introduced to the photochemistry of $Cp_2Mo(H)_2$ and $Cp_2W(H)_2$ by M. L H. Green. He moved to York in 1983 where he became a full professor in 1991. Another formative event was the visit of W. D. Jones to York in 1989 which started the research on $Ru(H)_2(dmpe)_2$. Nowadays, his research includes the development of new photochemical methods and the use of photochemistry to in solar fuels. He also investigates the chemistry of C-F bond activation. He has received awards from the Royal Society of Chemistry, the Italian Chemical Society and the French Chemical Society. He became a Fellow of the Royal Society, the UK's national academy, in 2010. He has been very active in the women in science agenda for almost 15 years. He served as President of Dalton Division of the Royal Society of Chemistry. In 2015, he was elected a Fellow of the American Association for the Advancement of Science.

Barbara Procacci graduated from the Università degli Studi di Perugia in 2007. She completed her PhD in 2012 at the University of York under the supervision of Professor Robin Perutz working on photoinduced C-F, C-H, B-H and Si-H activation by Rh and Ru complexes focusing on mechanistic investigations. She then decided to take up a position in York as a postdoctoral research fellow to work on a project jointly supervised by Professor Simon Duckett and Professor Robin Perutz. Her work is aimed to develop NMR spectroscopy as a time-resolved technique to monitor light-initiated organometallic reactions which happen on a fast timescale.

ACKNOWLEDGMENTS

We acknowledge support from EPSRC. RNP is grateful to the many colleagues who have worked with him on metal hydride photochemistry.

ABBREVIATIONS:

Bpy 2,2' - Bipyridine

CASSCF	Complete active space configuration self-consistent field
CASPT	Complete Active Space with Second-order Perturbation Theory
CCI	Contracted configuration interaction
Cp	Cyclopentadienyl
Cp*	Pentamethylcyclopentadienyl
CT	Charge transfer
depe	1,2- bis(diethylphosphino)ethane
dfepe	1,2- bis(di(pentafluoroethyl)phosphino)ethane
dft	Density functional theory
dmpe	1,2- bis(dimethylphosphino)ethane
dmpm	1,2- bis(dimethylphosphino)methane
dpe	1,2-bis(phosphino)ethane
dppe	1,2- bis(diphenylphosphino)ethane
dppm	1,2- bis(diphenylphosphino)methane
dppv	*Cis*-1,2-bis(diphenylphosphino)ethene
Duphos	1,2-bis-2,5-dimethylphospholane
em	emission
etp	bis(diphenylphosphinoethyl)phenylphosphine
EPR	Electron paramagnetic resonance
ex	excitation
GC	Gas chromatography
HOMO	Highest occupied molecular orbital
IR	Infrared
KIE	Kinetic isotope effect
LF	Ligand field
LUMO	Lowest unoccupied molecular orbital
MCD	Magnetic circular dichroism
MLCT	Metal-to-ligand charge transfer
MRCI	Multi-reference configuration interaction
NHC	N-Heterocyclic carbene
NHE	Normal hydrogen electrode
NMR	Nuclear magnetic resonance
pdt	Propanedithiolate
PHIP	*para*-hydrogen induced polarization

phen	1,10-phenanthroline
pin	Pinacol
PP_3	Tris[2-(diphenylphosphino)ethyl]phosphine
rf	Radio frequency
SCF	Self-consistent field
SOMO	Singly occupied molecular orbital
tcne	Tetracyanoethylene
THF	Tetrahydrofuran
TOF	Turnover frequency
TON	Turnover number
Tp'	Tris(3,5-dimethyl-1-pyrazolyl)borate
Trip	2,4,6-triisopropylphenyl
triphos	$MeC(CH_2PPh_2)_3$
UV	Ultraviolet

REFERENCES

(1) Camus, A.; Cocevar, C.; Mestroni, G. Cobalt complexes of 2,2'-bipyridine and 1,10-phenanthroline .2. Reactions with molecular-hydrogen and conjugated dienes in presence of tertiary phosphines. *J. Organomet. Chem.* **1972**, *39*, 355-364.

(2) Giannotti, C.; Green, M. L. H. Photoindued insertion of bis-π-cyclopentadienyl tungsten into aromatic carbon-hydrogen bonds *J. Chem. Soc., Chem. Commun.* **1972**, 1114-1115.

(3) Arndtsen, B. A.; Bergman, R. G.; Mobley, T. A.; Peterson, T. H. Selective intermolecular carbon-hydrogen bond activation by synthetic metal-complexes in homogeneous solution. *Acc. Chem. Res.* **1995**, *28*, 154-162.

(4) Jones, W. D.; Feher, F. J. Comparative reactivities of hydrocarbon C-H bonds with a transition-metal complex. *Acc. Chem. Res.* **1989**, *22*, 91-100.

(5) Jones, W. D. Isotope effects in C-H bond activation reactions by transition metals. *Acc. Chem. Res.* **2003**, *36*, 140-146.

(6) Bandy, J. A.; Cloke, F. G. N.; Cooper, G.; Day, J. P.; Girling, R. B.; Graham, R. G.; Green, J. C.; Grinter, R.; Perutz, R. N. Decamethylrhenocene, $(\eta^5\text{-}C_5Me_5)_2Re$. *J. Am. Chem. Soc.* **1988**, *110*, 5039-5050.

(7) Torres, O.; Procacci, B.; Halse, M. E.; Adams, R. W.; Blazina, D.; Duckett, S. B.; Eguillor, B.; Green, R. A.; Perutz, R. N.; Williamson, D. C. Photochemical pump and nmr probe: Chemically created NMR coherence on a microsecond time scale. *J. Am. Chem. Soc.* **2014**, *136*, 10124-10131.

(8) Lukoyanov, D.; Khadka, N.; Yang, Z. Y.; Dean, D. R.; Seefeldt, L. C.; Hoffman, B. M. Reversible photoinduced reductive elimination of h_2 from the nitrogenase dihydride state, the $E_4(4H)$ janus intermediate. *J. Am. Chem. Soc.* **2016**, *138*, 1320-1327.

(9) Barrett, S. M.; Pitman, C. L.; Walden, A. G.; Miller, A. J. M. Photoswitchable hydride transfer from iridium to 1-methylnicotinamide rationalized by thermochemical cycles. *J. Am. Chem. Soc.* **2014**, *136*, 14718-14721.
(10) Suenobu, T.; Guldi, D. M.; Ogo, S.; Fukuzumi, S. Excited-state deprotonation and H/D exchange of an iridium hydride complex. *Angew. Chem., Int. Ed.* **2003**, *42*, 5492-5495.
(11) Shimogawa, R.; Takao, T.; Konishi, G.-i.; Suzuki, H. Photochemical reaction of diruthenium tetrahydride-bridged complexes with carbon dioxide: Insertion of CO_2 into a Ru-H bond versus C=O double-bond cleavage. *Organometallics* **2014**, *33*, 5066-5069.
(12) Suzuki, H.; Shimogawa, R.; Muroi, Y.; Takao, T.; Oshima, M.; Konishi, G. Bimetallic activation of 2-alkanones through photo-induced alpha-hydrogen abstraction mediated by a dinuclear ruthenium tetrahydride complex. *Angew. Chem., Int. Ed.* **2013**, *52*, 1773-1776.
(13) Artero, V.; Chavarot-Kerlidou, M.; Fontecave, M. Splitting water with cobalt. *Angew. Chem., Int. Ed.* **2011**, *50*, 7238-7266.
(14) Dempsey, J. L.; Brunschwig, B. S.; Winkler, J. R.; Gray, H. B. Hydrogen evolution catalyzed by cobaloximes. *Acc. Chem. Res.* **2009**, *42*, 1995-2004.
(15) Stoll, T.; Castillo, C. E.; Kayanuma, M.; Sandroni, M.; Daniel, C.; Odobel, F.; Fortage, J.; Collomb, M. N. Photo-induced redox catalysis for proton reduction to hydrogen with homogeneous molecular systems using rhodium-based catalysts. *Coord. Chem. Rev.* **2015**, *304*, 20-37.
(16) Esswein, A. J.; Nocera, D. G. Hydrogen production by molecular photocatalysis. *Chem. Rev.* **2007**, *107*, 4022-4047.
(17) Lomoth, R.; Ott, S. Introducing a dark reaction to photochemistry: Photocatalytic hydrogen from FeFe hydrogenase active site model complexes. *Dalton Trans.* **2009**, 9952-9959.
(18) Wang, W. G.; Rauchfuss, T. B.; Bertini, L.; Zampella, G. Unsensitized photochemical hydrogen production catalyzed by diiron hydrides. *J. Am. Chem. Soc.* **2012**, *134*, 4525-4528.
(19) Pitman, C. L.; Miller, A. J. M. Molecular photoelectrocatalysts for visible light-driven hydrogen evolution from neutral water. *ACS Catal.* **2014**, *4*, 2727-2733.
(20) Balzani, V.; Ceroni, P.; Juris, A. *Photochemistry and photophysics, concepts, research and applications*; Wiley-VCH, 2014.
(21) Ito, T. Oxidative addition reactions involving molybdenum polyhydrides. *Bull. Chem. Soc. Jpn.* **1999**, *72*, 2365-2377.
(22) Perutz, R. N.; Torres, O.; Vlček, A. J. Photochemistry of metal carbonyls In *Comprehensive inorganic chemistry II*; Reedijk, J., Poeppelmeier, K., Eds.; Elsevier: Oxford, 2013; Vol. 8, Ch. 8.06 p. 229-253.
(23) Grebenik, P.; Grinter, R.; Perutz, R. N. Metallocenes as reaction intermediates. *Chem. Soc. Rev.* **1988**, *17*, 453-490.
(24) Perutz, R. N. Tilden lecture - organometallic intermediates - ultimate reagents. *Chem. Soc. Rev.* **1993**, *22*, 361-369.
(25) Andrews, L. Matrix infrared spectra and density functional calculations of transition metal hydrides and dihydrogen complexes. *Chem. Soc. Rev.* **2004**, *33*, 123-132.
(26) Rest, A. J.; Turner, J. J. Evidence for production of hydridotetracarbonylmanganese $HMn(CO)_4$ on reversible photolysis of hydridopentacarbonylmanganese $HMn(CO)_5$ in argon at 15 degrees k. *J. Chem. Soc. D, Chem. Commun.* **1969**, 375-&.
(27) Church, S. P.; Poliakoff, M.; Timney, J. A.; Turner, J. J. The generation in solid co of the radical $Mn(CO)_5$. *J. Mol. Struct.* **1982**, *80*, 159-162.
(28) Symons, M. C. R.; Sweany, R. L. An electron-spin resonance study of matrix-isolated pentacarbonylmanganese(0) - formation from photolyzed pentacarbonylhydridomanganese(I). *Organometallics* **1982**, *1*, 834-836.

(29) Church, S. P.; Poliakoff, M.; Timney, J. A.; Turner, J. J. Photochemistry of matrix-isolated $HMn(CO)_5$ - evidence for 2 isomers of $HMn(CO)_4$. *Inorg. Chem.* **1983**, *22*, 3259-3266.
(30) Blakney, G. B.; Allen, W. F. Electronic spectra of some pentacarbonyl compounds of manganese and rhenium. *Inorg. Chem.* **1971**, *10*, 2763-2770.
(31) Hachey, M. R. J.; Daniel, C. The spectroscopy of $HMn(CO)_5$: A casscf/mrci and caspt2 ab initio study. *Inorg. Chem.* **1998**, *37*, 1387-1391.
(32) Brahim, H.; Daniel, C.; Rahmouni, A. Spin-orbit absorption spectroscopy of transition metal hydrides: A TD-DFT and MS-CASPT2 study of $HM(CO)_5$ (M = Mn, Re). *Int. J. Quantum Chem.* **2012**, *112*, 2085-2097.
(33) Eyermann, C. J.; Chung-Phillips, A. Electronic-structure of $HMn(CO)_5$, $H_2Fe(CO)_4$, and $HCo(CO)_4$ - molecular-orbitals, transition energies, and photoactive states. *J. Am. Chem. Soc.* **1984**, *106*, 7437-7443.
(34) Daniel, C. The photochemistry of transition-metal hydrides - a CASSCF/CCI study of the photodissociation of $HMn(CO)_5$. *J. Am. Chem. Soc.* **1992**, *114*, 1625-1631.
(35) Miller, F. D.; Sanner, R. D. Activation of benzene carbon hydrogen-bonds via photolysis or thermolysis of $(\eta^5\text{-}C_5Me_5)_2Zr(alkyl)H$ - isolation of $(\eta^5\text{-}C_5Me_5)_2Zr(C_6H_5)H$ and its conversion to a complex containing a tetramethylfulvene ligand. *Organometallics* **1988**, *7*, 818-825.
(36) Liu, D. K.; Brinkley, C. G.; Wrighton, M. S. Photochemistry of iron and ruthenium carbonyl-complexes - evidence for light-induced loss of carbon-monoxide and reductive elimination of triethylsilane from cis-mer-$HM(SiEt_3)(CO)_3(PPh_3)$. *Organometallics* **1984**, *3*, 1449-1457.
(37) Glueck, D. S.; Winslow, L. J. N.; Bergman, R. G. Iridium alkoxide and amide hydride complexes - synthesis, reactivity, and the mechanism of O-H and N-H reductive elimination. *Organometallics* **1991**, *10*, 1462-1479.
(38) Ford, P. C.; Hintze, R. E.; Petersen, J. D. Photochemistry of the heavier elements In *Concepts of inorganic photochemistry*; Adamson, A. W., Fleischauer, P. D., Eds.; Wiley: New York, 1975, Ch. 5 p. 203-267.
(39) Garg, K.; Matsubara, Y.; Ertem, M. Z.; Lewandowska-Andralojc, A.; Sato, S.; Szalda, D. J.; Muckerman, J. T.; Fujita, E. Striking differences in properties of geometric isomers of $Ir(tpy)(ppy)H^+$: Experimental and computational studies of their hydricities, interaction with CO_2, and photochemistry. *Angew. Chem., Int. Ed.* **2015**, *54*, 14128-14132.
(40) Bianchini, C.; Barbaro, P.; Meli, A.; Peruzzini, M.; Vacca, A.; Vizza, F. Thermal and photochemical C-H bond activation reactions at iridium-π -coordination vs C-H cleavage of ethene, styrene, and phenylacetylene. *Organometallics* **1993**, *12*, 2505-2514.
(41) Montiel-Palma, V.; Perutz, R. N.; George, M. W.; Jina, O. S.; Sabo-Etienne, S. Two photochemical pathways in competition: Matrix isolation, time-resolved and nmr studies of cis- $Ru(PMe_3)_4(H)_2$. *Chem. Commun.* **2000**, 1175-1176.
(42) Green, M. L. H.; Berry, M.; Couldwell, C.; Prout, K. Photoinduced insertion of tungsten into a C-H bond of tetramethylsilane. *New J. Chem.* **1977**, *1*, 187-188.
(43) Ketkov, S. Y.; Kutyreva, V. V.; Ob'edkov, A. M.; Domrachev, G. A. Gas-phase electronic absorption spectra of metallocene dihydrides $M(\eta^5\text{-}C_5H_5)_2H_2$ (M = Mo, W). *J. Organomet. Chem.* **2002**, *664*, 106-109.
(44) Geoffroy, G. L.; Bradley, M. G. Photochemistry of transition-metal hydride complexes .3. Photoinduced elimination of molecular-hydrogen from $Mo(\eta^5\text{-}C_5H_5)_2H_2$. *Inorg. Chem.* **1978**, *17*, 2410-2414.
(45) Green, M. L. H.; O'Hare, D. The activation of carbon-hydrogen bonds. *Pure Appl. Chem.* **1985**, *57*, 1897-1910.

(46) Graham, R. G.; Grinter, R.; Perutz, R. N. Optical determination of magnetization behavior - a study of unstable metallocenes by magnetic circular-dichroism. *J. Am. Chem. Soc.* **1988**, *110*, 7036-7042.
(47) Bell, T. W.; Haddleton, D. M.; McCamley, A.; Partridge, M. G.; Perutz, R. N.; Willner, H. Photochemical isomerization of metal ethene to metal vinyl hydride complexes - a matrix-isolation and solution nmr-study. *J. Am. Chem. Soc.* **1990**, *112*, 9212-9226.
(48) Hill, J. N.; Perutz, R. N.; Rooney, A. D. Laser-induced fluorescence of rhenocene in low-temperature matrices - selective excitation and emission. *J. Phys. Chem.* **1995**, *99*, 531-537.
(49) Petri, S. H. A.; Neumann, B.; Stammler, H. G.; Jutzi, P. Silyl complexes of molybdenum and tungsten - synthesis, reactivity and structure. *J. Organomet. Chem.* **1998**, *553*, 317-329.
(50) Koloski, T. S.; Pestana, D. C.; Carroll, P. J.; Berry, D. H. Monobis(silyl) and bis(silyl) complexes of molybdenum and tungsten - synthesis, structures, and Si29 nmr trends. *Organometallics* **1994**, *13*, 489-499.
(51) Nakajima, T.; Mise, T.; Shimizu, I.; Wakatsuki, Y. A photochemical route to heterometallic complexes - synthesis and structural characterization of dinuclear and trinuclear complexes having a molybdenocene or tungstenocene unit. *Organometallics* **1995**, *14*, 5598-5604.
(52) Bergamini, P.; Sostero, S.; Traverso, O. Photochemistry of phosphine hydride complexes of iron group-metals. *J. Organomet. Chem.* **1986**, *299*, C11-C14.
(53) Hall, C.; Jones, W. D.; Mawby, R. J.; Osman, R.; Perutz, R. N.; Whittlesey, M. K. Matrix-isolation and transient photochemistry of $Ru(dmpe)_2H_2$ - characterization and reactivity of $Ru(dmpe)_2$ (dmpe = $Me_2PCH_2CH_2PMe_2$). *J. Am. Chem. Soc.* **1992**, *114*, 7425-7435.
(54) Callaghan, P. L.; Fernandez-Pacheco, R.; Jasim, N.; Lachaize, S.; Marder, T. B.; Perutz, R. N.; Rivalta, E.; Sabo-Etienne, S. Photochemical oxidative addition of B-H bonds at ruthenium and rhodium. *Chem. Commun.* **2004**, 242-243.
(55) Belt, S. T.; Scaiano, J. C.; Whittlesey, M. K. Determination of metal hydride and metal-ligand (L = CO, N_2) bond-energies using photoacoustic calorimetry. *J. Am. Chem. Soc.* **1993**, *115*, 1921-1925.
(56) Osman, R.; Perutz, R. N.; Rooney, A. D.; Langley, A. J. Picosecond photolysis of a metal dihydride - rapid reductive elimination of dihydrogen from $Ru(dmpe)_2H_2$ (dmpe=$(CH_3)_2PCH_2CH_2P(CH_3)_2$). *J. Phys. Chem.* **1994**, *98*, 3562-3563.
(57) Whittlesey, M. K.; Mawby, R. J.; Osman, R.; Perutz, R. N.; Field, L. D.; Wilkinson, M. P.; George, M. W. Transient and matrix photochemistry of $Fe(dmpe)_2H_2$ (dmpe = $Me_2PCH_2CH_2PMe_2$) - dynamics of C-H and H-H activation. *J. Am. Chem. Soc.* **1993**, *115*, 8627-8637.
(58) Cronin, L.; Nicasio, M. C.; Perutz, R. N.; Peters, R. G.; Roddick, D. M.; Whittlesey, M. K. Laser flash-photolysis and matrix-isolation studies of $Ru(R_2PCH_2CH_2PR_2)H_2$ (R=C_2H_5, C_6H_5, C_2F_5) - control of oxidative addition rates by phosphine substituents. *J. Am. Chem. Soc.* **1995**, *117*, 10047-10054.
(59) Nicasio, M. C.; Perutz, R. N.; Walton, P. H. Transient photochemistry, matrix isolation, and molecular structure of cis-$Ru(dmpm)_2H_2$ (dmpm = $Me_2PCH_2PMe_2$). *Organometallics* **1997**, *16*, 1410-1417.
(60) Osman, R.; Pattison, D. I.; Perutz, R. N.; Bianchini, C.; Casares, J. A.; Peruzzini, M. Photochemistry of $M(PP_3)H_2$ (M = Ru, Os; PP_3 = $P(CH_2CH_2PPH_2)_3$): Preparative, nmr, and time-resolved studies. *J. Am. Chem. Soc.* **1997**, *119*, 8459-8473.
(61) Montiel-Palma, V.; Pattison, D. I.; Perutz, R. N.; Turner, C. Photochemistry of $Ru(etp)(CO)H_2$ (etp = $PHP(CH_2CH_2PPH_2)_2$): Fast oxidative addition and coordination following exclusive dihydrogen loss. *Organometallics* **2004**, *23*, 4034-4039.

(62) Nicasio, M. C.; Perutz, R. N.; Tekkaya, A. Photochemistry of $Os(dmpe)_2H_2$: Matrix, transient solution, and nmr studies of 16-electron $Os(dmpe)_2$ (dmpe = $Me_2PCH_2CH_2PMe_2$). *Organometallics* **1998**, *17*, 5557-5564.

(63) Osman, R.; Pattison, D. I.; Perutz, R. N.; Bianchini, C.; Peruzzini, M. Pulsed-laser photolysis of $Os(PP_3)H_2$ $PP_3=P(CH_2CH_2PPH_2)_3$ - kinetic selectivity for reaction with methane. *J. Chem. Soc., Chem. Commun.* **1994**, 513-514.

(64) Vendrell, O.; Moreno, M.; Lluch, J. M. Fast hydrogen elimination from the $Ru(PH_3)_3(CO)(H)_2$ and $Ru(PH_3)_4(H)_2$ complexes in the first singlet excited states: A diabatic quantum dynamics study. *J. Chem. Phys.* **2004**, *121*, 6258-6267.

(65) Macgregor, S. A.; Eisenstein, O.; Whittlesey, M. K.; Perutz, R. N. A theoretical study of $M(PH_3)_4$ (M = Ru or Fe), models for the highly reactive d^8 intermediates $M(dmpe)_2$ (dmpe = Me_2PCH_2-CH_2PMe_2). Zero activation energies for addition of CO and oxidative addition of H_2. *J. Chem. Soc., Dalton Trans.* **1998**, 291-300.

(66) Ogasawara, M.; Macgregor, S. A; Streib, W. E.; Folting, K.;Eisenstein, O.;Caulton, K.G. Characterization and reactivity of an unprecedented unsaturated zero-valent ruthenium species: isolable, yet highly reactive. *J. Am. Chem. Soc.* **1996**, *118*, 10189-10199..

(67) Sweany, R. L. Matrix photolysis of tetracarbonyldihydridoiron - evidence for oxidative addition of dihydrogen on tetracarbonyliron. *J. Am. Chem. Soc.* **1981**, *103*, 2410-2412.

(68) Heitz, M. C.; Daniel, C. Photodissociation dynamics of organometallics: Quantum simulation for the dihydride complex $H_2Fe(CO)_4$. *J. Am. Chem. Soc.* **1997**, *119*, 8269-8275.

(69) Heitz, M. C.; Guillaumont, D.; Cote-Bruand, I.; Daniel, C. Photodissociation and electronic spectroscopy of transition metal hydrides carbonyls: Quantum chemistry and wave packet dynamics. *J. Organomet. Chem.* **2000**, *609*, 66-76.

(70) Vallet, V.; Bossert, J.; Strich, A.; Daniel, C. The electronic spectroscopy of transition metal di-hydrides $H_2M(CO)_4$ (M = Fe,Os): A theoretical study based on casscf/ms-caspt2 and td-dft. *Phys. Chem. Chem. Phys.* **2003**, *5*, 2948-2953.

(71) Vallet, V.; Strich, A.; Daniel, C. Spin-orbit effects on the electronic spectroscopy of transition metal dihydrides $H_2M(CO)_4$ (M = Fe, Os). *Chem. Phys.* **2005**, *311*, 13-18.

(72) Ampt, K. A. M.; Burling, S.; Donald, S. M. A.; Douglas, S.; Duckett, S. B.; Macgregor, S. A.; Perutz, R. N.; Whittlesey, M. K. Photochemical isomerization of N-heterocyclic carbene ruthenium hydride complexes: In situ photolysis, parahydrogen, and computational studies. *J. Am. Chem. Soc.* **2006**, *128*, 7452-7453.

(73) Merwin, R. K.; Ontko, A. C.; Houlis, J. F.; Roddick, D. M. Synthesis and characterization of CpMn(dfepe)(L) complexes (dfepe = $(C_2F_5)_2PCH_2CH_2P(C_2F_5)_2$; L = CO, H_2, N_2): An unusual example of a dihydride to dihydrogen photochemical conversion. *Polyhedron* **2004**, *23*, 2873-2878.

(74) Casey, C. P.; Tanke, R. S.; Hazin, P. N.; Kemnitz, C. R.; McMahon, R. J. Kinetic generation of cis-$C_5H_5(CO)_2ReH_2$ from the reaction of $C_5H_5(CO)_2Re(\mu\text{-}H)Pt(H)(PPh_3)_2$ with diphenylacetylene. *Inorg. Chem.* **1992**, *31*, 5474-5479.

(75) Jones, W. D.; Maguire, J. A.; Rosini, G. P. Thermal and photochemical substitution reactions of $CpRe(PPh_3)_2H_2$ and $CpRe(PPh_3)H_4$. Catalytic insertion of ethylene into the C-H bond of benzene. *Inorg. Chim. Acta* **1998**, *270*, 77-86.

(76) Jones, W. D.; Feher, F. J. Isotope effects in arene C-H bond activation by $(C_5Me_5)Rh(PMe_3)$. *J. Am. Chem. Soc.* **1986**, *108*, 4814-4819.

(77) Jones, W. D.; Rosini, G. P.; Maguire, J. A. Photochemical C-H activation and ligand exchange reactions of $CpRe(PPh_3)_2H_2$. Phosphine dissociation is not involved. *Organometallics* **1999**, *18*, 1754-1760.

(78) Ko, J. J.; Bockman, T. M.; Kochi, J. K. Photoinduced hydrometalation and hydrogenation of activated olefins with molybdenum and tungsten dihydrides (Cp_2MH_2). *Organometallics* **1990**, *9*, 1833-1842.

(79) Brewer, K. J.; Murphy, W. R.; Moore, K. J.; Eberle, E. C.; Petersen, J. D. Visible-light production of molecular-hydrogen by sensitization of a cobalt dihydride complex. *Inorg. Chem.* **1986**, *25*, 2470-2472.
(80) Webster, L. R.; Ibrahim, S. K.; Wright, J. A.; Pickett, C. J. Solar fuels: Visible-light-driven generation of dihydrogen at p-type silicon electrocatalysed by molybdenum hydrides. *Chem. Eur. J.* **2012**, *18*, 11798-11803.
(81) Graff, J. L.; Sobieralski, T. J.; Wrighton, M. S.; Geoffroy, G. L. Photophysical and photochemical behavior of tetrahydridobis(bis(1,2-diphenylphosphino)ethane)molybdenum and tungsten -optical-emission and photo-reduction of alkenes. *J. Am. Chem. Soc.* **1982**, *104*, 7526-7533.
(82) Pierantozzi, R.; Geoffroy, G. L. Photoinduced elimination of H_2 from $MoH_4(diphos)_2$ and $MoH_4(PPh_2Me)_4$. *Inorg. Chem.* **1980**, *19*, 1821-1822.
(83) Ito, T.; Matsubara, T. Insertion of carbon-dioxide into a molybdenum hydrogen-bond - photochemical formation of hydridoformato complex of molybdenum(II). *J. Chem. Soc., Dalton Trans.* **1988**, 2241-2242.
(84) Ito, T.; Tosaka, H.; Yoshida, S.; Mita, K.; Yamamoto, A. Selective activation of olefinic C-H bonds - reaction of a hydridomolybdenum complex with methacrylic esters to form hydrido alkenyl complexes. *Organometallics* **1986**, *5*, 735-739.
(85) Ito, T.; Matsubara, T.; Yamashita, Y. Selective C-O bond-cleavage of allylic esters using $MoH_4(PH_2PCH_2CH_2PPH_2)_2$ under light irradiation to give hydridocarboxylatomolybdenum(II) complexes. *J. Chem. Soc., Dalton Trans.* **1990**, 2407-2412.
(86) Kurishima, S.; Matsuda, N.; Tamura, N.; Ito, T. Bidentate cyclic imido complexes of molybdenum(ii) - preparation, solution behavior and x-ray crystal-structure. *J. Chem. Soc., Dalton Trans.* **1991**, 1135-1141.
(87) Ito, T.; Kurishima, S.; Tanaka, M.; Osakada, K. Oxidative addition of n-substituted amides to molybdenum(ii) involving N-H bond-cleavage to give (η^2-N-acylamido-N,O)hydridomolybdenum(II) complexes - X-ray molecular-structure of the 7-coordinate complex $MoH(N(COCH_3)CH_3)((C_6H_5)_2PCH_2CH_2P(C_6H_5)_2)_2$. *Organometallics* **1992**, *11*, 2333-2335.
(88) Eguillor, B.; Caldwell, P. J.; Cockett, M. C. R.; Duckett, S. B.; John, R. O.; Lynam, J. M.; Sleigh, C. J.; Wilson, I. Detection of unusual reaction intermediates during the conversion of $W(N_2)_2(dppe)_2$ to $W(H)_4(dppe)_2$ and of H_2O into H_2. *J. Am. Chem. Soc.* **2012**, *134*, 18257-18265.
(89) Sweany, R. L. Photolysis of hexacarbonylchromium in hydrogen-containing matrices - evidence of simple adducts of molecular-hydrogen. *J. Am. Chem. Soc.* **1985**, *107*, 2374-2379.
(90) Sweany, R. L. Photolysis of (cyclopentadienyl)tricarbonylhydridometal and (pentamethylcyclopentadienyl)tricarbonylhydridometal complexes of tungsten and molybdenum in dihydrogen-containing matrices - evidence for adducts of molecular-hydrogen. *J. Am. Chem. Soc.* **1986**, *108*, 6986-6991.
(91) Wang, X.; Andrews, L. Infrared spectra and theoretical calculations for Fe, Ru, and Os metal hydrides and dihydrogen complexes. *J. Phys. Chem. A* **2009**, *113*, 551-563.
(92) Doherty, M. D.; Grills, D. C.; Huang, K. W.; Muckerman, J. T.; Polyansky, D. E.; van Eldik, R.; Fujita, E. Kinetics and thermodynamics of small molecule binding to pincer-PCP rhodium(I) complexes. *Inorg. Chem.* **2013**, *52*, 4160-4172.
(93) Loges, B.; Boddien, A.; Junge, H.; Noyes, J. R.; Baumann, W.; Beller, M. Hydrogen generation: Catalytic acceleration and control by light. *Chem. Commun.* **2009**, 4185-4187.

(94) Foley, H. C.; Morris, R. H.; Targos, T. S.; Geoffroy, G. L. Photoinduced elimination of H_2 from $Pt_2H_3(dppm)_2PF_6$ and $Pt_2H_2Cl(dppm)_2$ PF_6. *J. Am. Chem. Soc.* **1981**, *103*, 7337-7339.
(95) Esswein, A. J.; Veige, A. S.; Nocera, D. G. A photocycle for hydrogen production from two-electron mixed-valence complexes. *J. Am. Chem. Soc.* **2005**, *127*, 16641-16651.
(96) Alvarez, C. M.; Garcia, M. E.; Ruiz, M. A.; Connelly, N. G. Diphenylphosphide-bridged diiron derivatives of $Fe_2(\eta^5\text{-}C_5H_5)_2(\mu\text{-}H)(\mu\text{-}PPh_2)(CO)_2$. *Organometallics* **2004**, *23*, 4750-4758.
(97) Procopio, L. J.; Berry, D. H. Dehydrogenative coupling of trialkylsilanes mediated by ruthenium phosphine complexes - catalytic synthesis of carbosilanes. *J. Am. Chem. Soc.* **1991**, *113*, 4039-4040.
(98) Brunner, H.; Peter, H. Optically-active transition-metal complexes .100. Photochemically induced cis-trans-isomerization in optically-active phosphido bridged iron complexes of the type $(CpFe(\mu\text{-}PR_2)CO)_2$ and $(Cp_2Fe_2(\mu\text{-}H)(\mu\text{-}PR_2)$ $(CO)_2)$. *J. Organomet. Chem.* **1990**, *393*, 411-422.
(99) Brunner, H.; Rotzer, M. Enantioselective catalysis .78. Optically-active phosphido-bridged iron complex $(\eta^5\text{-}C_5H_5)_2Fe_2(\mu\text{-}H)(\mu\text{-}PMen_2)(CO)_2$ - synthesis, isomerization, catalysis. *J. Organomet. Chem.* **1992**, *425*, 119-124.
(100) Yu, Y.; Sadique, A. R.; Smith, J. M.; Dugan, T. R.; Cowley, R. E.; Brennessel, W. W.; Flaschenriem, C. J.; Bill, E.; Cundari, T. R.; Holland, P. L. The reactivity patterns of low-coordinate iron-hydride complexes. *J. Am. Chem. Soc.* **2008**, *130*, 6624-6638.
(101) Heyduk, A. F.; Nocera, D. G. Hydrogen produced from hydrohalic acid solutions by a two-electron mixed-valence photocatalyst. *Science* **2001**, *293*, 1639-1641.
(102) Elgrishi, N.; Teets, T. S.; Chambers, M. B.; Nocera, D. G. Stability-enhanced hydrogen-evolving dirhodium photocatalysts through ligand modification. *Chem. Commun.* **2012**, *48*, 9474-9476.
(103) Barrett, S. M.; Slattery, S. A.; Miller, A. J. M. Photochemical formic acid dehydrogenation by iridium complexes: Understanding mechanism and overcoming deactivation. *ACS Catal.* **2015**, *5*, 6320-6327.
(104) Dombray, T.; Werncke, C. G.; Jiang, S.; Grellier, M.; Vendier, L.; Bontemps, S.; Sortais, J. B.; Sabo-Etienne, S.; Darcel, C. Iron-catalyzed C-H borylation of arenes. *J. Am. Chem. Soc.* **2015**, *137*, 4062-4065.
(105) Castro, L. C. M.; Bezier, D.; Sortais, J. B.; Darcel, C. Iron dihydride complex as the pre-catalyst for efficient hydrosilylation of aldehydes and ketones under visible light activation. *Adv. Synth. Catal.* **2011**, *353*, 1279-1284.
(106) Yu, M. M.; Jing, H. Z.; Liu, X.; Fu, X. F. Visible-light-promoted generation of hydrogen from the hydrolysis of silanes catalyzed by rhodium(III) porphyrins. *Organometallics* **2015**, *34*, 5754-5758.
(107) Perutz, R. N. Photochemical-reactions involving matrix-isolated atoms. *Chem. Rev.* **1985**, *85*, 77-96.
(108) Perutz, R. N. Photochemistry of small molecules in low-temperature matrices. *Chem. Rev.* **1985**, *85*, 97-127.
(109) Bondybey, V. E.; Smith, A. M.; Agreiter, J. New developments in matrix isolation spectroscopy. *Chem. Rev.* **1996**, *96*, 2113-2134.
(110) Khriachtchev, L.; Rasanen, M.; Gerber, R. B. Noble-gas hydrides: New chemistry at low temperatures. *Acc. Chem. Res.* **2009**, *42*, 183-191.
(111) Bell, S. E. J.; Hill, J. N.; McCamley, A.; Perutz, R. N. Laser-induced fluorescence of reactive metallocenes $(\eta^5\text{-}C_5H_5)_2Re$, $(\eta^5\text{-}C_5H_5)_2W$, $(\eta^5\text{-}C_5H_5)_2Mo$ and $(\eta^5\text{-}C_5Me_5)_2Re$. *J. Phys. Chem.* **1990**, *94*, 3876-3878.

(112) Schott, D.; Callaghan, P.; Dunne, J.; Duckett, S. B.; Godard, C.; Goicoechea, J. M.; Harvey, J. N.; Lowe, J. P.; Mawby, R. J.; Muller, G.; Perutz, R. N.; Poli, R.; Whittlesey, M. K. The reaction of $M(CO)_3(Ph_2PCH_2CH_2PPh_2)$ (M = Fe, Ru) with parahydrogen: Probing the electronic structure of reaction intermediates and the internal rearrangement mechanism for the dihydride products. *Dalton Trans.* **2004**, 3218-3224.

(113) Wang, X.; Andrews, L.; Infante, I.; Gagliardi, L. Matrix infrared spectroscopic and computational investigation of late lanthanide metal hydride species $MH_X(H_2)_Y$ (M = Tb-Lu, x=1-4, y=0-3). *J. Phys. Chem. A* **2009**, *113*, 12566-12572.

(114) Bitterwolf, T. E.; Linehan, J. C.; Shade, J. E. Solution and nujol matrix photochemistry of $(\eta^5\text{-}C_5H_5)_2Os_2(CO)_4$ and nujol matrix photochemistry of $(\eta^5\text{-}C_5H_4CH_3)_2Ru_2(CO)_4$ and $(\eta^5\text{-}C_5H_5)M(CO)_2H$, where M = Ru and Os. *Organometallics* **2001**, *20*, 775-781.

(115) Macrae, V. A.; Green, J. C.; Greene, T. M.; Downs, A. J. Thermal and photoyltic reactions of group 12 metal atoms in HCl-doped argon matrixes: Formation and characterization of the hydride species HMCl (M = Zn, Cd, or Hg). *J. Phys. Chem. A* **2004**, *108*, 9500-9509.

(116) Reinartz, S.; White, P. S.; Brookhart, M.; Templeton, J. L. Syntheses of platinum(IV) aryl dihydride complexes via arene C-H bond activation. *Organometallics* **2001**, *20*, 1709-1712.

(117) Cho, H. G.; Andrews, L. Methane activation by laser-ablated V, Nb, and Ta atoms: Formation of CH_3-MH, CH_2=MH_2, CH=MH_3-, and $(CH_3)_2MH_2$. *J. Phys. Chem. A* **2006**, *110*, 3886-3902.

(118) Girling, R. B.; Grebenik, P.; Perutz, R. N. Vibrational-spectra of terminal metal-hydrides - solution and matrix-isolation studies of $(\eta\text{-}C_5H_5)_2MH_n\ X^+$ (M = Re, Mo, W, Nb, Ta, n = 1-3, x = 0, 1). *Inorg. Chem.* **1986**, *25*, 31-36.

(119) Bakac, A. Photoinduced insertion of molecular oxygen into metal-hydrogen bonds. *J. Photochem. Photobiol. A, Chem* **2000**, *132*, 87-89.

(120) Chetwynd-Talbot, J.; Grebenik, P.; Perutz, R. N. Photochemical-reactions of $W(\eta\text{-}C_5H_5)_2L_n$, $Mo(\eta\text{-}C_5H_5)_2L_n$, $Cr(\eta\text{-}C_5H_5)_2L_n$, $V(\eta\text{-}C_5H_5)_2$ in in low-temperature matrices - detection of tungstenocene and molybdenocene. *Inorg. Chem.* **1982**, *21*, 3647-3657.

(121) Partridge, M. G.; McCamley, A.; Perutz, R. N. Photochemical generation of 16-electron $Rh(\eta^5\text{-}C_5H_5)\text{-}(PMe_3)$ and $Ir(\eta^5\text{-}C_5H_5)(PMe_3)$ in low-temperature matrices - evidence for methane activation. *J. Chem. Soc., Dalton Trans.* **1994**, 3519-3526.

(122) Bloyce, P. E.; Rest, A. J.; Whitwell, I. Photochemistry of carbonyl(η^5-cyclopentadienyl)dihydridoiridium in frozen gas matrices at ca 12 K - infrared evidence relating to C-H activation. *J. Chem. Soc., Dalton Trans.* **1990**, 813-821.

(123) Colombo, M.; George, M. W.; Moore, J. N.; Pattison, D. I.; Perutz, R. N.; Virrels, I. G.; Ye, T. Q. Ultrafast reductive elimination of hydrogen from a metal carbonyl dihydride complex; a study by time-resolved IR and visible spectroscopy. *J. Chem. Soc., Dalton Trans.* **1997**, 2857-2859.

(124) Frederix, P.; Adamczyk, K.; Wright, J. A.; Tuttle, T.; Ulijn, R. V.; Pickett, C. J.; Hunt, N. T. Investigation of the ultrafast dynamics occurring during unsensitized photocatalytic H_2 evolution by an FeFe -hydrogenase subsite analogue. *Organometallics* **2014**, *33*, 5888-5896.

(125) Campian, M. V.; Perutz, R. N.; Procacci, B.; Thatcher, R. J.; Torres, O.; Whitwood, A. C. Selective photochemistry at stereogenic metal and ligand centers of cis-Ru(diphosphine)$_2$(H)$_2$: Preparative, NMR, solid state, and laser flash studies. *J. Am. Chem. Soc.* **2012**, *134*, 3480-3497.

(126) Procacci, B.; Jiao, Y.; Evans, M. E.; Jones, W. D.; Perutz, R. N.; Whitwood, A. C. Activation of B-H, Si-H, and C-F bonds with Tp'Rh(PMe_3) complexes: Kinetics, mechanism, and selectivity. *J. Am. Chem. Soc.* **2015**, *137*, 1258-1272.

(127) Blazina, D.; Dunne, J. P.; Aiken, S.; Duckett, S. B.; Elkington, C.; McGrady, J. E.; Poli, R.; Walton, S. J.; Anwar, M. S.; Jones, J. A.; Carteret, H. A. Contrasting photochemical and thermal reactivity of $Ru(CO)_2(PPh_3)$(dppe) towards hydrogen rationalised by parahydrogen NMR and DFT studies. *Dalton Trans.* **2006**, 2072-2080.
(128) Xiao, Z. L.; Hauge, R. H.; Margrave, J. L. Reactions of vanadium and titanium with molecular-hydrogen in Kr and Ar matrices at 12 K. *J. Phys. Chem.* **1991**, *95*, 2696-2700.
(129) Andrews, L.; Cho, H. G.; Wang, X. Reactions of methane with titanium atoms: CH_3TiH, CH_2=TiH_2, agostic bonding, and $(CH_3)_2TiH_2$. *Inorg. Chem.* **2005**, *44*, 4834-4842.
(130) Cho, H. G.; Wang, X. F.; Andrews, L. Reactions of methane with hafnium atoms: CH_2=HfH_2, agostic bonding, and $(CH_3)_2HfH_2$. *Organometallics* **2005**, *24*, 2854-2861.
(131) Cho, H. G.; Wang, X. F.; Andrews, L. The C-H activation of methane by laser-ablated zirconium atoms: CH_2=ZrH_2, the simplest carbene hydride complex, agostic bonding, and $(CH_3)_2ZrH_2$. *J. Am. Chem. Soc.* **2005**, *127*, 465-473.
(132) Wang, G. J.; Gong, Y.; Chen, M. H.; Zhou, M. F. Methane activation by titanium monoxide molecules: A matrix isolation infrared spectroscopic and theoretical study. *J. Am. Chem. Soc.* **2006**, *128*, 5974-5980.
(133) Margulieux, G. W.; Semproni, S. P.; Chirik, P. J. Photochemically induced reductive elimination as a route to a zirconocene complex with a strongly activated N_2 ligand. *Angew. Chem., Int. Ed.* **2014**, *53*, 9189-9192.
(134) Foust, D. F.; Rogers, R. D.; Rausch, M. D.; Atwood, J. L. Photoinduced reactions of $(\eta^5\text{-}C_5H_5)_2NbH_3$ and $(\eta^5\text{-}C_5H_5)_2Nb(CO)H$ and $(\eta^5\text{-}C_5H_5)_2TaH_3$ and $(\eta^5\text{-}C_5H_5)_2Ta(CO)H$ and the molecular-structure of $(\eta^5\text{-}C_5H_5)_2Ta(CO)H$. *J. Am. Chem. Soc.* **1982**, *104*, 5646-5650.
(135) Baynham, R. F. G.; Chetwyndtalbot, J.; Grebenik, P.; Perutz, R. N.; Powell, M. H. A. Photochemistry of $Nb(\eta^5\text{-}C_5H_5)_2(H)CO$,$Ta(\eta^5\text{-}C_5H_5)_2(H)CO$ and $Nb(\eta^5\text{-}C_5H_5)_2H_3$,$Ta(\eta^5\text{-}C_5H_5)_2H_3$ in low-temperature matrices. *J. Organomet. Chem.* **1985**, *284*, 229-242.
(136) Braunschweig, H.; Gross, M.; Kraft, K. Synthesis and reactivity of 2 disilaniobocenophanes. *J. Organomet. Chem.* **2011**, *696*, 568-571.
(137) Darensbourg, D. J.; Incorvia, M. J. Solution photochemistry of anionic metal-carbonyl hydride derivatives - substitution and dimer disruption processes in μ-$H[M(CO)_5]_2^-$ (M = Cr and W). *Inorg. Chem.* **1979**, *18*, 18-22.
(138) Hynes, R. C.; Preston, K. F.; Springs, J. J.; Williams, A. J. EPR studies of $M(CO)_5^-$ radicals trapped in single-crystals of $PPN^+HM(CO)_5^-$ *Organometallics* **1990**, *9*, 2298-2304.
(139) Alt, H. G.; Mahmoud, K. A.; Rest, A. J. Photolysis of the cyclopentadienyl(hydrido) complexes $C_5H_5M(CO)_3H$ (M=Cr, Mo, W) in matrices and in solution - characterization of $C_5H_5W(CO)_2H_2$ and $C_5Me_5W(CO)_2H_2$. *Angew. Chem., Int. Ed.* **1983**, *22*, 544-545.
(140) Brumas-Soula, B.; Dahan, F.; Poilblanc, R. Transition-metal derivatives of the functionalized cyclopentadienyl ligand. XVI. Synthesis of the bridged complexes $[(\mu\text{-}\eta^5\text{-}C_5H_4PPh_2)M(CO)_2]_2$ (M = Cr, Mo, W). X-ray crystal structure of the dihydride derivative $[(\mu\text{-}\eta^5\text{-}C_5H_4PPh_2)W(CO)_2H]_2$. *New J. Chem.* **1998**, *22*, 15-23.
(141) Mahmoud, K. A.; Rest, A. J.; Alt, H. G. Photochemistry of tricarbonyl (η^5-cyclopentadienyl)hydrido complexes of molybdenum and tungsten and of dicarbonyl(η^5-cyclopentadienyl)(ethylene)hydridotungsten in solution and in frozen gas matrices at 12-k. *J. Chem. Soc., Dalton Trans.* **1984**, 187-197.
(142) Alt, H. G.; Mahmoud, K. A.; Rest, A. J. Matrix-isolation studies of hydroformylation intermediates - infrared spectroscopic evidence for stepwise substitution of ethylene into (η^5-cyclopentadienyl)tri-carbonyl(hydrido)molybdenum and (η^5-cyclopentadenyl)tri-carbonyl(hydrido)tungsten complex followed by insertion into the metal hydrogen-bond. *J. Organomet. Chem.* **1983**, *243*, C5-C9.

(143) Sweany, R. L. Formation of adducts of molecular-hydrogen and dicarbonyl(η^5 cyclopentadienyl)hydridomolybdenum in low-temperature matrices. *Organometallics* **1986**, *5*, 387-388.
(144) Cho, H. G.; Andrews, L. Infrared spectra of CH_3-MoH, CH_2=MoH_2, and $CHMoH_3$ formed by activation of CH_4 by molybdenum atoms. *J. Am. Chem. Soc.* **2005**, *127*, 8226-8231.
(145) Cho, H.-G.; Andrews, L. Infrared spectra and density functional calculations of CH_2=MHX and CH=MH_2X complexes prepared in reactions of methyl halides with Mo and W atoms. *J. Phys. Chem. A* **2006**, *110*, 13151-13162.
(146) Hoffman, N. W.; Brown, T. L. Thermal and photo-chemical substitution-reactions of tricarbonyl(cyclopentadienyl)hydrido compounds of tungsten and molybdenum. *Inorg. Chem.* **1978**, *17*, 613-617.
(147) Sakaba, H.; Ishida, K.; Horino, H. Synthesis of a silylene- and hydride-bridged re-w heterobimetallic complex and its photolysis to form novel silenyl-bridged heterobimetallic complexes. *Chem. Lett.* **1998**, 149-150.
(148) Angeles Alvarez, M.; Esther Garcia, M.; Ruiz, M. A.; Toyos, A.; Fernanda Vega, M. Heterometallic derivatives of the unsaturated ditungsten hydride $W_2(\eta^5$-$C_5H_5)_2(\eta)(\mu$-$PCy_2)(CO)_2$. *Inorg. Chem.* **2013**, *52*, 7068-7077.
(149) Xiao, Z. L.; Hauge, R. H.; Margrave, J. L. Reactions and photochemistry of chromium and molybdenum with molecular-hydrogen at 12-K. *J. Phys. Chem.* **1992**, *96*, 636-644.
(150) Geoffroy, G. L.; Bradley, M. G. Photoinduced elimination of H_2 from $Mo(\eta^5$-$C_5H_5)_2H_2$ - generation of molybdenocene. *J. Organomet. Chem.* **1977**, *134*, C27-C31.
(151) Berry, M.; Davies, S. G.; Green, M. L. H. Photoinduced synthesis of binuclear molybdenocene and tungstenocene derivatives - catalytic deoxygenation of epoxides by metallocenes. *J. Chem. Soc., Chem. Commun.* **1978**, 99-100.
(152) Jones, W. D.; Chin, R. M.; Crane, T. W.; Baruch, D. M. Carbon sulfur bond-cleavage in thiophene by group-6 metallocenes. *Organometallics* **1994**, *13*, 4448-4452.
(153) Grebenik, P.; Downs, A. J.; Green, M. L. H.; Perutz, R. N. Infrared spectroscopic evidence for photo-chemical generation of the metallocenes $(\eta$-$C_5H_5)_2$M (M = Mo Or W) in low-temperature matrices. *J. Chem. Soc., Chem. Commun.* **1979**, 742-744.
(154) Perutz, R. N.; Scaiano, J. C. Transient spectroscopy and kinetics of monomeric molybdenocene $Mo(\eta$-$C_5H_5)_2$ in solution. *J. Chem. Soc., Chem. Commun.* **1984**, 457-458.
(155) Cloke, F. G. N.; Day, J. P.; Green, J. C.; Morley, C. P.; Swain, A. C. Bis(η-pentamethylcyclopentadienyl) complexes of molybdenum, tungsten and rhenium via metal vapor synthesis. *J. Chem. Soc., Dalton Trans.* **1991**, 789-796.
(156) Baxley, G. T.; Avey, A. A.; Aukett, T. M.; Tyler, D. R. Photoactivation of water by Cp_2'Mo and photochemical studies of Cp_2MoO. Investigation of a proposed water-splitting cycle and preparation of a water-soluble molybdocene dihydride. *Inorg. Chim. Acta* **2000**, *300*, 102-112.
(157) Labella, L.; Chernega, A.; Green, M. L. H. Syntheses and reactions of ansa- 2,2-bis(η-cyclopentadienyl)propane -tungsten and ansa- 2,2-bis(η-cyclopentadienyl)propane - molybdenum compounds. *J. Chem. Soc., Dalton Trans.* **1995**, 395-402.
(158) Churchill, D. G.; Bridgewater, B. M.; Parkin, G. Modeling aspects of hydrodesulfurization at molybdenum: Carbon-sulfur bond cleavage of thiophenes by ansa molybdenocene complexes. *J. Am. Chem. Soc.* **2000**, *122*, 178-179.
(159) Churchill, D. G.; Bridgewater, B. M.; Zhu, G.; Pang, K. L.; Parkin, G. Carbon-hydrogen versus carbon-chalcogen bond cleavage of furan, thiophene and selenophene by ansa molybdenocene complexes. *Polyhedron* **2006**, *25*, 499-512.

(160) Braunschweig, H.; Gross, M.; Radacki, K.; Rothgaengel, C. Intramolecular activation of a disila[2]molybdenocenophanedihydride: Synthesis and structure of a [1],[1]metalloarenophane. *Angew. Chem., Int. Ed.* **2008**, *47*, 9979-9981.
(161) Arnold, T.; Braunschweig, H.; Gross, M.; Kaupp, M.; Muller, R.; Radacki, K. Electronic structure and reactivity of a [1],[1]disilamolybdenocenophane. *Chem. Eur. J.* **2010**, *16*, 3014-3020.
(162) Barral, M. D.; Green, M. L. H.; Jimenez, R. Photochemical studies on binuclear hydrido-molybdenocene compounds. *J. Chem. Soc., Dalton Trans.* **1982**, 2495-2498.
(163) Bitterwolf, T. E.; Saygh, A.; Haener, J. L.; Fierro, R.; Shade, J. E.; Rheingold, A. L.; Liable-Sands, L.; Alt, H. G. Synthesis and photolysis of $[M(CO)_3H]_2(\eta^5,\eta^5\text{-}C_5H_4CH_2C_5H_4)$, where M = Mo and W. Photochemical 'twist' rearrangement of $M_2(CO)_6(\eta^5,\eta^5\text{-}C_5H_4CH_2C_5H_4)$ to give $[M(CO)_3][M(CO)_3H](\eta^5,\eta^5{:}\eta^1\text{-}C_5H_4CH_2C_5H_3)$, where M = Mo and W. The molecular structure $[Mo(CO)_3][Mo(CO)_3Cl](\eta^5,\eta^5{:}\eta^1\text{-}C_5H_4CH_2C_5H_3)$. *Inorg. Chim. Acta* **2002**, *334*, 54-58.
(164) Carrasco, M.; Curado, N.; Alvarez, E.; Maya, C.; Peloso, R.; Poveda, M. L.; Rodriguez, A.; Ruiz, E.; Alvarez, S.; Carmona, E. Experimental and theoretical studies on arene-bridged metal-metal-bonded dimolybdenum complexes. *Chem. Eur. J.* **2014**, *20*, 6092-6102.
(165) Elmitt, K.; Green, M. L. H.; Forder, R. A.; Jefferso.I; Prout, K. Photoinduced insertion of tungsten into a methyl C-H bond in p-xylene and mesitylene - crystal-structure of $(\eta\text{-}C_5H_5)_2WCH_2(3,5\text{-}Me_2C_6H_3)_2$. *J. Chem. Soc., Chem. Commun.* **1974**, 747-748.
(166) Berry, M.; Elmitt, K.; Green, M. L. H. Photoinduced insertion of tungsten into aromatic and aliphatic carbon-hydrogen bonds by bis(η-cyclopentadienyl)tungsten derivatives. *J. Chem. Soc., Dalton Trans.* **1979**, 1950-1958.
(167) Farrugia, L.; Green, M. L. H. Photoinduced insertion of tungsten into methanol giving a tungsten-methyl derivative. *J. Chem. Soc., Chem. Commun.* **1975**, 416-417.
(168) Cox, P. A.; Grebenik, P.; Perutz, R. N.; Robinson, M. D.; Grinter, R.; Stern, D. R. Electronic-structure of molybdenocene and tungstenocene - detection of paramagnetism by magnetic circular-dichroism in argon matrices. *Inorg. Chem.* **1983**, *22*, 3614-3620.
(169) Kunkely, H. Photochemical hydrogen transfer from bis(i-propylcyclopentadienyl) tungsten dihydride to 9,10-phenanthrenequinone induced by outer sphere charge transfer excitation. *Inorg. Chem. Commun.* **1998**, *1*, 200-202.
(170) Wang, X. F.; Andrews, L. Matrix infrared spectra and density functional theory calculations of molybdenum hydrides. *J. Phys. Chem. A* **2005**, *109*, 9021-9027.
(171) Wang, X. F.; Chertihin, G. V.; Andrews, L. Matrix infrared spectra and dft calculations of the reactive MH_x (x=1, 2, and 3), $(H_2)MH_2$, MH_2^+, and MH_4^- (M = Sc, Y, and La) species. *J. Phys. Chem. A* **2002**, *106*, 9213-9225.
(172) Kang, S. K.; Albright, T. A.; Eisenstein, O. The structure of d^0 ML_6 complexes. *Inorg. Chem.* **1989**, *28*, 1611-1613.
(173) Wang, X. F.; Andrews, L.; Infante, I.; Gagliardi, L. Infrared spectra of the $WH_4(H_2)_4$ complex in solid hydrogen. *J. Am. Chem. Soc.* **2008**, *130*, 1972-1978.
(174) Dziegielewski, J. O.; Gilbortnowska, R.; Mrzigod, J.; Malecki, J. G. Hydride complexes of tungsten in photocatalytic dinitrogen reduction. *Polyhedron* **1995**, *14*, 1375-1379.
(175) Pivovarov, A. P.; Ioffe, L. M.; Gak, Y. V.; Makhaev, V. D.; Borisov, A. P.; Borodko, Y. G. Intramolecular hydrogen transfer from the alkyl substituent of a phosphine ligand to a metal atom upon the irradiation of tungsten phosphine hydride complexes. *Bull. Acad. Sci USSR Div. Chem. Sci.* **1987**, *36*, 928-930.
(176) Shima, T.; Hou, Z. Heterometallic polyhydride complexes containing yttrium hydrides with different Cp ligands: Synthesis, structure, and hydrogen-uptake/release properties. *Chem. Eur. J.* **2013**, *19*, 3458-3466.

(177) Church, S. P.; Poliakoff, M.; Timney, J. A.; Turner, J. J. Synthesis and characterization of the pentacarbonylmanganese(0) radical, $Mn(CO)_5$, in low-temperature matrices. *J. Am. Chem. Soc.* **1981**, *103*, 7515-7520.

(178) Fairhurst, S. A.; Morton, J. R.; Perutz, R. N.; Preston, K. F. Electron-paramagnetic-res spectra of $KrMn(CO)_5$ and $KrFe(CO)_5^+$ in a krypton matrix. *Organometallics* **1984**, *3*, 1389-1391.

(179) Frigyes, D.; Fogarasi, G. Isomers of manganese tetracarbonyl hydride: A density functional study of structure and vibrational spectra. *Organometallics* **1999**, *18*, 5245-5251.

(180) Clarke, M. J.; Howdle, S. M.; Jobling, M.; Poliakoff, M. Solvent-free impregnation of dinuclear metal-complexes into polyethylene - use of supercritical CO_2 and the in-situ photochemical assembly of $Mn_2(CO)_{10}$ from $HMn(CO)_5$. *Inorg. Chem.* **1993**, *32*, 5643-5644.

(181) Albertin, G.; Antoniutti, S.; Bettiol, M.; Bordignon, E.; Busatto, F. Synthesis, characterization, and reactivity of cationic molecular hydrogen complexes of manganese(i). *Organometallics* **1997**, *16*, 4959-4969.

(182) Bogdan, P. L.; Sullivan, P. J.; Donovan, T. A.; Atwood, J. D. Photocatalysis of hydrogenation and isomerization of alkenes by cis-$HMn(CO)_4PPh_3$. *J. Organomet. Chem.* **1984**, *269*, C51-C54.

(183) Karch, R.; Schubert, U. Transition metal silyl complexes .54. Hydrido disilanyl complexes $L_nM(H)SiR_2SiR_2H$ (L_nM=$MeCp(CO)_2Mn$, $Cp(CO)_2Re$, $(CO)_3(PPh_3)Fe$. *Inorg. Chim. Acta* **1997**, *259*, 151-160.

(184) Guillaumont, D.; Daniel, C. A quantum chemical investigation of the metal-to-ligand charge-transfer photochemistry. *Coord. Chem. Rev.* **1998**, *177*, 181-199.

(185) Chet wynd-Talbot, J.; Grebenik, P.; Perutz, R. N. Photochemistry of $(\eta\text{-}C_5H_5)_2ReH$ and $(\eta\text{-}C_5H_5)(\eta^2\text{-}C_5H_6)Re(CO)_2$ in low-temperature matrices - hydrogen loss and hydrogen migration. *J. Chem. Soc., Chem. Commun.* **1981**, 452-454.

(186) Chetwynd-Talbot, J.; Grebenik, P.; Perutz, R. N.; Powell, M. H. A. Photochemical studies of rhenium η-cyclopentadienyl complexes in matrices and in solution - detection of rhenocene and mechanisms of hydrogen transfer. *Inorg. Chem.* **1983**, *22*, 1675-1684.

(187) Cox, P. A.; Grebenik, P.; Perutz, R. N.; Graham, R. G.; Grinter, R. Rhenocene - magnetic circular-dichroism and laser-induced fluorescence in nitrogen matrices. *Chem. Phys. Lett.* **1984**, *108*, 415-419.

(188) Bossert, J.; Amor, N. B.; Strich, A.; Daniel, C. Electronic spectroscopy of $HRe(CO)_5$: A CASSCF/CASPT2 and TD-DFT study. *Chem. Phys. Lett.* **2001**, *342*, 617-624.

(189) Albertin, G.; Antoniutti, S.; Garcia-Fontan, S.; Carballo, R.; Padoan, F. Preparation, characterisation and reactivity of a series of classical and non-classical rhenium hydride complexes. *J. Chem. Soc., Dalton Trans.* **1998**, 2071-2081.

(190) Bolano, S.; Bravo, J.; Castro, J.; del Carmen Marin, M.; Garcia-Fontan, S. Synthesis, characterization and crystal structure of cis,mer- $ReH(CO)_2\{PPh(OMe)_2\}_3$. *Inorg. Chem. Commun.* **2009**, *12*, 916-918.

(191) Menon, R. K.; Brown, T. L. Excited-state properties of (μ-pyridyl)(μ-hydrido)dirhenium octacarbonyl and related dirhenium carbonyl-complexes. *Inorg. Chem.* **1989**, *28*, 1370-1379.

(192) Ball, R. G.; Campen, A. K.; Graham, W. A. G.; Hamley, P. A.; Kazarian, S. G.; Ollino, M. A.; Poliakoff, M.; Rest, A. J.; Sturgeoff, L.; Whitwell, I. Synthesis, x-ray crystal structure and photochemistry of (η^5-pentamethylcyclopentadienyl)(dicarbonyl)(dihydrido)rhenium in cyclohexane and liquid xenon solutions and in low temperature media at about 12 K. *Inorg. Chim. Acta* **1997**, *259*, 137-149.

(193) Jones, W. D.; Maguire, J. A. The activation of methane by rhenium - catalytic h/d exchange in alkanes with $CpRe(PPh_3)_2H_2$. *Organometallics* **1986**, *5*, 590-591.
(194) Epstein, R. A.; Gaffney, T. R.; Geoffroy, G. L.; Gladfelter, W. L.; Henderson, R. S. Photoinduced fragmentation of $H_3Re_3(CO)_{12}$ and $H_3Mn_3(CO)_{12}$. *J. Am. Chem. Soc.* **1979**, *101*, 3847-3852.
(195) Roberts, D. R.; Geoffroy, G. L. Reversible insertion of CO_2 into the Re-H bond of photogenerated $ReH(Ph_2PCH_2CH_2PPh_2)_2$. *J. Organomet. Chem.* **1980**, *198*, C75-C78.
(196) Bradley, M. G.; Roberts, D. A.; Geoffroy, G. L. Photogeneration of reactive $ReH(diphos)_2$ - its reversible coordination of CO_2 and activation of aromatic C-H bonds. *J. Am. Chem. Soc.* **1981**, *103*, 379-384.
(197) Perthuisot, C.; Fan, M. X.; Jones, W. D. Catalytic thermal C-H activation with manganese complexes - evidence for η^2-H_2 coordination in a neutral manganese complex and its role in c-h activation. *Organometallics* **1992**, *11*, 3622-3629.
(198) Roberts, D. A.; Geoffroy, G. L. Definitive examples of polyhydride complexes which do not eliminate H_2 in the primary photochemical-reaction - photo-dissociation of PR_3 from $ReH_3(PR_3)_4$ and $ReH_5(Pr_3)_3$ complexes. *J. Organomet. Chem.* **1981**, *214*, 221-231.
(199) Bergamo, M.; Beringhelli, T.; D'Alfonso, G.; Garavaglia, L.; Mercandelli, P.; Moret, M.; Sironi, A. Hydrido-carbonyl rhenium clusters with a square geometry of the metal core. Synthesis and x-ray characterization of the novel $Re_4(\mu\text{-}H)_3(CO)_{16}^-$ anion. *J. Cluster Sci.* **2001**, *12*, 223-242.
(200) Adams, R. D.; Captain, B.; Smith, M. D.; Beddie, C.; Hall, M. B. Unsaturated platinum-rhenium cluster complexes. Synthesis, structures and reactivity. *J. Am. Chem. Soc.* **2007**, *129*, 5981-5991.
(201) Geoffroy, G. L.; Epstein, R. A. Photoinduced de-clusterification of $HCCo_3(CO)_9$, $CH_3CCo_3(CO)_9$, and $HFeCo_3(CO)_{12}$. *Inorg. Chem.* **1977**, *16*, 2795-2799.
(202) Geoffroy, G. L.; Bradley, M. G. Photochemical generation of chlorohydridotristriphenylphosphineruthenium, $RuHCl(PPh_3)_3$. *J. Chem. Soc., Chem. Commun.* **1976**, 20-21.
(203) Geoffroy, G. L.; Bradley, M. G. Photochemistry of transition-metal hydride complexes .2. $RuClH(CO)(PPh_3)_3$, $RuH_2(CO)(PPh_3)_3$, and $RuClH(CO)_2(PPh_3)_2$. *Inorg. Chem.* **1977**, *16*, 744-748.
(204) Hoyano, J. K.; Graham, W. A. G. Hydrogen-mediated photolysis of $(\eta\text{-}C_5Me_5)Os(CO)_2H$ - synthesis of $(\eta\text{-}C_5Me_5)Os(CO)H_3$ and multiply bonded diosmium compounds. *J. Am. Chem. Soc.* **1982**, *104*, 3722-3723.
(205) McCamley, A.; Perutz, R. N.; Stahl, S.; Werner, H. Intermolecular and intramolecular photochemical C-H activation in matrices and in solution with (η^6-arene)(carbonyl)osmium complexes. *Angew. Chem., Int. Ed.* **1989**, *28*, 1690-1692.
(206) Hayes, P. G.; Gribble, C. W.; Waterman, R.; Tilley, T. D. A hydrogen-substituted osmium stannylene complex: Isomerization to a metallostannylene complex via an unusual α-hydrogen migration from tin to osmium. *J. Am. Chem. Soc.* **2009**, *131*, 4606-4607.
(207) Baker, M. V.; Field, L. D. Reaction of sp^2 C-H bonds in unactivated alkenes with bis(diphosphine) complexes of iron. *J. Am. Chem. Soc.* **1986**, *108*, 7433-7434.
(208) Baker, M. V.; Field, L. D. Reaction of ethylene with a coordinatively unsaturated iron complex, $Fe(depe)_2$ - sp^2 C-H bond activation without prior formation of a pi-complex. *J. Am. Chem. Soc.* **1986**, *108*, 7436-7438.
(209) Baker, M. V.; Field, L. D. Reaction of C-H bonds in alkanes with bis(diphosphine) complexes of iron. *J. Am. Chem. Soc.* **1987**, *109*, 2825-2826.
(210) Buys, I. E.; Field, L. D.; Hambley, T. W.; McQueen, A. E. D. Photochemical-reactions of $cis\text{-}FeH)_2(Me_2PCH_2CH_2PMe_2)_2$ with thiophenes - insertion into C-H and C-S bonds. *J. Chem. Soc., Chem. Commun.* **1994**, 557-558.

(211) Field, L. D.; George, A. V.; Messerle, B. A. Methane activation by an iron phosphine complex in liquid xenon solution. *J. Chem. Soc., Chem. Commun.* **1991**, 1339-1341.
(212) Baker, M. V.; Field, L. D. Cyclometallation reactions in the $Fe(dprpe)_2$ system dprpe=1,2-bis(dipropylphosphino)ethane. *Aust. J. Chem.* **1999**, *52*, 1005-1011.
(213) Pelton, E. J.; Blank, D. A.; McNeill, K. Dechlorination of chlorinated ethylenes by a photochemically generated iron(0) complex. *Dalton Trans.* **2013**, *42*, 10121-10128.
(214) Harvey, J. N.; Poli, R. Computational study of the spin-forbidden H_2 oxidative addition to 16-electron Fe(0) complexes. *Dalton Trans.* **2003**, 4100-4106.
(215) Poli, R. Open shell organometallics: A general analysis of their electronic structure and reactivity. *J. Organomet. Chem.* **2004**, *689*, 4291-4304.
(216) Ozin, G. A.; McCaffrey, J. G. The photoreversible oxidative-addition, reductive-elimination reactions $Fe+H_2$ reversible-FeH_2 in low-temperature matrices. *J. Phys. Chem.* **1984**, *88*, 645-648.
(217) Ozin, G. A.; McCaffrey, J. G.; Parnis, J. M. Photochemistry of transition-metal atoms - reactions with molecular-hydrogen and methane in low-temperature matrices. *Angew. Chem., Int. Ed.* **1986**, *25*, 1072-1085.
(218) Rubinovitz, R. L.; Nixon, E. R. The photochemical $Fe+H_2$ reaction in Ar-matrix and Kr-matrix by irradiation in the visible region. *J. Phys. Chem.* **1986**, *90*, 1940-1944.
(219) Chertihin, G. V.; Andrews, L. Infrared-spectra of FeH, FeH_2, and FeH_3 in solid argon. *J. Phys. Chem.* **1995**, *99*, 12131-12134.
(220) Mawby, R. J.; Perutz, R. N.; Whittlesey, M. K. Matrix photochemistry of $Ru(CO)_2(PMe_3)_2H_2$ and $Ru(CO)_3(PMe_3)_2$ - formation of $Ru(CO)_2(PMe_3)_2\cdots S$ (S=Ar, CH_4, Xe). *Organometallics* **1995**, *14*, 3268-3274.
(221) Burn, M. J.; Bergman, R. G. A study of the silanolysis of triphenylsilane and p-methoxyphenol catalyzed by $(PMe_3)_4RuH_2$ and the stoichiometric reactions of $(PMe_3)_4Ru(H)(OC_6H_4\text{-}p\text{-}X)$ (X=Me, OMe) with Ph_3SiH. *J. Organomet. Chem.* **1994**, *472*, 43-54.
(222) Morton, D.; Colehamilton, D. J.; Utuk, I. D.; Panequesosa, M.; Lopezpoveda, M. Hydrogen-production from ethanol catalyzed by group-8 metal-complexes. *J. Chem. Soc., Dalton Trans.* **1989**, 489-495.
(223) Kletzin, H.; Werner, H. Aryl(hydrido)ruthenium complexes by C-H addition - isolation of a 4-membered metallacycle as intermediate. *Angew. Chem., Int. Ed.* **1983**, *22*, 873-874.
(224) Morris, R. H.; Shiralian, M. Benzene carbon hydrogen-bond activation using $Ru(C_6Me_6)PH(C_6H_{11})_2H_2$. *J. Organomet. Chem.* **1984**, *260*, C47-C51.
(225) Hartwig, J. F.; Andersen, R. A.; Bergman, R. G. Alkyl, aryl, hydrido, and acetate complexes of $(dmpm)_2Ru$ dmpm = bis(dimethylphosphino)methane - reductive elimination and oxidative addition of C-H bonds. *Organometallics* **1991**, *10*, 1710-1719.
(226) Field, L. D.; Wilkinson, M. P. Synthesis and reactions of dihydridobis 1,2-bis(bis(trifluoromethyl)phosphino)ethane ruthenium(II) , $RuH_2(dfmpe)_2$. *Organometallics* **1997**, *16*, 1841-1845.
(227) Bianchini, C.; Casares, J. A.; Osman, R.; Pattison, D. I.; Peruzzini, M.; Perutz, R. N.; Zanobini, F. C-H bond cleavage in thiophenes by $P(CH_2CH_2PPh_2)_3Ru$. Uv flash kinetic spectroscopy discloses the ruthenium-thiophene adduct which precedes c-h insertion. *Organometallics* **1997**, *16*, 4611-4619.
(228) Boddien, A.; Loges, B.; Gartner, F.; Torborg, C.; Fumino, K.; Junge, H.; Ludwig, R.; Beller, M. Iron-catalyzed hydrogen production from formic acid. *J. Am. Chem. Soc.* **2010**, *132*, 8924-8934.
(229) Burkhardt, E. W.; Geoffroy, G. L. Photoassisted synthesis of mixed-metal clusters - PPN $CoOs_3(CO)_{13}$, $H_2RuOs_3(CO)_{13}$, and $H_2FeOs_3(CO)_{13}$. *J. Organomet. Chem.* **1980**, *198*, 179-188.

(230) Kiel, W. A.; Ball, R. G.; Graham, W. A. G. Carbonyl-η-hexamethylbenzene complexes of osmium - carbon-hydrogen activation by $(\eta\text{-}C_6Me_6)Os(CO)(H)_2$. *J. Organomet. Chem.* **1990**, *383*, 481-496.
(231) Graff, J. L.; Wrighton, M. S. Photochemistry and photocatalytic activity of a polynuclear metal-carbonyl hydride - dodecacarbonyltetrahydridotetraruthenium. *J. Am. Chem. Soc.* **1980**, *102*, 2123-2125.
(232) Bentsen, J. G.; Wrighton, M. S. Photochemistry of $H_4Ru_4(CO)_{12}$ in rigid alkane matrices at low-temperature - spectroscopic detection and characterization of coordinatively unsaturated $H_4Ru_4(CO)_{11}$. *J. Am. Chem. Soc.* **1984**, *106*, 4041-4043.
(233) Nakajima, T.; Shimizu, I.; Kobayashi, K.; Wakatsuki, Y. Synthesis of triangular and tetrahedral heteronuclear metal clusters using hydride complexes of cyclopentadienylrhodium and -ruthenium as the precursors. *Organometallics* **1998**, *17*, 262-269.
(234) Sweany, R. L. Photolysis of matrix-isolated hydridotetracarbonylcobalt(I) - evidence for metal-hydrogen bond homolysis. *Inorg. Chem.* **1980**, *19*, 3512-3516.
(235) Sweany, R. L. Photolysis of matrix-isolated hydridotetracarbonylcobalt(I) - comparison of the probabilities of carbonyl loss with hydrogen-atom loss. *Inorg. Chem.* **1982**, *21*, 752-756.
(236) Daniel, C.; Heitz, M. C.; Lehr, L.; Schroder, T.; Warmuth, B. Dynamics of photochemical-reactions - simulation by quantum calculations for transition-metal hydrides. *Int. J. Quantum Chem.* **1994**, *52*, 71-88.
(237) Heitz, M. C.; Ribbing, C.; Daniel, C. Spin-orbit induced radiationless transitions in organometallics: Quantum simulation of the intersystem crossing processes in the photodissociation of $HCo(CO)_4$. *J. Chem. Phys.* **1997**, *106*, 1421-1428.
(238) Sweany, R. L. Evidence for tricarbonyltrihydridocobalt(III) - synthesis from tricarbonylhydridocobalt(I) in matrices. *J. Am. Chem. Soc.* **1982**, *104*, 3739-3740.
(239) Sweany, R. L.; Russell, F. N. Photolysis of tetracarbonylmethylcobalt(i) and tetracarbonylhydridocobalt(I) in inert-gas and hydrogen-containing matrices - the reaction of 16-electron, coordinatively unsaturated complexes with dihydrogen. *Organometallics* **1988**, *7*, 719-727.
(240) Endicott, J. F.; Wong, C. L.; Inoue, T.; Natarajan, P. Photoinduced oxygenation of trans-aquohydridotetraamminerhodium(III) - evidence for a transition-metal chain carrier. *Inorg. Chem.* **1979**, *18*, 450-454.
(241) Bakac, A.; Thomas, L. M. Macrocyclic rhodium(III) hydrides and a monomeric rhodium(II) complex. *Inorg. Chem.* **1996**, *35*, 5880-5884.
(242) Moriyama, H.; Yabe, A.; Matsui, F. Photoenhanced homogeneous catalytic-hydrogenation of olefins following XeCl excimer laser excitation of $RhH(CO)(PPh_3)_3$. *J. Mol. Catal.* **1989**, *50*, 195-202.
(243) Yoshida, T.; Okano, T.; Otsuka, S. Activation of water-molecules .4. Generation of dihydrogen from water by rhodium(I) hydrido and rhodium(0) carbonyl-compounds. *J. Am. Chem. Soc.* **1980**, *102*, 5966-5967.
(244) Fox, D. J.; Duckett, S. B.; Flaschenriem, C.; Brennessel, W. W.; Schneider, J.; Gunay, A.; Eisenberg, R. A model iridium hydroformylation system with the large bite angle ligand xantphos: Reactivity with parahydrogen and implications for hydroformylation catalysis. *Inorg. Chem.* **2006**, *45*, 7197-7209.
(245) Ziessel, R. Photocatalysis - mechanistic studies of homogeneous photochemical water gas shift reaction catalyzed under mild conditions by novel cationic iridium(III) complexes. *J. Am. Chem. Soc.* **1993**, *115*, 118-127.
(246) Jones, W. D.; Feher, F. J. The mechanism and thermodynamics of alkane and arene carbon-hydrogen bond activation in $(C_5Me_5)Rh(PMe_3)(R)H$. *J. Am. Chem. Soc.* **1984**, *106*, 1650-1663.

(247) Periana, R. A.; Bergman, R. G. Rapid intramolecular rearrangement of a hydridocyclopropylrhodium complex to a rhodacyclobutane - independent synthesis of the metallacycle by addition of hydride to the central carbon-atom of a cationic rhodium pi-allyl complex. *J. Am. Chem. Soc.* **1984**, *106*, 7272-7273.
(248) Periana, R. A.; Bergman, R. G. Oxidative addition of rhodium to alkane C-H bonds - enhancement in selectivity and alkyl group functionalization. *Organometallics* **1984**, *3*, 508-510.
(249) Periana, R. A.; Bergman, R. G. Isomerization of the hydridoalkylrhodium complexes formed on oxidative addition of rhodium to alkane C-H bonds - evidence for the intermediacy of η^2-alkane complexes. *J. Am. Chem. Soc.* **1986**, *108*, 7332-7346.
(250) Periana, R. A.; Bergman, R. G. C-c activation of organic small ring compounds by rearrangement of cycloalkylhydridorhodium complexes to rhodacycloalkanes - synthesis of metallacyclobutanes, including one with a tertiary M-C bond, by nucleophilic-addition to π-allyl complexes. *J. Am. Chem. Soc.* **1986**, *108*, 7346-7355.
(251) Perutz, R. N.; Sabo-Etienne, S. The sigma-cam mechanism: Sigma complexes as the basis of sigma-bond metathesis at late-transition-metal centers. *Angew. Chem., Int. Ed.* **2007**, *46*, 2578-2592.
(252) Evans, M. E.; Li, T.; Jones, W. D. C-H vs C-C bond activation of acetonitrile and benzonitrile via oxidative addition: Rhodium vs nickel and Cp* vs Tp ' (Tp ' = hydrotris(3,5-dimethylpyrazol-1-yl)borate, Cp* = η^5-pentamethylcyclopentadienyl). *J. Am. Chem. Soc.* **2010**, *132*, 16278-16284.
(253) Wick, D. D.; Jones, W. D. Synthesis, characterization, and C-H/C-C cleavage reactions of two rhodium-trispyrazolylborate dihydrides. *Inorg. Chim. Acta* **2009**, *362*, 4416-4421.
(254) Tanabe, T.; Brennessel, W. W.; Clot, E.; Eisenstein, O.; Jones, W. D. Synthesis, structure, and reductive elimination in the series Tp'Rh(PR_3)(Ar-F) H; determination of rhodium-carbon bond energies of fluoroaryl substituents. *Dalton Trans.* **2010**, *39*, 10495-10509.
(255) Tanabe, T.; Evans, M. E.; Brennessel, W. W.; Jones, W. D. C-H and C-CN bond activation of acetonitrile and succinonitrile by Tp'Rh(PR_3). *Organometallics* **2011**, *30*, 834-843.
(256) Wink, D. A.; Ford, P. C. A flash-photolysis investigation of dihydrogen elimination from phosphine complexes of iridium(III) and rhodium(III) - $H_2IrCl(CO)(PPh_3)_2$, $H_2IrCl(PPh_3)_3$, and $H_2RhCl(PPh_3)_3$. *J. Am. Chem. Soc.* **1986**, *108*, 4838-4842.
(257) Itagaki, H.; Murayama, H.; Saito, Y. Photocatalysis of rhcl(pcy_3)$_2$ for cyclohexane dehydrogenation - thermal-dissociation of C-H bond and photoelimination of H_2. *Bull. Chem. Soc. Jpn.* **1994**, *67*, 1254-1257.
(258) Geoffroy, G. L.; Hammond, G. S.; Gray, H. B. Photochemical reductive elimination of oxygen, hydrogen, and hydrogen chloride from iridium complexes. *J. Am. Chem. Soc.* **1975**, *97*, 3933-3936.
(259) Geoffroy, G. L.; Pierantozzi, R. Photochemistry of transition-metal hydride complexes .1. Photoinduced elimination of molecular-hydrogen from $IrClH_2(PPh_3)_3$ and $IrH_3(PPh_3)_3$. *J. Am. Chem. Soc.* **1976**, *98*, 8054-8059.
(260) Schultz, R. H. Unusual behavior in the 308 nm flash photolysis of Vaska's complex. *J. Organomet. Chem.* **2003**, *688*, 1-4.
(261) Janowicz, A. H.; Bergman, R. G. C-H activation in completely saturated-hydrocarbons - direct observation of M + R-H$\rightarrow$M(R)(H). *J. Am. Chem. Soc.* **1982**, *104*, 352-354.
(262) Bergman, R. G. Activation of alkanes with organotransition metal-complexes. *Science* **1984**, *223*, 902-908.
(263) Janowicz, A. H.; Bergman, R. G. Activation of C-H-bonds in saturated-hydrocarbons on photolysis of (η^5-C_5Me_5)(PMe_3)IrH_2 - relative rates of reaction of the intermediate with

different types of C-H-bonds and functionalization of the metal-bound alkyl-groups. *J. Am. Chem. Soc.* **1983**, *105*, 3929-3939.

(264) Peterson, T. H.; Golden, J. T.; Bergman, R. G. Evidence for the intervention of different c-h activating intermediates in the irradiation of (η^5-C_5Me_5)(PMe_3)IrH_2 and the reaction of (η^5-C_5Me_5)(PMe_3)Ir(H)(Cl) with strong base. Detection and spectroscopic characterization of (η^5-C_5Me_5)(PMe_3)Ir(Li)(Cl), an intermediate in the dehydrohalogenation reaction. *J. Am. Chem. Soc.* **2001**, *123*, 455-462.

(265) Foo, T.; Bergman, R. G. Synthesis and C-H activation reactions of (η^5-indenyl)(trimethylphosphine)iridium alkyl and hydride complexes. *Organometallics* **1992**, *11*, 1801-1810.

(266) Bloyce, P. E.; Rest, A. J.; Whitwell, I.; Graham, W. A. G.; Holmessmith, R. Photoactivation of alkanes by carbonyl(η^5-cyclopentadienyl)dihydridoiridium - solution and matrix-isolation studies. *J. Chem. Soc., Chem. Commun.* **1988**, 846-848.

(267) Crowfoot, L.; Ozin, G. A.; Ozkar, S. Intrazeolite carbonyl(η^5-cyclopentadienyl)dihydridoiridium(III) ($CpIr(CO)H_2$-M56Y, where M = H, Li, Na, K, Rb, and Cs). *J. Am. Chem. Soc.* **1991**, *113*, 2033-2040.

(268) Burk, M. J.; Crabtree, R. H.; McGrath, D. V. Thermal and photochemical catalytic dehydrogenation of alkanes with $IrH_2(CF_3CO_2)(PR_3)_2$ (R = C_6H_4F-p and cyclohexyl). *J. Chem. Soc., Chem. Commun.* **1985**, 1829-1830.

(269) Gerard, H.; Eisenstein, O.; Lee, D. H.; Chen, J. Y.; Crabtree, R. H. Unifying the mechanisms for alkane dehydrogenation and alkene H/D exchange with $IrH_2(O_2CCF_3)(PAr_3)_2$: The key role of CF_3CO_2 in the "sticky" alkane route. *New J. Chem.* **2001**, *25*, 1121-1131.

(270) Ferrari, A.; Polo, E.; Ruegger, H.; Sostero, S.; Venanzi, L. M. Photochemistry of dihydrido(hydrotris(3,5-dimethylpyrazolyl)borato)(Z-cyclooctene)iridium. Synthetic intermediates and mechanism of the photochemical formation of hydridophenyl(hydrotris(3,5-dimethylpyrazolyl)borato)(trimethyl phosphite)iridium. *Inorg. Chem.* **1996**, *35*, 1602-1608.

(271) Sweany, R. L.; Polito, M. A.; Moroz, A. Photolysis of tetracarbonylnickel in dihydrogen-containing matrices - evidence for the formation of a complex of molecular-hydrogen. *Organometallics* **1989**, *8*, 2305-2308.

(272) Sostero, S.; Traverso, O.; Ros, R.; Michelin, R. A. Photoinduced reductive elimination of cyanoalkanes from hydridocyanoalkyl complexes of platinum(II). *J. Organomet. Chem.* **1983**, *246*, 325-329.

(273) Clark, H. C.; Ferguson, G.; Hampden-Smith, M. J.; Ruegger, H.; Ruhl, B. L. The chemistry of platinum hydrides .30. The chemical and structural effects of steric overcrowding in the compounds *cis*- and *trans*-H[R_3Sn]Pt(PCy_3)$_2$,R = Ph, Cl. *Can. J. Chem.* **1988**, *66*, 3120-3127.

(274) Chan, D.; Duckett, S. B.; Heath, S. L.; Khazal, I. G.; Perutz, R. N.; Sabo-Etienne, S.; Timmins, P. L. Platinum bis(tricyclohexylphosphine) silyl hydride complexes. *Organometallics* **2004**, *23*, 5744-5756.

(275) Brown, M. P.; Cooper, S. J.; Frew, A. A.; Manojlovicmuir, L.; Muir, K. W.; Puddephatt, R. J.; Thomson, M. A. The di-μ-bis(diphenylphosphino)methane-μ-hydrido-bis[methylplatinum(II)]cation - synthesis, molecular-structure, and chemical-properties. *J. Chem. Soc., Dalton Trans.* **1982**, 299-305.

(276) Boaretto, R.; Sostero, S.; Traverso, O. Photochemistry of platinum phosphine complexes. Perspective in C-H bond activation. *Inorg. Chim. Acta* **2002**, *330*, 59-62.

(277) Cho, H.-G.; Andrews, L. Infrared spectra of CH_3-MH, CH_3-M, and CH_3-MH- prepared via methane activation by laser-ablated Au, Ag, and Cu atoms. *Dalton Trans.* **2011**, *40*, 11115-11124.

(278) Dhayal, R. S.; Liao, J.-H.; Lin, Y.-R.; Liao, P.-K.; Kahlal, S.; Saillard, J.-Y.; Liu, C. W. A nanospheric polyhydrido copper cluster of elongated triangular orthobicupola array: Liberation of h_2 from solar energy. *J. Am. Chem. Soc.* **2013**, *135*, 4704-4707.

(279) Girod, M.; Krstic, M.; Antoine, R.; MacAleese, L.; Lemoine, J.; Zavras, A.; Khairallah, G. N.; Bonacic-Koutecky, V.; Dugourd, P.; O'Hair, R. A. J. Formation and characterisation of the silver hydride nanocluster cation $Ag_3H_2((Ph_2P)_2CH_2)^+$ and its release of hydrogen. *Chem. Eur. J.* **2014**, *20*, 16626-16633.

Graphical Abstract